UNIVERSIDADE DE LISBOA

FACULDADE DE CIÊNCIAS

Ciências
ULisboa

Solar Energy Potential in a Changing Climate:

Iberia and Azores Assessment Combining Dynamical and Statistical Downscaling Methods

Doutoramento em Sistemas Sustentáveis de Energia

Clarisse Magarreiro

Tese orientada por:
Professor Doutor Miguel C. Brito
Professor Doutor Pedro M. M. Soares

Documento especialmente elaborado para a obtenção do grau de doutor

2016

UNIVERSIDADE DE LISBOA

FACULDADE DE CIÊNCIAS

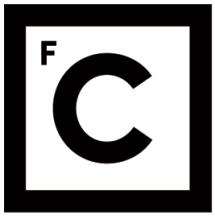

Ciências
ULisboa

Solar Energy Potential in a Changing Climate:

Iberia and Azores Assessment Combining Dynamical and Statistical Downscaling Methods

Doutoramento em Sistemas Sustentáveis de Energia

Clarisse Magarreiro

Tese orientada por:
Professor Doutor Miguel C. Brito
Professor Doutor Pedro M. M. Soares

Júri:
Presidente:
- Dr. João C. C. Catalão Fernandes

Vogais:
- Dr. Eduardo M. V. Brito de Azevedo
- Dr. João C. Andrade dos Santos
- Dr. João M. de Almeida Serra
- Dr. Pedro M. M. Soares

Documento especialmente elaborado para a obtenção do grau de doutor

Fundação para a Ciência e a Tecnologia, SFRH/BD/79544/2011

2016

Acknowledgements

I would like to thank my two advisors, Prof. Miguel Centeno Brito and Prof. Pedro Matos Soares for their scientific guidance, friendship, motivation, for dealing with my frustrations and deadlines. To Prof. Miguel I am especially grateful for his serenity and stabilizing presence which helped me so much in moments of self-doubt and to Prof. Pedro for constantly challenging me to go beyond what I thought I was capable which lead me to grow immensely not only scientifically but also personally.

I am also thankful to Rita Cardoso for all the help in the statistical analysis, for the ideas and comments throughout the development of the thesis especially in the co-authored scientific papers.

To Ricardo Tomé, for solving the technical problems of the cluster and for providing the data of the WRF model for the Azores and also to Daniela Lima who, together with Rita, helped in obtaining the WRF data for Iberian Peninsula. Thank you.

I am grateful to Martin Widmann for hosting me at University of Birmingham during my 5 weeks visit. Thank you for being willing to share your knowledge and for making me feel welcomed in Birmingham. I have enjoyed working with you immensely.

Não existem palavras que quantifiquem o quão grata estou aos meus pais, Teresa e Manuel, e à minha irmã, Ana, que sempre me motivaram e apoiaram de todas as maneiras possíveis durante todo este processo. Viveram comigo intensamente todas as conquistas e dificuldades que encontrei nos últimos anos e, portanto, considero este trabalho como um pedaço de cada um deles.

Ao Ricardo, pela paciência inesgotável que teve ao me acompanhar em todos os momentos críticos e por ser diariamente um suporte inigualável e inquestionável durante todo o desenvolvimento do meu trabalho. Obrigado por me ajudares a tornar tudo mais fácil e por me impulsionares sempre no meu crescimento consciencial.

I extend also my appreciation to Prof. João Serra who, by being the MIT Portugal Program coordinator of the Sustainable Energy Systems at Faculdade de Ciências da Universidade de Lisboa, was always available to solve any bureaucratic situation concerning the development of the PhD.

I acknowledge the funding I received from the Portuguese Science Foundation (FCT), under the doctoral grant SFRH/BD/79544/2011 and the MIT Portugal Program on Sustainable Energy Systems for the framework provided. I also acknowledge the funding obtained in the framework of the Short Term Scientific Missions of COST Action (European Cooperation in Science and Technology): Validating and Integrating Downscaling Methods for Climate Change Research (VALUE) which allowed me to develop part of my work in my 5 weeks stay at the University of Birmingham.

To all, thank you!

Abstract

The proper characterization of solar radiation resource is essential for the design of any solar energy harnessing systems which aims its optimal performance. To this end, the solar resource is often quantified through solar radiation measurements at meteorological stations. Unfortunately radiation data recorded on the desired location is often inexistent. Furthermore, the actual existing solar radiation databases have also a limited temporal span and, more frequently than desired, missing values and non-uniform formats. Also, such databases consist almost entirely of global solar radiation; variables such as the nature of the solar energy (direct or diffuse) are rarely recorded.

Atmospheric models can add value to solar energy applications by enabling solar resource assessments as they easily overcome the limited spatial and temporal coverage of irradiance measuring networks. Furthermore, climate models can be used for any region of the planet to assess the solar resource for not only present climate conditions but also to analyse its long-term past evolution and future tendency. Nowadays such models are a popular approach on the field of solar radiation forecasting but the quality evaluation of the solar radiation representation by such models is first of all a fundamental step to understand its usefulness. Having this in mind, in this thesis, a dynamical downscaling approach is used to evaluate simulated solar radiation at the Earth's surface which will then enable the characterization of the solar resource. The model output is also combined with a statistical downscaling approach used in its simplest form to minimize the model biases. The work focuses primarily in the Iberian Peninsula as its large climate gradients are representative of diverse meteorological conditions, enabling therefore the adaptation of the presented methods to other regions. Then, following the same methodology, the solar resource of the Azores archipelago is also addressed. The Azores region is often neglected in solar resource assessments and solar resource maps of the Earth's surface or even of Europe region. These methods are used to characterize the present climate renewable solar resource and analyse the impact of climate change on its projections for the end of the 21st century for both Iberia Peninsula and Azores archipelago.

Atmospheric numerical models are however limited in the sense that they only provide global solar radiation, the direct normal radiation and diffuse components are not common outputs to the user. Given this, the separation of global radiation into its diffuse and direct components is analysed in this thesis through models of diffuse solar radiation fraction. One important characteristic of these models is that they are empirically derived from site-specific measurements and a model developed and validated in a very specific climate type region may not hold its suitability to other regions. This thesis focuses on the assessment of such models only for the Azores region which has not been object of this type of analysis before.

Keywords: Solar Resource; Iberian Peninsula; Azores; Dynamical downscaling; Bias Correction

Resumo

A viabilidade técnica e económica de qualquer sistema energético solar que visa o seu desempenho óptimo é sustentada na existência de informação confiável e exacta sobre o recurso solar disponível no local pretendido para a sua implementação. Idealmente, a informação de recurso solar deve reunir características tais como valores médios e sua variabilidade no espaço e no tempo. Além disso três componentes da radiação solar são fundamentais na análise do recurso: radiação difusa, directa e global. A radiação difusa diz respeito à radiação dispersa existente como resultado das interacções da radiação extraterrestre com a atmosfera terrestre. A radiação directa é radiação que atinge a superfície terrestre directamente em linha com o disco solar e ao conjunto de radiação difusa e directa é chamado de radiação global (ou total). Os dados de radiação global são necessários para cálculos de cargas de aquecimento e arrefecimento em arquitectura; sistemas solares térmicos e fotovoltaicos mas, quando estão em causa sistemas de concentração, é indispensável possuir informação sobre a radiação directa.

Devido aos elevados custos de implementação e manutenção de estações meteorológicas que façam recolha de dados de radiação solar de forma consistente e fiável a probabilidade de pré-existirem dados de radiação registados nesse mesmo local é baixa. Como consequência a este facto, a densidade de pontos de medidas desta variável é limitada o que implica então que se recorra a métodos alternativos de avaliação do recurso. Uma base de dados de recurso solar pode ser construída com técnicas de interpolação aplicadas a dados climatológicos mas a estimação de dados através deste processo introduz erros nos dados espacialmente estimados que aumentam com a distância entre os pontos de interesse e o ponto onde foram realmente recolhidas as medidas de radiação solar.

Quando existentes, as medidas de radiação solar dizem respeito a, maioritariamente, valores de radiação solar global. Variáveis como radiação directa ou radiação difusa são pouco frequentes em bases de dados desta variável.

Hoje em dia também dados obtidos via satélite são usados para obter informação relativa à radiação solar que alcança a superfície terrestre. Os dados podem ser recolhidos

por satélites de órbita polar ou geoestacionários. Como os satélites de órbita polar facultam imagens com baixa resolução temporal, as imagens obtidas por satélites geoestacionários são as normalmente usadas em estudos de radiação solar. Este tipo de satélites garante imagens com uma resolução temporal que pode chegar aos 15 minutos e resolução espacial que pode atingir 1 km no ponto imediatamente abaixo do posicionamento do satélite. No entanto, dado que este tipo de satélites são posicionados num ponto longitudinal fixo acima do equador, a sua resolução espacial decai com a latitude e a sua relevância em latitudes acima dos 60-70° norte ou sul é bastante limitada. Os modelos atmosféricos podem então ser considerados como uma mais valia para estudos de recurso solar por facilitarem a obtenção de dados regularmente espaçados na superfície terreste e consistentes em termos temporais e formatação dos mesmos. Estes modelos simulam o sistema climático e quantificam a resposta climática às interacções entre os seus vários componentes. Entre os modelos atmosféricos é feita a distinção entre modelos globais e modelos regionais. Os modelos globais reproduzem as principais características do sistema climático, mas uma vez que são de demasiada baixa resolução para descrever adequadamente os processos de mesoescala, para aplicações regionais é então apropriado usar modelos regionais. Os modelos regionais simulam então o sistema climático em domínios espaciais limitados. Estes últimos requerem para a sua execução informação para as condições fronteira do sistema que é por sua vez fornecida pelos modelos globais. Ao processo de usar modelos regionais para representar subdomínios de modelos globais é denominado *dynamical downscaling* (redução de escala dinâmico). Uma vez que estes modelos são formulados usando princípios físicos, possuem grande potencial para capturar as características não lineares de mesoescala e fornecer informação coerente entre múltiplas variáveis meteorológicas. Além disto, os modelos atmosféricos são úteis não só para analisar as condições de clima presente mas também para estudo de tendências passadas e de clima futuro.

As simulações numéricas destes modelos não são no entanto imunes à existência de erros. No caso dos modelos regionais além dos erros inerentes da formulação do modelo (parametrização de processos de pequena escala) também estão susceptíveis a erros herdados através das condições fronteiras que são o resultado de simulações de modelos globais. Dado isto, é frequentemente usado uma qualquer abordagem estatística que constitua o pós-processamento dos resultados obtidos através dos modelos dinâmicos. Os modelos estatísticos usados envolvem tipicamente o desenvolvimento de relações entre os preditores adquiridos através dos modelos dinâmicos e a variável desejada (o preditante). Este processo além de ser conhecido como um simples pós-processamento estatístico é também referido neste contexto como *statistical downscaling* (redução de escala estatístico). Esta última definição evidencia que os resultados dos modelos atmosféricos, mesmo que se referindo a simulações de elevada resolução, podem ser submetidos a processamento adicional para obter um valor que foi sujeito a uma redução de escala ao ponto de ser equiparável a um valor obtido localmente.

Na presente tese, uma abordagem de *dynamical downscaling* é usada para avaliar simulações de radiação solar à superfície terrestre. No âmbito do presente trabalho este processo é representado pelo modelo atmosférico WRF (*Weather Research and Forecasting*). O WRF é um modelo de mesoescala de simulação de sistema climático com capacidade para funcionar tanto para a operacionalidade dos centros meteorológicos como para pesquisas atmosféricas. Reúne várias e diferentes escolhas em termos de parametrizações físicas incluindo microfísica; parametrização de cumulus; camada limite planetária; modelos de superfície terrestre e radiação de grande e pequeno comprimento de onda. Os resultados das simulações do modelo são combinados com uma abordagem de *statistical downscaling*. Em termos práticos, na tese, esta abordagem é representada por métodos que visam a correcção do viés dos dados simulados através da abordagem de *dynamical downscaling*. Estes métodos são usados para caracterizar o recurso solar em clima presente e para analisar o impacto do clima futuro nas projecções de recurso solar para o final do século XXI. O trabalho desenvolvido foca primeiramente a Península Ibérica dado que os seus gradientes de clima são representativos de diversas condições meteorológicas proporcionando assim a adaptação dos métodos apresentados a outras regiões. Além disto, a Península Ibérica é identificada como uma das regiões mais responsivas à mudança de clima futuro. O trabalho foca também, usando a mesma metodologia, a caracterização do recurso solar no arquipélago dos Açores. A região dos Açores é frequentemente negligenciada em estudos de recurso solar ou em publicações de mapas solares da Terra ou até mesma da Europa.

Uma vez que as simulações de radiação solar do modelo WRF irão ultrapassar as limitações encontradas em dados medidos *in situ* no que diz respeito à consistência espacial e temporal dos mesmos, há que considerar o facto de que os dados simulados dizem respeito apenas a radiação solar global. Assim, a separação da radiação solar global nas suas componentes difusa e directa é também analisada no âmbito da presente tese através de modelos de fracção de radiação difusa. Estes modelos têm como objectivo a estimação de radiação difusa numa superfície horizontal baseando se em dados de radiação solar global medidos na mesma superfície. Através da relação fundamental entre as componentes difusa, directa e global é então possível inferir não só os valores de radiação difusa como também os valores de radiação directa. A variedade existente deste tipo de modelos é consequência, principalmente, do tipo de parâmetros de entrada usados nos mesmos. Os mais simples e comuns são modelos que usam apenas informação da radiação global. Modelos mais sofisticados podem no entanto requerer parâmetros e variáveis meteorológicas tais como informação de nebulosidade, turbidez atmosférica ou temperatura. No geral, a maioria dos modelos de fracção de radiação difusa dependem de correlações entre o índice de céu limpo e a fracção de radiação difusa. Estas correlações são expressas em termos de polinómios de 1° a 4° grau, modelos logísticos ou até exponenciais. No entanto há que considerar uma importante limitação dos modelos de fracção de radiação difusa. Como são derivados empiricamente a partir de medidas *in situ*, um modelo desenvolvido e validado numa região com um clima muito específico pode não ser

adequado para uma outra qualquer região. No presente trabalho, este tópico é apenas explorado para o arquipélago dos Açores. Para a Península Ibérica é possível encontrar na literatura vários estudos onde este tipo de modelos foi desenvolvido e validado. No entanto, a região dos Açores não foi até então considerada neste tipo de estudos. Além disso, a região dos Açores é conhecida por ter um padrão de condições meteorológicas diferentes da Península Ibérica, caracterizado com uma maior ocorrência de estados nebulosos.

Palavras-Chave: Recurso solar; Península Ibérica; Açores; *Dynamical downscaling*; Correcção viés

Contents

List of Acronyms, Abbreviations and Symbols

BIAS	Bias Error
CDF	Cumulative Distribution Function
D	Diffuse radiation
G	Global radiation
GCM	Global climate model
G_{ex}	Global extraterrestrial radiation
I	Direct normal radiation
IP	Iberian Peninsula
k_d	Diffuse fraction
k_t	Clearness index
LR	Linear Regression
m	Air mass
MAE	Mean Absolute Error
MAPE	Mean Absolute Percentual Error
MOS	Model output statistics
PDF	Probability Density Function
PV	Photovoltaic
QM	Quantile mapping
r	Correlation coefficient
RCM	Regional climate model
RMSE	Root Mean Square Error
S	Skill Score
WRF	Weather Research and Forecasting
θ	Zenith angle
ρ	Clear sky index
σ_n	Normalized standard deviation
τ	Hour-to-hour variability index

List of Figures

List of Tables

Chapter 1

Introduction

1.1 Introduction

The technical and economic viability of a system deployment of any solar energy harnessing technology is directly dependent on the corresponding resource availability. Hence it is essential to have better understanding of the resource characteristics, such as means and variability in space and time, which will enable the appropriate design of the harnessing technology and the maximization of its performance. To this end, the solar resource is often quantified through solar radiation measurements at meteorological stations. However, deploying and maintaining a measuring network for solar radiation is costly and thus the spatial coverage of measured irradiance values is frequently limited and sparse. Furthermore, the existing solar radiation databases have also a limited temporal span and, more frequently than desired, missing values and non-uniform formats which may hinder their usefulness (Paulescu et al., 2013). Also, such databases consist almost entirely of global solar radiation; variables such as the nature of the solar energy (direct or diffuse) or the total cloud cover amount are rarely recorded on hourly basis.

Due to high initial investment and maintenance costs of deploying a solar radiation measurement network, and due to the limitations of the database spatial coverage, interpolation (or extrapolation) of available data for estimating a given location is often required. This estimation however introduces errors on the spatially simulated data which will increase with the distance between the point of interest and the data acquisition spot (Journée & Bertran, 2010). Presently, also satellite data is used to retrieve information over solar radiation at Earth's surface. The methods used to derive solar radiation from satellite imagery are often categorized into empirical or physical models (Badescu, 2008). Physical models rely on radiation-transfer equations to analyse the brightness seen by the satellite in different wavelengths using for that end precise information about the composition of the

atmosphere which must be acquired by accurately calibrated satellite sensors. Empirical models may, on the other hand, consist of only a simple regression between the satellite visible channel's recorded intensity and a measuring station at the Earth's surface (Kleissl, 2013). Nowadays however, most of currently used models contain both empirical and physical information (Badescu, 2008). Since polar orbit satellites provide a low temporal frequency of images, geostationary satellites are often used when information about solar radiation variability is required. Such satellites can offer a temporal resolution of up to 15 min and a spatial resolution reaching approximately 1 km at satellite nadir (subsatellite point) (Paulescu et al., 2013). However, geostationary satellites are always positioned above a fixed longitudinal point over the equator and consequently the spatial resolution decreases with the latitude (Badescu, 2008; Kleissl, 2013). Their use in latitudes beyond 60-70 degrees north or south is therefore rather limited (Badescu, 2008; Kleissl, 2013).

Atmospheric models can add value to solar energy applications by enabling solar resource assessments as they easily overcome the limited spatial and temporal coverage of irradiance measuring networks. Furthermore, climate models can be used for any region of the planet, have associated relatively low costs and missing data is not an issue. For regional applications it is appropriate to use regional climate models (RCMs), which are limited-area high-resolution models driven by boundary conditions from either standard simulations with global general circulation models (GCMs) or atmospheric reanalysis, which assimilate observational information (Giorgi, 1990; Rummukainen, 2010). Reanalysis-driven simulations aim to represent the actual weather during the last few decades, while standard GCM simulations are typically used to investigate the response of past and future climate to natural and anthropogenic forcing (Meehl et al., 2007). GCMs though are appropriate to capture the large-scale atmospheric circulations but, for understanding the local effects on regional areas RCMs must come into play. Local features that affect the atmospheric flow such as topography and coastal processes require finer resolution simulations to reproduce the observed weather (Soares et al., 2012a). The process of using high-resolution RCMs to represent regional sub-domains which assimilate beforehand either reanalysis or lower-resolution GCMs data as their boundary conditions is denominated dynamical downscaling. Since these models are formulated using physical principles, dynamical downscaling has the potential for capturing mesoscale to small-scale nonlinear effects and providing coherent information among multiple climate variables. Besides, such models can reliably reproduce a broad range of climates around the world which gives confidence in their ability to downscale realistically future climate (Christensen et al., 2007). Numerical models can then be useful not only to assess the solar resource for present climate conditions but also to analyse its long-term past evolution and future trends.

Simulations with RCMs, by relying on global models for their initial and boundary conditions, may inherit the biases of the global model on which it relies and besides, the RCM itself may cause bias on its output. A variety of errors may arise due to the necessary parameterizations for the numerous atmospheric small-scale processes that have to be parameterized in the dynamical downscaling process. Even without considering the

complexity of cloud simulation and its impact on the proper representation of solar radiation by the numerical models, deficiencies in water-vapour absorption, inaccurate representation of ozone and aerosols play an important part on possible causes of error on the simulation of irradiance (Kleissl, 2013). It is however extremely difficult to pinpoint the source of model errors due to the strong feedback and interactions among physical processes in the atmosphere (Kleissl, 2013). In reanalysis-driven simulations the errors from the driving conditions are reduced, but substantial RCM-generated biases are still present (Kotlarski et al. 2014; Soares et al., 2012b; van der Linden and Mitchell, 2009). Given this, statistical approaches are used to post-process the results of the dynamical models. In addition to offering a way to deal with model biases, they can also provide quantities not represented by the numerical model or be used for downscaling from the grid-cell scale to a given location (Wilks, 2006). The statistical methods typically involve the establishment of links between the grid-scale or large-scale predictors and the desired predictand variable. This process is referred to as statistical post-processing or statistical downscaling. This latter term highlights that the atmospheric numerical model output, even if referring to a high-resolution dynamical downscaling, can be further processed to obtain a downscaled value of the desired variable at a given location from the grid-cell scale of the model. The statistical downscaling concept in the scope of the present thesis is discussed in detail in Chapter 3.

Atmospheric numerical models are becoming a popular approach on the field of solar radiation forecasting and resource assessment but the quality evaluation of the solar radiation representation by such models is first of all a fundamental step to understand its usefulness. In this thesis, a dynamical downscaling approach is evaluated and used to simulate solar radiation at the Earth's surface. The model output is also combined with a statistical downscaling approach to minimize the model biases. These methods are used to characterize the present climate renewable solar resource and analyse the impact of future climate on its projections for the end of the 21st century. The work focuses primarily in the Iberian Peninsula, since its large climate gradients are representative of diverse meteorological conditions, enabling therefore the adaptation of the presented methods to other regions. Furthermore, the Iberian Peninsula has been identified as one of the most vulnerable regions to global climate change (Giorgi, 2006). The present work also addresses, with the same methodology, the solar resource of the Azores archipelago. The Azores region is often neglected in solar resource assessments and solar resource maps of the Earth's surface or even in Europe region.

The following sections included in this chapter describe some basic concepts and background for the motivation and aims of the thesis, which are collected in Section 1.5.

1.2 Solar radiation at Earth's Surface

At the top of Earth's atmosphere, the beam of nearly parallel incident sunrays is referred to as extraterrestrial radiation. The integration of the extraterrestrial spectrum

over all wavelengths defines the solar constant. The solar constant represents the averaged flux density of incoming solar radiation on a unitary surface perpendicular to the rays at the mean Sun–Earth distance (Paulescu et al., 2013). The actual power density of the solar constant varies slightly since the Earth-Sun distance changes as the Earth moves in its elliptical orbit around the sun, and because the sun's emitted power is not constant. However since this variations are typically small this value is considered as constant. The currently accepted value for solar constant is 1366 W/m^2 (Kleissl, 2013; Badescu, 2008; Paulescu et al., 2013) but some oscillation on this number may be found on literature of around ± $7W/m^2$ (Kleissl, 2013). When the solar radiation flux passes through the Earth's atmosphere, its spectral distribution is modified by absorption and scattering processes. Thus the radiation at the Earth's surface varies widely. Also, local variations in the atmosphere, such as water vapour, clouds, pollution, geographic location of the region in interest, season of the year and the time of day are factors that contribute to its variation.

Solar energy resource assessments typically require the knowledge of the two components of solar radiation at the Earth's surface: diffuse radiation (D), the scattered radiation, resulted from the interactions of the extraterrestrial radiation with the Earth's atmosphere, and the direct or beam radiation (I) arriving on the ground directly in line from the solar disk. The sum of the direct and diffuse components is called global (or total) radiation (G). When combined, these quantities are often referred to the horizontal plane and are related according to the following:

$$G_{horizontal} = I_{normal} \times \cos(\theta_z) + D_{horizontal} \quad (1)$$

where $\theta_z$refers to the solar zenith angle which is used to convert the direct normal radiation to direct horizontal. The term ''global'' is associated to the fact that the solar radiation is received from the entire 2π solid angles of the sky. When solar radiation on a tilted (non-horizontal) surface is being analysed, an additional term describing the reflected radiation from the ground has to be considered. This additional term is the diffuse hemispherical radiation affected by a conversion coefficient taking into account the sky view factor. In the scope of the present thesis the focus lies on horizontal quantities only and, henceforth, when referring to global or diffuse radiation it is implied that it concerns to the horizontal plane.

The most common instrumentation used for solar radiometric measures consist of pyrheliometers and pyranometers. The former records direct beam radiation and have an angle field of view restricted to admit only beam radiation with some inadvertent circumsolar contribution from the Sun's aureole. Pyranometer measure the total hemispherical (global) horizontal radiation. They may be coupled with a shading device (to obstruct the sun disk and therefore the beam irradiation) in order to measure diffuse horizontal radiation. This though requires tracking the Sun with the blocking device throughout the day. A lower cost alternative is often used which consist of a fixed band or ring of opaque material placed to shadow the pyranometer throughout the day. Either way, the deployment and maintenance cost of these types of instruments are high and often,

solar radiation measurements include only records of global horizontal radiation. Nonetheless, direct and diffuse radiation characteristics are also important, in particular when concentrating solar energy systems are considered.

Since direct and diffuse radiation data are relatively uncommon, models for estimating these solar components from the more prevalent global radiation data are available. This topic is further developed in Section 1.4.

1.3 Solar radiation data simulated by atmospheric models

Historical solar radiation data have already been examined in several studies with focus on the investigation of trends (Gilgen et al., 1998) and possible causes for the global dimming/brightening of the solar radiation at the Earth's surface (Liang and Xia, 2005; Che et al.,2005; Liepert, 2002; Power, 2003; Ohmura, 2009; Stanhill, 1998; Stanhill and Ianetz, 1997; Romanou et al., 2007; Wild et al., 2005, Sanchez-Lorenzo et al., 2009 , Chiacchio et al., 2015). Solar radiation data obtained from atmospheric models have been used as a solar resource assessment tool (reviewed in Chapter 4) and to analyse future projections (reviewed in Chapter 5). A considerable number of studies have also employed numerical atmospheric models in the context of short-term forecasting (Lorenz et al.,2009 ; Rincón et al., 2010 ; Lara-Fanego et al., 2012 ; Perez et al., 2013 ; Ohtake et al., 2013 ; Pelland et al., 2013 ; Kosmopoulos et al., 2015). These studies have been emerging in recent years because since renewable solar energy is inherently variable, its integration on the grid presents a major challenge to grid operators and utilities (Kleissl, 2013).

In atmospheric models, global radiation is required for predictions of the model's energy budget and therefore direct normal radiation and diffuse components are not common outputs. Also, since often these models do not account for the atmospheric aerosols in the radiative transfer equation, global radiation is a more accurate radiometric value to be available to the user as is a much less sensitive variable to the aerosol optical properties than direct and diffuse radiations (Jimenez et al., 2015). Presently some efforts have already being made to overcome this issue. Jimenez et al. (2015) developed a model built on the WRF (Weather Research and Forecasting) modelling framework – WRF-Solar – with the aim to fulfil the needs of the solar energy industry focusing the forecast of solar radiation quantities including global, diffuse and direct radiation. This WRF extension has been validated for clear-sky conditions. Solar radiation simulations for partly cloudy and cloudy conditions are yet to be explored. The WRF-Solar adds the surface irradiance components to the model output when the existing shortwave parameterization in WRF calculates the direct and diffuse radiative transfer equations. When the shortwave scheme do not explicitly solves the direct and diffuse components but provides global radiation at the surface, the WRF-Solar estimates the direct and diffuse radiation using a regression model which takes into account not only the simulated global radiation but also the optical air mass and the clearness index (Jimenez et al., 2015).

Despite these recent advances made by WRF-Solar, most atmospheric models only provide global horizontal radiation. Also, one should underline that even in this specific model in situations where the shortwave parameterization does not calculate the direct and diffuse radiative transfer equations, there is the need to resort to models for partition of global radiation into its diffuse and direct components.

1.4 Models of diffuse solar fraction

As pointed out in Sections 1.2 and 1.3, the diffuse component of global solar radiation is not generally measured in meteorological stations and it is not provided in the majority of atmospheric models. Consequently, it is very useful to have a method to estimate the diffuse radiation on a horizontal surface based on the available data of global solar radiation (measured or simulated) on a surface. These models are often referred as to separation models (Gueymard and Ruiz-Arias, 2016). They aim to estimate the diffuse fraction (portion of diffuse component from global radiation) and then use the fundamental equation (Eq. 1) between global radiation and its components to also obtain the value of the direct radiation.

The range of diffuse solar radiation models differ mainly on the parameters used as input. The simplest, and most commons, are models which only use global radiation information (e.g. Liu & Jordan, 1960; Erbs et al., 1982). More sophisticated models may require meteorological parameters such as information from clouds, atmospheric turbidity, temperature or precipitable water content (e.g. Kasten, 1983; Hollands and Crha, 1987). Overall, most models rely on correlations with the clearness index (ratio of horizontal extraterrestrial radiation and horizontal global radiation measured at the Earth's surface) to estimate the diffuse fraction. These are expressed in terms of 1^{st} to 4^{th} degree polynomials, logistic or exponential models (Miguel et al., 2001; Jacovides et al., 2006). Models available in literature and some of their formulations are further reviewed in Chapter 7.

One important drawback of such models is that they are empirically derived from site-specific measurements and so, a model developed and validated in a specific climate type region may not hold its suitability for other regions.

Recently Gueymard and Ruiz-Arias (2016) undertook an unprecedented level of effort to gather and analyse the available separation models existing in literature until present date. The authors assessed the performance of 140 models using data from 54 stations which they clustered into four different climate zones of the world (tropical; temperate; arid and high-albedo). The object of their work was the validation and climate sensitivity analysis of direct normal radiation estimations obtained via the separation models. One major finding of the authors was that most separation models that were developed using hourly radiation data are not properly designed to operate correctly under high clearness index conditions: the errors of the models are exacerbated by cloud enhancement and high-albedo induced effects. Cloud enhancement is associated to situations when the clearness

index reaches high values, sometimes even over-unity values (Gueymard and Ruiz-Arias, 2016). This behaviour of the clearness index is attributed to cases in which global irradiance exceeds its theoretical clear sky value. It can occur due to reflection from the sides of clouds or in cases where a thin high-level cloud deck scatters at high intensity while permitting some beam radiation to still penetrate it (Engerer, 2015).

1.5 Aims and outline

The main objective of the current thesis is to assess the solar radiation resource provided by the combination of dynamical and statistical downscaling methods for present and future climate. With this it will be provided a quality solar resource map for the Iberian Peninsula and the Azores archipelago. Along the thesis, the statistical downscaling approach will only be represented by bias correction methods applied to the dynamical downscaled simulations.

As already mentioned, the work focuses primarily in the Iberian Peninsula as its large climate gradients are representative of diverse meteorological conditions, enabling therefore the adaptation of the presented methods to other regions. Besides, the Iberian Peninsula has been identified as one of the most responsive regions to global climate change (Giorgi, 2006). Afterwards, the same methodology is used to assess the solar resource of the Azores archipelago. The Azores region has been often neglected in solar resource assessments and solar resource maps of the world or even for the European region.

In this thesis the atmospheric model used for simulation of high-resolution global solar radiation data is WRF. The WRF is a state-of-the-art, mesoscale numerical weather prediction system designed to function for both operational forecasting and atmospheric research. It gathers many different choices for physical parametrizations including microphysics, cumulus parameterization, planetary boundary layer, land surface models, longwave and shortwave radiation (Skamarock et al., 2008). The WRF extension WRF-Solar is not considered in the present thesis because, as already mentioned in Section 1.3 it has been validated for only clear-sky conditions and its performance for partly cloudy and cloudy conditions is yet to be explored.

Given that the combination of bias correction with the simulated solar radiation data provided by WRF will overcome the limitations found in observations regarding the temporal and spatial consistency of data availability, one additional topic should be addressed: the fact that its output consists of global radiation only. Thus, it requires the implementation of separation of global radiation into its diffuse and direct components, which in this work is performed by developing a model of diffuse solar radiation fraction. This latter issue is only discussed for the Azores archipelago since diffuse solar radiation fraction models for the Iberian Peninsula have already been thoroughly considered in the literature (Reindl et al., 1990; Miguel et al., 2001; Boland et al., 2008; Ridley et al., 2010;

Ruiz-Arias et al., 2010). The Azores region, on the other hand, has not been object of this type of analysis before. Furthermore, mid latitude islands are not abundant and the typical Atlantic climate of Azores Islands is not very common in other regions.

The aims of the thesis are addressed and presented following the structure below:

- The solar radiation simulated by the WRF model for Iberian Peninsula present climate is evaluated through comparison with measured values of global radiation gathered across the region. The WRF output is then combined with bias correction methods and a solar resource map is presented (Chapter 4).
- The future projections of solar radiation for the end of the 21st century in Iberia Peninsula are analysed. The simulated WRF values are also subjected to bias correction and a solar resource map is obtained, but in this case for future climate (Chapter 5).
- Following the methodologies used in the analysis of the WRF solar radiation values for Iberian Peninsula, the same process is used to assess the solar resource of the Azores archipelago. The simulated values for present climate and future projections for the mid and end of the 21st century are addressed (Chapter 6).
- Focusing on the Azores archipelago, the separation of global radiation into its diffuse and direct components is analysed using models of diffuse solar fraction. Several models available in literature are tested using high-quality measured data of global and diffuse radiation. The model with best performance is then adapted to further minimize the errors on the simulation of the diffuse fraction (Chapter 7).

For the better organization of the thesis, the data sets used in the thesis are detailed in Chapter 2 and a description of the methodology fundamentals are presented in Chapter 3. Finally, the main conclusions and future work are collected in Chapter 8.

Henceforth, throughout the thesis, “solar radiation” and “solar resource” should be interpreted as referring to global solar radiation. The term “radiation” and “irradiance” are used as referring to the same quantity which is the power per unit area (W/m^2) received from the Sun in a given horizontal surface.

1.6 Publications

This thesis is sustained by three original publications on international peer-review journals which are, at the time the thesis was printed, published or under review:

- Magarreiro C., Widmann M., Soares P.M.M., Cardoso R. and Brito M.C. (2016) Solar energy resource from bias-corrected regional climate simulations: an Iberian irradiance assessment. Submitted to *Energy*. (Chapter 4)

- Magarreiro C., Cardoso R., Widmann M., Brito M.C. and Soares P.M.M (2016) Combining high resolution dynamical downscaling and quantile mapping for future projections of the Iberian Solar Resource. Under review in *International Journal of Climatology*. (Chapter 5)

- Magarreiro C., Brito M.C. and Soares P.M.M. (2014) Assessment of diffuse radiation models for cloudy atmospheric conditions in the Azores region, *Solar Energy*, 108, 538-547. (Chapter 7)

A collaboration made during the development of the PhD led to an additional co-authored publication which is not included in the thesis and which is also under review at the time the thesis was printed:

- Perdigão J., Salgado R., Magarreiro C., Soares P.M.M., Costa M.J. and Dasari H. (2016) An Iberian Climatology of solar radiation obtained from WRF regional climate simulations for 1950-2010 period. Under review in *Solar Energy*.

Finally, the main results from Chapter 7 are also part of a Conference Proceedings:

- Magarreiro C., Brito M., Soares P.M.M., Azevedo E., (2014) Assessment of diffuse radiation models in Azores, Geophysical Research Abstracts, 16, EGU2014-5748, EGU General Assembly 2014, Vienna, Austria, 27 April – 02 May 2014.

Note: Parts of the text included in Chapters 1, 2 and 3 are taken from the three publications in which this thesis is sustained and that are listed above. For coherence and to avoid replication of information, the correspondent sections of the chapters 4, 5 and 7 which relate to the chapters mentioned above were updated to a shorter version. For a complete version of the published papers, the reader may want to consult the papers themselves.

1. Introduction

Chapter 2

Description of the data sets used

2.1 Ground based observations and study regions

As in any evaluation experiment, high quality observational data sets are essential to avoid misleading conclusions.

Iberian Peninsula

The geomorphological complexity and the climate gradients influenced by the Atlantic Ocean and Mediterranean Sea characterize the large weather variability of Iberian Peninsula. The highlands of the northwest are among the wettest regions in Europe and a significant North-South precipitation gradient is present in Iberia (Cardoso et al., 2013). Also, like in other Mediterranean regions, Iberia climate is characterized by large interannual variability (Soares et al., 2012b). The Köppen climate classification (Peel et al., 2007), divides the Iberian climate into temperate climate without dry season and mild/warm summers in the north and the Iberian cordillera; temperate climate with hot and dry summers in the center, south and southwest region; steppe climate in the Ebro valley and southeastern region and continental climate without dry season and mild summers in the Pyrenees.

For the assessment of the Iberian Peninsula solar resource in Chapters 4 and 5, local observations of global solar radiation gathered at 64 meteorological stations over Iberia were used. For Portugal, data was provided by IPMA (Portuguese Weather Service, 16 stations) while for Spain, by AEMET (Spanish Weather Service, 48 stations). The pyranometers used to obtain data in the Portuguese stations were Kipp and Zonen models CM11 (Kipp & Zonen, 2000) and CMP11 (Kipp & Zonen, 2015) and in the Spanish stations Kipp and Zonen models CM11 and CM21 (Kipp & Zonen, 2000). The time period of the

observations varies amongst stations. Data from Portuguese stations cover the period from January 2000 – December 2011 and data from Spanish stations cover the period January 2000 – December 2010. The datasets used are daily mean values of global solar radiation (W/m2). From AEMET, the data featured daily mean records of solar radiation values while from IPMA, data was provided on hourly records. In this case daily means were determined only for days where no missing hourly value was existent between the sunrise and sunset hour. The data sets present different amounts of missing values among the stations but, given the nature of the meteorological variable here analysed (highly influenced by clouds presence/absence), no interpolation technique was considered to fill the missing data as that could lead to misleading conclusions. It is a fact that measures of global solar radiation at a specific site continuously and accurately over the long term (measured by pyranometers) are far from being abundant and so all available measures were included in this study (even in the locations where data was available for only 2 years). The locations of the local measurements stations with respective number of valid daily values (from 686 to 4366) are shown in Figure 2.1 in Section 2.3.

Azores

The Azores archipelago is constituted by 9 islands which are clustered in 3 groups: the western group with the islands Flores and Corvo; the central group with the islands Graciosa, Terceira, São Jorge, Faial and Pico and the eastern group with the islands São Miguel and Santa Maria. The Azores has a mild climate highly conditioned by the Atlantic Ocean in terms of temperature and it is frequently under the influence of low pressure systems linked to weather fronts with high humidity content which cross the ocean. The climate is classified as humid subtropical, rainy between September and March due to the presence of low pressure systems from the polar front and less rainy on the remaining months as a result of the Azores High. The Azores climate is also shaped by the topography of each island and the mutual influence among the closest islands as is the case of Pico, São Jorge and Faial (Tomé, 2013).

The global solar radiation measurements datasets available and used in the assessment of the Azores solar resource for present and future climate presented in Chapter 6 are multi-year daily mean data for the islands Faial; Terceira; Graciosa; Pico; Flores; Corvo; Sta Maria and two locations in São Miguel, Ponta Delgada and Nordeste (Fig. 2.2b). The multi-year daily mean data is available at the Green Islands Project website (Green Islands Azores Project, 2015) and was constructed from measurements made by the Azores delegation of the Portuguese Weather Service (IPMA) with pyranometers Kipp & Zonen CM11(Kipp & Zonen, 2000) during the period 1999-2009. An average daily value was determined for each day of the year according to the available measurements at the correspondent site. The measurements used cover different parts of 1999-2009 time period among the locations analysed.

In Chapter 7, the applicability of a set of models for prediction of hourly diffuse fraction from global radiation is tested for the Azores region. In this specific study the analysis was performed with global and diffuse solar radiation data from Graciosa Island available from the Atmospheric Radiation Measurements (ARM) Climate Research Facility, and collected in the field campaign - Clouds, Aerosol and Precipitation in the Marine Boundary Layer (CAP-MBL). The ARM Mobile Facility was deployed from May 2009 to December 2010 and included, among others, measurements of broadband shortwave downwelling irradiances (global, diffuse and direct). The ARM instrument SKYRAD used consisted of: Black&White Pyranometer, Model 8-48; Normal Incidence Pyrheliometer, Model NIP; Precision Spectral Pyranometer, Model PSP, all manufactured by Eppley Laboratories, Inc. The tracker is the Kipp and Zonen Model 2AP.

The data available in ARM includes a quality assessment for radiation measurements which uses climatological analysis of the surface radiation to define reasonable limits for testing the data for unusual data values (Long and Shi, 2006). The correction is applied not only to diffuse but also to global radiation measurements. The irradiance variables are available with a time step of 60 seconds, but were aggregated to hourly mean values. The location of the ARM station matches the location of the Graciosa Island multi-year daily mean data described above.

2.2 Cloud fractional cover

Satellite observations of cloud fractional coverage is used to assess the skill of the WRF – ERA-Interim simulation in the process of representing cloudy condition, in particular in the Iberian region (Chapter 4).

Iberian Peninsula

Cloud fractional coverage (percentage of cloud presence in the sky) is obtained from the CM SAF cloud property data set using SEVIRI (CLAAS) derived from the EUMETSAT Satellite Application Facility on Climate Monitoring (Stengel et al., 2014). This pixel-based CLAAS dataset has approximately 4km spatial (0.05° x 0.05° latitude-longitude grid) resolution for daily averages spanning from 2004 to 2011. The cloud detection obtained in this product is presented as cloud fractional coverage defined as the fraction of cloudy pixels per grid square compared to the total number of analysed pixels in the grid square. The detailed definition of the cloud fractional coverage product is presented by Kniffka et al. (2013) and Stengel et al. (2014). Since the simulated cloud fraction is provided for every model level and the satellite data is simply a 2D representation of a 3D field, the approach proposed by Sundqvist et al. (1989) and Morcrette et al. (2000) is followed to derive the

WRF values. This method uses a random-maximum overlapping approach which takes into account cloud tilting and vertical overlapping of cloud layers.

Azores

In Azores the WRF – ERA-Interim cloud fractional coverage simulated values were not addressed in the present study. However cloud information is used to assess the impact of the existent cloud cover on the statistical performance of the diffuse fraction models covered in Chapter 7. Due to the detailed ARM campaign it was possible to obtain observational cloud cover data from the same location of the solar radiation measurements. The data was retrieved by a Total Sky Imager (TSI) which captures images of the sky during daylight hours. The raw sky images are then processed to infer fractional sky cover. Each pixel of the image is analysed to account for thin or thick (opaque) clouds. The sum of thin and opaque represents the total cloud cover.

2.3 WRF climate simulations

The WRF is a state-of-the-art, mesoscale numerical weather prediction system designed to work for both operational forecasting and atmospheric research. It gathers many different choices for physical parametrizations including microphysics, cumulus parameterization, planetary boundary layer, land surface models, longwave and shortwave radiation (Skamarock et al., 2008).

The physical parameterizations chosen for the simulations of both Iberian Peninsula and Azores archipelago include the microphysics WSM6 class single-moment (MP6) scheme by Hong and Lim (2006), the planetary boundary layer scheme of Mellor-Yamada-Janjić (Janjić 2001) and the Betts-Miller-Janjić cumulus scheme (Betts 1986; Betts and Miller 1986; Janjić 1990, 1994, 2000). The simulations use the Unified Noah Land-Surface-Model (Chen and Dudhia 2001). The shortwave and longwave radiation schemes rely on the NCAR Community Atmospheric Model (CAM 3.0, Collins et al. 2004).

WRF was setup with two nested grids for both regions. Nudging was applied to the outermost regional model domain using the forcing fields. Nudging relaxes the regional model simulations towards the driving global climate model simulations, preventing possible drift of regional model solution from that of the driving global model over a long term. The inner nested domains are not nudged because it allows the mesoscale model to freely develop fine-scale features and generate its internal variability (Zhang et al., 2009).

The model simulations were preformed to characterize the present and future climate conditions. For present climate the WRF model was driven at the lateral boundaries by the ERA-Interim reanalysis (Dee et al., 2011). For the future climate, the simulations comprise a historical period which represents the free-running simulations for present climate and the

future projections. This latter simulations were both forced by the EC-EARTH global model (Hazeleger et al., 2010) and in agreement with the Representative Concentration Pathways (RCP)8.5 (Riahi et al., 2011).

The RCPs form a set of greenhouse gas concentration and emissions pathways designed to support research on impacts and potential policy responses to climate change (Moss et al. 2010). Compared to the total set of RCPs, RCP8.5 corresponds to the pathway with the highest greenhouse gas emissions. For RCP8.5 no specific climate mitigation target is included until the end of the 21st century (Riahi et al., 2011).

The studies of Soares et al. (2012b) and Cardoso et al. (2013) include a detailed setup of the WRF simulation used in this thesis and present a thorough analysis and evaluation of precipitation and temperature revealing the high quality results achieved for Iberian Peninsula. Considering the same region, the quality of the WRF simulation forced by ERA-Interim is also documented for others meteorological variables besides precipitation and temperature such as cloud cover and wind (Rios-Entenza et al. 2014, Soares et al. 2014, Martins et al. 2016). In the context of renewable energy, Campaniço et al. (2016) also used this simulation to characterize the climate cooling potential for buildings in Iberia.

Iberia Peninsula

The WRF simulation used for the Iberian Peninsula analysis has 9km horizontal grid spacing and has been produced by nesting the 9km domain in a parent grid with 27 km resolution (Fig. 2.1a) having both grids being centred in Iberia. The present climate synchronized simulation covers the period 1989-2012. For climate change assessment, the historical reference baseline model simulation covers from 1970 to 2000, and the future scenario simulation ranges from 2070-2100.

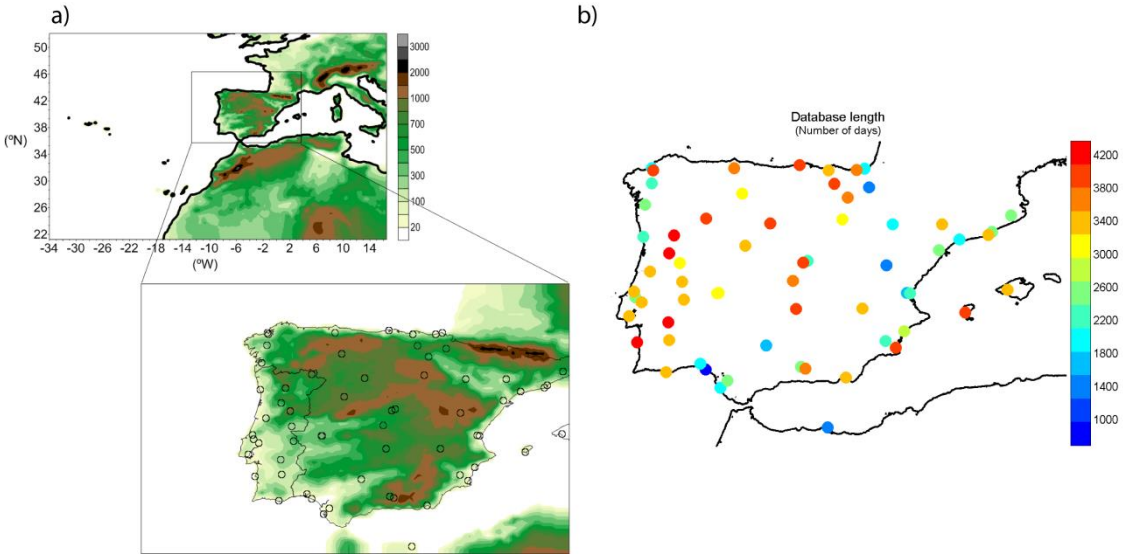

Figure 2.1 (a) WRF model outermost (full, dx = 27 km), and inner (zoomed area, dx = 9 km) domains with corresponding WRF topography and (b) location of ground measurement stations with corresponding number of valid days used in this study.

Azores

For Azores the WRF simulation considers a 6km horizontal grid spacing nested into a coarser grid of 24 km (Fig. 2.2a). The 24 km outer domain is centred on the central group of the Azores archipelago. To minimize the computational costs, and considering the extent of the Azores archipelago, 3 different 6km inner domains corresponding to the different archipelago groups (western, central and eastern) were considered. For the Azores, the reanalysis driven present climate synchronized simulation covers the period 1989-2010. The historical reference baseline simulation covers 1989-2010. The future projection simulations cover the 2040-2059 period for representation of the 21st mid-century and the 2080-2099 period for representation of the end of the century.

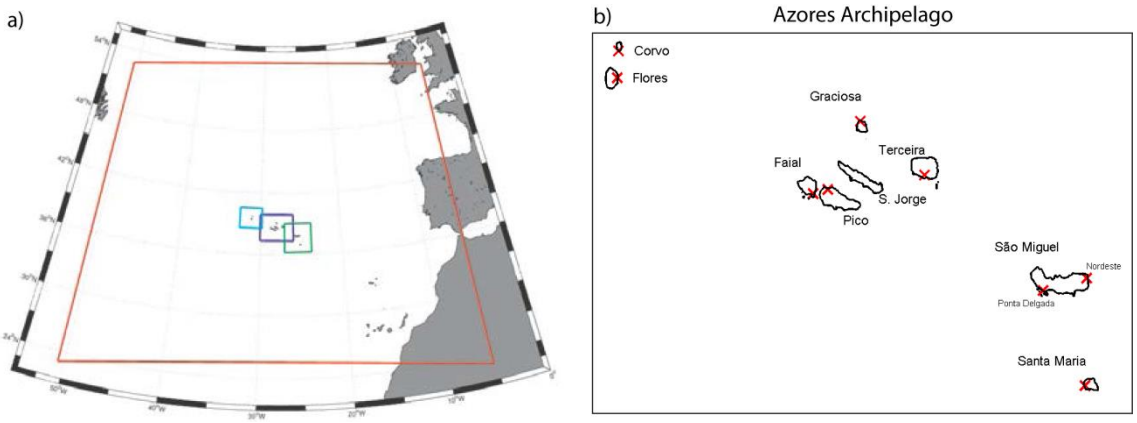

Figure 2.2 (a) WRF model outermost (dx = 24 km, orange), and inner (dx = 6 km) domains (cyan: western group; purple: central group; green: eastern group) and (b) location of the ground measurements stations used in the present study (red crosses).

Chapter 3

Methodology fundamentals

3.1 Standard statistical errors

The quality of the simulated data is assessed by means of standard statistical errors. Throughout the thesis the following scores are used: MAE (Mean Absolute Error), RMSE (Root Mean Square Error), BIAS and probability density functions (PDF) matching scores. For all these error scores absolute values as well as relative errors (as percentages) are computed. Relative errors are obtained by dividing the absolute values through the mean observations of the correspondent observations. The statistical errors are named equal for both absolute and relative magnitudes but are always followed by the respective units which differentiates them. In the particular case of the MAE its relative magnitudes are hereafter referred as MAPE (Mean Absolute Percentage Error). Normalized standard deviation, the ratio between of simulated and observed solar radiation standard deviations, (σ_n) and correlation coefficient (r) are also determined. The error measures are defined as follows:

$$MAE = \frac{1}{N}\sum_{i=1}^{N}|M_i - O_i| \tag{2}$$

$$RMSE = \left[\frac{1}{N}\sum_{i=1}^{N}(M_i - O_i)^2\right]^{0.5} \tag{3}$$

$$BIAS = \frac{1}{N}\sum_{i=1}^{N}(M_i - O_i) \tag{4}$$

$$r = \frac{\sum_{i=1}^{N}(O_i - \bar{O}) * (M_i - \bar{M})}{\left[\sum_{i=1}^{N}(O_i - \bar{O})^2 * \sum_{i=1}^{N}(M_i - \bar{M})^2\right]^{0.5}} \tag{5}$$

$$\sigma_n = \sigma_M / \sigma_O \quad (6)$$

where N is the number of data, M_i is the i^{th} estimated value, O_i is the i^{th} observed value and $\bar{M}$ and $\bar{O}$ the corresponding estimated and observed mean values. MAE and RMSE reflect the time synchronized record matching ability of the model's estimates, with RMSE giving higher weight to large deviations to observations. Moreover, it is also important to assess if the model predicted values describe the measured solar radiation distributions, i.e. to evaluate the PDFs, and quantify how observational and model PDFs match. If the simulated variables values can represent an entire distribution of the corresponding observation, it ensures the existence of an inherent capability to simulate the full range of values and not only their mean. Thus, to measure the agreement of simulated and observed PDF the skill score (S) proposed by Perkins et al. (2007) was computed according to:

$$S = \sum_1^N minimum(Z_p, Z_m) \quad (7)$$

where N is the number of bins used to calculate the PDF for a given region, Z_p is the relative frequency of values in a given bin from the model and Z_m is the frequency of values in a given bin from the measured data. If the model PDF is identical to the observed PDF, the skill score (S) will equal 1 (or, in percentage, 100).

3.2 Statistical downscaling

To minimize the errors and improve the results of the numerical models used in climate assessments, statistical downscaling may be used to account for obtaining subgrid-scale information from coarser resolution fields, derive variables not directly provided by the numerical models but related to available variables or to reduce systematic errors. The statistical downscaling concept is based on the determination of links between large-scale atmospheric variables (predictors) and local or regional variables (predictands) (Maraun et al., 2010).

The concept of statistical downscaling is generally associated to the notion that it is one of the possible options to generate regional climate information as it is dynamical downscaling. Indeed, they are the two main approaches used for generating information below the grid scale of an Atmosphere- Ocean General Circulation Model (GCM) which given its complexity present horizontal resolution that ranges from 400 to 125 km (Christensen et al., 2007). However, both approaches can also be combined. It should be noted that the use of dynamic downscaling does not eliminate the need for statistical downscaling and bias correction because bias inherited from both the GCM simulation that drives the regional climate model at the outer boundary combined with bias generated by the RCMs models themselves can be substantial (Wood et al. 2004).

Statistical downscaling methods cover regression-type models including both linear and nonlinear relationships, unconditional or conditional weather generators for generating synthetic sequences of local variables, techniques based on weather classification that draw on the more skilful attributes of models to simulate circulation patterns, and analogue methods that seek equivalent weather states from the historical record (Wilby et al., 2004). Depending on the variables considered as predictors, two different classifications/ approaches are differentiated in statistical downscaling: perfect prognosis (or perfect prog) and model output statistics (MOS) (Wilks, 2006). In perfect prog statistical relationships are found between observations of the desired predictand(s) and observations of the predictor variables which are then applied to model output. The perfect prog technique does not correct for possible errors or biases of the numerical models because it assumes that the model variables are as perfect as observations (Wilks, 2006). On the other hand, the MOS approach can account for systematic model errors since it uses statistical relationships obtained between observed predictands and predictors from the numerical models. MOS versatility derives from its ability to be used as a downscaling method or as a bias correction method. When applied to observations on the same spatial scale as the model output MOS is a pure correction, while it includes an additional downscaling component when applied to observations on smaller scales (Maraun et al., 2010).

Both perfect prog and MOS can further be classified into event or distributional-wise techniques. For event-wise one refers to day to day correspondence of predictors and predictands and for distributional-wise the focus is the different aspects of the probability distribution functions (PDFs) (Casanueva, 2016).

The present thesis focuses on the use of statistical downscaling as a bias correction approach combined with high resolution dynamical downscaling (which is represented through the use of WRF model as a regional climate modelling). Considering its nature, this approach is designated in literature as solely bias correction methods. These methods are assumed to be stationary, i.e., the correction algorithm and its parameterization for current climate conditions are also valid for future conditions (Teutschbein and Seibert, 2012) however some studies have already been developed in order to overcome this issue (Li et al, 2010; Amengual et al., 2012). The methods used in the thesis are related to only MOS, more specifically bias correction ones. The following section describes then the basics of the MOS methods used in this thesis.

3.3 Model Output Statistics

The predictors for the MOS method can in principle be any simulated variables that are related to the predictand. In the present work, for simplicity, the homogeneous approach is considered, i.e. the predictor for the MOS method will be solely the WRF simulated solar radiation. As mentioned in the section above, the MOS approach can be applied by means

of event-wise and distributional methods. For an event-wise method a pairwise time series is needed and so it can only be considered to reanalysis driven RCMs (Eden et al., 2014).

The range of methods used as bias correction can go from simple factor scaling to multi-variable bias correction for particular combinations of variables (Casanueva, 2016). Teutschbein and Seibert (2012) present an extensive review and evaluation of bias correction methods used in combination with RCMs. The authors explore linear scaling, local intensity scaling, power transformation, variance scaling and distribution transfer and transformation.

For the purposes of the present thesis two MOS approach are considered. For reanalysis-driven WRF simulations (Chapter 4 and Section 6.3) a pairwise setup is possible. Having this in mind the first MOS approach tested is regression. Through careful visual inspections of individual scatter plots of daily mean solar radiation observations versus simulated WRF values for all the meteorological stations, a linear regression was considered to be an appropriate choice. So, the relation between the measured solar global radiation values (x_{obs}) and the corresponding WRF simulated values (x_{mod}) for each location are modelled as

$$x_{obs} = \beta + \alpha\, x_{mod} + \epsilon \tag{8}$$

The regression parameters (β and α) are then applied to the simulated output to obtain the corrected values. It is used a deterministic approach, i.e. the noise term (ϵ) is not added for the correction.

The second approach followed is a non-parametric QM (which will be compared with the linear regression in the reanalysis-driven WRF simulations analysis). This method corrects errors in the shape of the statistical distribution (Themßl et al., 2011): for a given variable, the cumulative density function (CDF) of a simulation is matched with the CDF of the observations generating a correction function depending on the quantile. The correction function is used to obtain the corrected estimate of the simulated variable quantile by quantile and for the simulated WRF solar radiation ($x_{mod_{corr}}$) it is calculated as

$$x_{mod_{corr}} = {F_{obs}}^{-1}(F_{mod}(x_{mod})) \tag{9}$$

where *F* and F^{-1} denote the empirical CDF and its inverse of the observations (obs) or model data (mod) and x_{mod} the raw output of the model. The schematic diagram of Figure 3.1 exemplifies the method. The value of the RCM-simulated data is searched on the empirical CDF of the RCM simulations together with its corresponding cumulative probability. Thereafter, the value of observed data of that same cumulative probability is located on the empirical CDF of observations. Finally, this value is used as the corrected value for the RCM. In this thesis the 99 percentiles are corrected and linear interpolation is used for the values between two percentiles (Déqué, 2007). Constant extrapolation is applied for values outside the calibration range, i.e. the correction function of the last percentile is applied to all the values above it. The QM approach has often been used in climate assessments concerning

precipitation and temperature (Themeßl et al., 2011; Ines and Hansen, 2006; Boé et al; 2007; Teutschbein and Seibert, 2012; Piani et al., 2010, Wilcke et al., 2013) but not for solar radiation, to the best knowledge of the author.

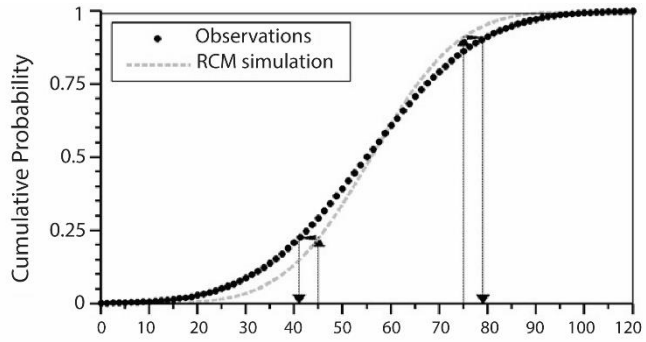

Figure 3.1 Schematic representation of the QM method. Solid black dots shows observations CDF and dashed line shows model simulation CDF. Illustration from Teutschbein and Seibert (2012).

Variables such as precipitation and temperature allow the use of a parametric approach of QM (Teutschbein and Seibert, 2012; Piani et al., 2010; Ines and Hansen, 2006) where theoretical CDFs are estimated for both the observed and estimated data. However such approach may become problematic for variables that do not fit to theoretical distribution functions (Themeßl et al., 2011).

3.4 Validation framework of the MOS

The standard skill estimates based on residual sums of squares are often optimistically biased. This is a consequence of the fitting process which, by definition, chooses parameters that adapt the model to the data as closely as possible and is known as artificial skill (von Storch et al., 2001 and Wilks, 2006). In order to avoid this artificial skill statistical models have to be validated on data that have not been used for calibration. Essentially, what is desired is a measure of how the statistical models will perform when used on data not involved in the fitting. Cross validation is an especially appropriate tool for this purpose: the data is divided into learning and validation data sets (corresponding 'validation' to the data points which are left out) and the model is fitted to the learning data and tested on the validation subset (Von Storch et al., 2001). The number of points left out can range from one to more than half of the available dataset (Barnston and van den Dool, 1993).

The holdout method (or splitting method) is one of the frequently known and simplest cross-validation alternatives. It involves splitting the data into two different sets: the training set and the testing set. The function is fitted using the training set only. Then the fitted function is asked to predict the output values for the data in the testing set (it has never seen these output values before). The errors it makes are accumulated for both splits to give the absolute test error of the model. Its evaluation however can have a high variance because it depends heavily on which data points end up in the training set and which end up

in the test set, and thus the evaluation may be significantly different depending on how the division is made (Casanueva, 2016). The leave-one-out method is also well known for this subject. In this approach the fitting procedure is repeated *n* times, each time with a sample of size *n*−1, because one of the predictands and its corresponding predictor set are left out (Wilks, 2006). This technique is however very expensive to compute. The cross-validation method most widely used for model evaluation standard procedures is the k-fold cross-validation (Gutiérrez et al, 2013) where the data set is divided into k subsets, and the holdout method is repeated k times. It attempts to produce a more rigorous validation through the use of multiple calibration/validation period combinations within reasonable computational time.

In the present thesis, following Maraun et al. (2015), a five-fold cross validation is applied. The data set is separated into 5 subsets and a function is fitted using the training set only. Then that function is used to predict the data in the testing set and the method is repeated 5 times. Each time, one of the 5 subsets is used as the test set and the other 4 subsets are put together to form a training set. Given the observations data sets characteristics (Section 2.1), each individual data set had a different training period. As example, if a given observational data set has valid values from, let's say, 2003 to 2008, the last 6 years of the historical simulation (2007-2012, if for instance the historical simulation comprises the period 1989-2012) are used. Simulated data values which correspond to missing data on the observations are then removed.

Chapter 4

Iberian Peninsula solar energy resource from bias-corrected regional climate simulation: a present climate assessment

The proper characterization of solar radiation resource is essential for the design of all solar energy harnessing systems. The power generation from photovoltaic systems, in particular, is often forecasted by means of atmospheric models. Besides its utility for forecasting, they enable a more accurate resource characterization by providing long periods of solar radiation estimates with extensive spatial coverage.

In this chapter, the Weather Research and Forecasting model (WRF) is used in combination with statistical bias correction to simulate global solar radiation for the Iberian Peninsula. Daily observations of irradiance are used to assess the quality of the simulation and fit the bias correction methods. Simulated cloud cover is also analysed, anticipating that deviations from the observations may be consistent with those obtained for the solar radiation data. A satellite derived dataset is used to perform this analysis.

Two bias correction methods, a linear regression and a quantile mapping, are compared. The model with best performance is used to derive the Iberian Peninsula solar resource maps for the present climate.

The results of this Chapter were submitted to *Energy* in August 2016 and were under review when the thesis was printed.

4.1 Background

A considerable number of studies have employed numerical atmospheric models in the context of energy resource research, with emphasis on short-term forecasting (Lorenz et al.,2009 ; Rincón et al., 2010 ; Lara-Fanego et al., 2012 ; Perez et al., 2013 ; Ohtake et al., 2013 ; Pelland et al., 2013 ; Kosmopoulos et al., 2015) and future projections (Crook et al., 2011 ; Gaetani et al., 2014 ; Panagea et al., 2014 ; Wild et al., 2015). Some studies have also investigated recent trends in surface solar irradiance (Romanou et al., 2007) focussing mainly on the dimming/brightening phenomenon (Sanchez-Lorenzo et al., 2009, Chiacchio et al., 2015).

Solar radiation data obtained from atmospheric models have also been used as a solar resource assessment tool. Santos-Alamillos et al. (2012) analysed solar radiation and wind simulated by the WRF model (Weather Research and Forecast, Skamarock et al., 2008) for 2007 with a 9km resolution to assess the spatiotemporal balancing between solar and wind energy resources over the Southern Iberian Peninsula region. The balancing effect refers to conditions where strong solar energy compensates weak wind energy and vice versa, and is relevant to find optimal distribution of wind farms and solar energy plants that minimize the variability of total energy input into the power supply system. Jerez et al. (2013b) explored the same topic but for the entire Iberian Peninsula using data from a 10km resolution simulation with the MM5 model (Grell et al., 1994), which corresponds to an older model core of WRF.

Recently, Alexandri et al. (2015) assessed the ability of the RegCM4 (Giorgi et al., 2012) RCM with 50km resolution to simulate surface solar radiation patterns over Europe evaluating model output from 2000-2009 against satellite observations on a monthly basis. The main result found was a low negative bias over land and a low positive bias over ocean although considering the entire model domain the overall bias was determined to be +1.5% and +3.3%, respectively, for the two complementary datasets which constitute the satellite observations (2000-2005 and 2006-2009). Besides analysing solar radiation the authors explored the relative contribution of other meteorological variables that determine the transmission of solar radiation through the atmosphere such as cloud fractional coverage, cloud optical thickness, aerosol optical depth, single-scattering albedo, among others.

Katragkou et al. (2015) evaluated six WRF simulations over Europe with different physical configurations and evaluated their performances in simulating a set of meteorological variables, including shortwave downward radiation at the surface and total cloud cover. For solar global radiation the set of simulations was compared to satellite observations from the International Satellite Cloud Climatology Project (ISCCP, Rossow and Dueñas, 2004) with spatial resolution of 280km and using seasonal averages (summer and winter) for the time period 1990–2008. The results showed that, for winter, all six simulations overestimated solar radiation throughout the domain particularly in the North and Central region of Europe. For summer four of the six simulations overestimated the solar radiation in the entire domain but particularly over land and in Central Europe (bias of

around 40-60%). The remaining two simulations overestimated it along the Southern and South-eastern Europe and underestimated in the North and Central parts. From these two simulations the authors suggest that the underestimation of downward radiation at the surface could be linked to a 40–50% overestimation of cloudiness. A similar study by García-Díez et al. (2015) used a multi-variable analysis of a set of WRF simulation to improve the understanding of the physical realism of the model and to identify sources of error compensation. Regarding global solar radiation and cloud fraction the authors analysed their biases in the summer season and found that they are correlated. The majority of the simulations indicated, for that season, an overestimation of solar radiation in agreement with an underestimation of cloud cover.

As discussed in Chapter 3 simulations with RCMs have errors due to bias in the large-scale atmospheric conditions that drive the RCM as well as due to the RCM model itself. The MOS approach is particularly suited for solar radiation forecasting as the correction of simulated grid-scale radiation can be expected to give better results than using large-scale meteorological field as in a Perfect Prog approach. Several studies have incorporated some type of statistical post-processing to solar radiation forecasts output from numerical models. Polynomial regressions (Lorenz et al., 2009 ; Mathiesen and Kleissl, 2011) and Kalman filter (Rincón et al., 2011; Pelland et al., 2013; Diagne et al., 2014) are common approaches in this field.

As shown, atmospheric models are becoming a popular approach on the field of solar radiation forecasting and resource assessment. The quality evaluation of the solar radiation representation by such models is then a crucial step to understand its usefulness. As already mentioned, errors in the solar radiation output from any numerical model may have a variety of sources, although, it is known that cloud related parameterization schemes are one of the main sources of bias in such models (Otkin et al., 2008; Kleissl, 2013, García-Díez et al., 2015) and that they are often prone to underestimation of cloud fields (Zhang et al., 2015).

The objective of this chapter is to benchmark WRF as a tool to provide consistent temporal and spatial high resolution solar radiation maps and to validate its performance. It is further investigated to what extent the results can be enhanced by applying MOS methods. Since in this simulation setup the simulated and observed meteorological situations are in sync, quantile mapping (QM) and linear regression are used and compared. It is used the WRF model, a meteorological highly customizable mesoscale RCM with sophisticated physical parameterizations. In recent years, WRF has become increasingly popular in the field of solar radiation forecasting and has been employed in a number of studies (Rincón et al., 2011; Ruiz-Arias et al., 2012; Perez et al., 2013; Diagne et al., 2014; Mathiesen et al., 2014). It is also analysed simulated cloud cover anticipating that deviations from the observations may be consistent with those obtained for the solar radiation data. In the present study a satellite derived dataset is used to perform this analysis. Despite its limited accuracy, cloud data obtained from satellite is valuable for evaluation of simulated cloud fields especially when observations with sufficient temporal and spatial resolution are

scarce (Otkin et al., 2008). To obtain a solar resource map for the entire Iberian Peninsula the station-wise corrections obtained from the observations data are interpolated and combined with the simulated PDF of each gridpoint domain for the full simulation period. This approach yields spatially complete fields that include the local details simulated by the RCM and that are based on a longer reference period than the solar radiation observations.
In Section 4.2 the data and methods used in this study are presented: the WRF model data, the observational dataset (solar radiation measurements and satellite-derived dataset cloud fractional coverage), MOS methodologies applied to the WRF solar radiation output, the comparison method and error statistics for the assessment of the solar radiation and cloud fractional coverage WRF simulations. The results and discussion of the performed analysis as well as a characterization of the spatial and temporal distribution of solar radiation in Iberian Peninsula are presented in Section 4.3. In Section 4.4 a solar resource map for Iberian Peninsula is given and finally, conclusions of the study are drawn in Section 4.5.

4.2 Data and methods

WRF simulation

The Iberian Peninsula WRF simulation used in this chapter has been driven at the lateral boundaries by the ERA-Interim reanalysis (Dee et al., 2011) and refers to a 9km horizontal resolution for the period 1989-2012 (Section 2.2).

Observations

The WRF solar radiation simulation is evaluated with measures of global solar radiation from 64 meteorological stations across the Iberian Peninsula. Data was provided by both the Portuguese (IPMA) and Spanish (AEMET) Weather Services. Data from Portuguese stations cover the period from January 2000 – December 2011 and data from Spanish stations the period January 2000 – December 2010 (see Section 2.1). The time range of the observations varies amongst stations (Fig. 2.1b).

The misrepresentation of cloudy conditions in numerical models is often suggested as a source of inaccuracy in the simulated solar radiation (Kleissl, 2013). To address this issue and assess its impact on the simulated radiation, the WRF simulated cloud fractional coverage is compared to satellite observations. These were obtained from the CM SAF cloud property data set (Stengel et al., 2014) derived from the EUMETSAT Satellite Application Facility on Climate Monitoring and consist of daily averages spanning from 2004 to 2011 (Section 2.3).

Model Output Statistics

Since reanalysis-driven WRF simulations are used to provide the predictor a pairwise setup is possible. Having this in mind the first MOS approach to consider is linear regression. The regression parameters are applied to the simulated output to obtain the corrected values. It is used a deterministic approach, i.e. the noise term (ϵ) is not added for the correction. The second approach followed is a non-parametric QM, which will be compared with the linear regression. This method corrects errors in the statistical distribution (Section 3.3).

Evaluation methods

The simulated daily solar irradiance is evaluated as well as the cloud fractional coverage. The WRF radiation values are compared with surface observations using the nearest model gridpoint to the radiation observations. The simulated cloud fractional coverage for this WRF gridpoint is compared with the nearest gridpoint in the CLASS satellite dataset.

The quality of the WRF model is assessed by means of standard statistical errors: MAE (Mean Absolute Error), RMSE (Root Mean Square Error), BIAS and by probability density functions (PDF) matching scores. For all these error measures absolute values as well as relative errors (as percentages) are computed (see Section 3.1).

When testing the linear regression and the quantile mapping models, in order to avoid artificial skill (Von Storch et al., 2001; Wilks, 2006), a five-fold cross-validation approach is used (Section 3.4).

4.3 Results and discussion

Global solar radiation

The statistical errors obtained from the comparison between simulated and observed mean daily values of horizontal global solar radiation are presented in Figure 4.1. BIAS (Fig. 4.1a); MAPE (Fig. 4.1c); RMSE (Fig. 4.1e) are shown in relative magnitude (%; the corresponding absolute results – W/m^2 – are presented in Appendix A, Fig. A1); correlation coefficient (Fig. 4.1b); normalized standard deviation (Fig. 4.1d) and PDF skill score (%, Fig. 4.1f) are also displayed.

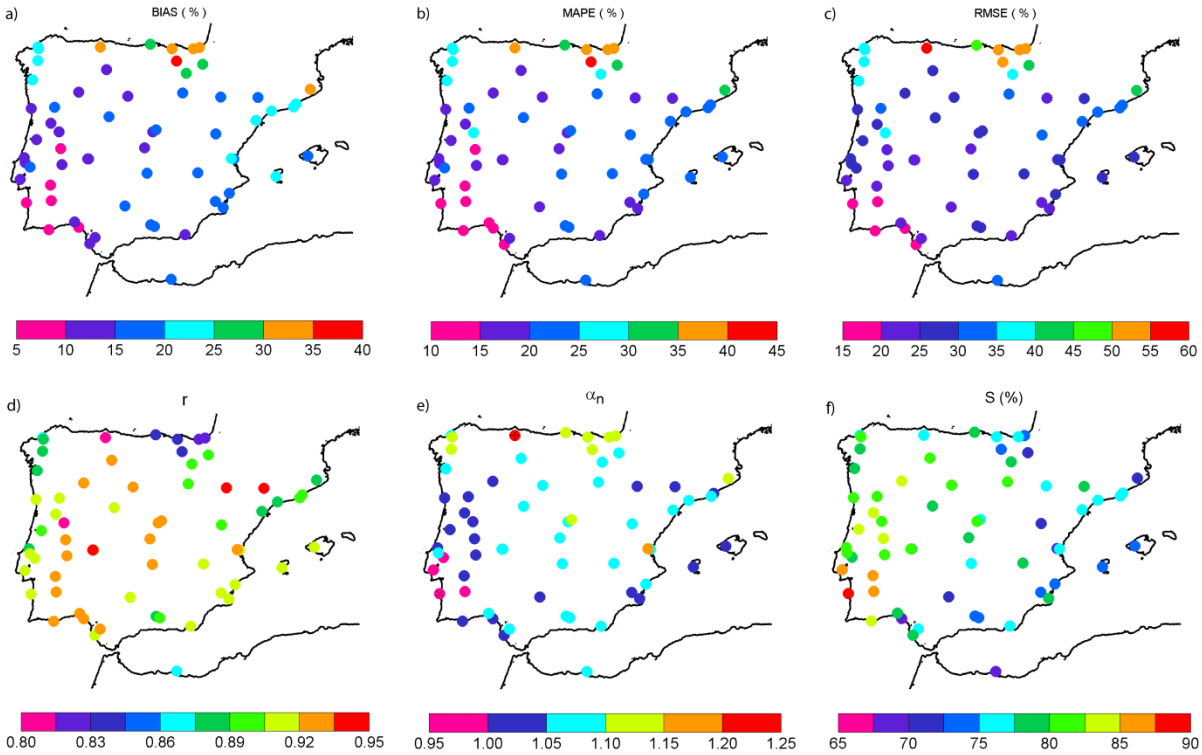

Figure 4.1 Statistical performance results for daily observations of global solar radiation versus WRF simulated data obtained for the Iberian Peninsula: BIAS (a), MAPE (b) and RMSE (c) are shown in relative magnitude (%, top row). Correlation coefficient (d), normalized standard deviation (e) and PDF skill score (%, f) results are also shown (bottom row).

The BIAS shows an overestimation of daily global radiation values by the WRF model over the entire Iberian Peninsula, where the majority of the locations show a positive bias of around 15%. The highest deviations are mainly in the North region, with BIAS magnitudes up to 40% of the observed daily radiation. In contrast, the lowest errors predominate in the Southwest, with magnitude close to 5%. This Northeast-Southwest pattern also occurs in the MAPE and RMSE statistical results. This contrast may be associated with cloudy skies typical of Northern climate of the Basque country, Cantabria, Galicia and Asturias, which has a high frequency of cloudy conditions, and the comparatively very low frequency of clouds in the South. The similarity between BIAS and MAPE values indicate the systematic overestimation by the model.

The skill score results (Fig. 4.1f) confirm that the WRF model simulates the distributions of global solar radiation better in the Southwest. It is noticeable that the lower scores are not confined to the Northeast as the Eastern part of Iberia has a concentration of lower values of skill score. Locations with at least above 85% skill score are only present in the Southwest part of Portugal. The majority of locations with normalized standard deviation values between 0.95 and 1.05 were found to be predominantly located in Portugal and, to a lesser extent, in other parts of the Iberian Peninsula, mainly the South and Mediterranean coastline (Fig. 4.1d). In Spain most of the modelled solar radiation values present variance that deviates around 5 to 15 % from the variance of the observed data.

The correlations between simulation and observations are high, (Fig. 4.1b) ranging from approximately 0.8 to 0.95, most of them are above 0.88. It is also in the North – Northeast Iberian coast that the lower values were found as well as in the Serra da Estrela, which is the location at highest altitude in Portugal. The highest correlations occur mostly in the centre of the Peninsula, while the coastal areas have lower performance, indicating the difficulty of WRF in simulating the coastal cloud development and dissipation. These results indicate, nevertheless, that the solar radiation temporal variability is satisfactorily simulated by the WRF and MOS correction is justified (Eden et al., 2012).

The statistical errors after pooling together the individual stations datasets, i.e., the average of the stations relative errors, indicate an Iberia overall BIAS, MAPE and RMSE of approximately 18%; 22% and 30%, respectively. These overall statistical results were also computed for Portugal and Spain separately due to their different temporal span (2000-2011 vs 2000-2010) and were found to be slightly higher in the stations located in Spain (Table 4.1).

Table 4.1 Statistical performance results for annual average data obtained from Iberian Peninsula after pooling together the individual stations datasets. Results from Portugal and Spain individual set of stations are also shown. MAE, RMSE and MBE are shown in absolute (W/m^2) and in relative magnitude (%).

	MAE		**RMSE**		**BIAS**	
	W/m^2	*%*	*W/m^2*	*%*	*W/m^2*	*%*
Portugal	33.2	17.1	49.1	25.3	21.9	11.4
Spain	41.9	23.3	57.2	31.8	35.5	19.8
Iberian Peninsula	39.6	21.7	55.1	30.2	32.2	17.7

The error results may be compared to the study by Alexandri et al. (2015); its model configuration and comparison to satellite observations instead of *in situ* measurements was designed with a purpose analogous to the present investigation and includes an analysis of solar radiation over the Iberian Peninsula. The spatial distribution of the BIAS in the Iberian Peninsula found by Alexandri et al., (2015) showed overestimation (up to 30%) along the Iberia coastlines, whereas the model underestimates solar radiation in its central area (up to -20%). However, the average BIAS for the entire Iberian Peninsula indicated overestimation of 0.14% and 1.66 % depending on the satellite observations used. The correlation coefficients were 0.96 and 0.97; σ_n 1.13 and 1.14 and RMSE 28.45 and 24.70 W/m^2. It should be mention that their analysis was based on monthly values. Correlations are also expected to be higher and the RMSE lower than the values found here. Similarly, the work of Katragkou et al. (2015), using models with a much coarser resolution, also demonstrated an overestimation of solar radiation in Europe by different configurations of the WRF model, particularly intense in Central and Southern regions with bias of around 40-60%.

Cloud fractional coverage

To investigate the link between global solar radiation and cloud cover in WRF the simulated cloud fractional coverage (%) is compared with satellite observations at the station locations used for the radiation analysis. Due to data availability (observational and model) the analysis is performed for the period 2004-2011. The error is quantified by BIAS, MAPE and RMSE and Figure 4.2 shows that WRF underestimates clouds at all locations: the BIAS (Fig. 4.2a) ranges from approximately -75% to -15%. Lower to moderate underestimation is found mainly in the West and central regions, while strong underestimation occurs in the Southeast along the Mediterranean coast. This region is known to have frequent clear skies, but when cloudy conditions arise, they are predominantly characterized by sparse and convective clouds with a very local type precipitation regime which can only be properly modelled in WRF with higher resolutions (< 4km) (Clark et al., 2009). These large BIAS values in fact correspond to small amounts of cloud cover.

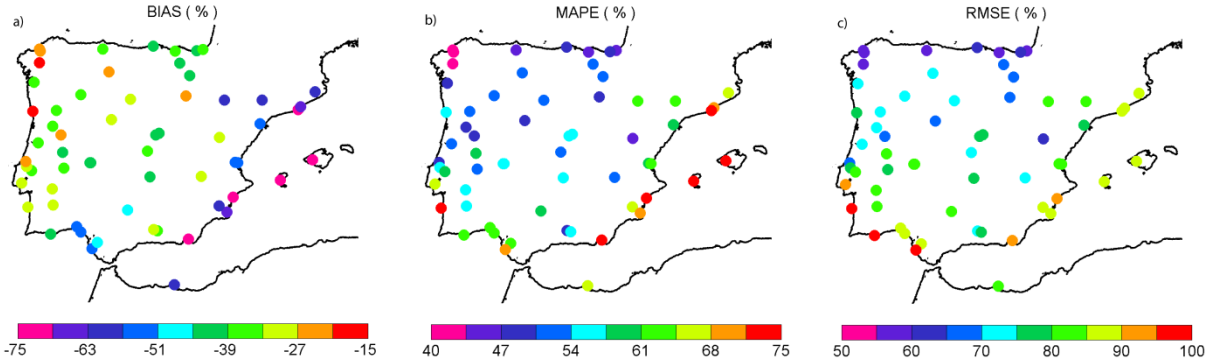

Figure 4.2 Cloud fraction coverage WRF – satellite comparison of average daily values: BIAS (%, a), MAPE (%, b) and RMSE (%, c).

The cloud cover BIAS results, with opposite sign to those for solar radiation, are an indication that the limitations of the WRF model to simulate solar radiation is linked to the misrepresentation of the cloud fractional coverage field. Other authors have also identified this link between solar radiation positive BIAS and negative cloud fractional coverage bias in simulations of the WRF model. Katragkou et al. (2015) found a 50% underestimation of cloud cover in southern Europe. In García-Díez et al. (2015) a negative cloud cover bias appears predominantly over the Mediterranean Sea and its surrounding countries and Alexandri et al. (2015) also obtained an overall cloud fractional coverage underestimation by the RegCM4 model over Iberian Peninsula with bias of -13.7%.

The MAE and RMSE values vary from approximately 16% to 40% and 25% to 48%, respectively. Their spatial distribution is similar to the BIAS distribution with lower MAE and RMSE concentrated in the West and central region and higher values in the Northeast and along Southeast coast.

It should be mentioned that the satellite observational cloud fractional coverage data is known to overestimate cloud cover (Kniffka et al., 2013) since pixels with partial cloud

cover are counted as 'cloud' and are thus not properly distinguished from those with full cloud cover. This overestimation is largest over ocean surfaces but is limited to 10%. Thus the underestimation calculated for WRF cloud fractional coverage should be considered slightly less intense than what the statistical numerical results imply.

Model output statistics

The systematic biases of the simulated solar radiation characterized above are here corrected with linear regression (LR) and quantile mapping (QM). The comparison between these methods allows us to select the most appropriate to obtain a solar resource map for the Iberian Peninsula in present climate. Figure 4.3 shows the cross-validated relative BIAS, the normalized standard deviation and the skill score for both methods. The BIAS of the WRF solar radiation data is reduced to negligible values (around 0%) by LR (Fig.4.3b-c). The QM however, does not reach such low values but it also reduces significantly the BIAS compared to the uncorrected WRF solar radiation data. The maximum BIAS value obtained after QM correction is approximately 9% but almost 80% of the individual stations datasets attain BIAS values that are below 5%. Regardless the MOS method used, the MAPE was also reduced from 11-41% to 10-32.5 % (Appendix A, Fig. A2a-b) and the relative RMSE from 15-55% to 15-45% (Appendix A, Fig. A2d-e). The skill score statistic (S) though (Fig.4.3 g-h) gives a lead to the QM method over the LR which is confirmed by the normalized frequencies of the error values (Fig.4.3i). Almost 70% of the locations analysed with QM method attained skill scores over 85%. The LR results vary in its majority between 75 and 82%. Another advantage of the QM correction over LR is that QM achieves closer results to perfect variance ratios (Fig.4.3f), whereas LR shows an underestimation (Fig. 4.3e), which is a basic property of non-randomized LR because it only captures the explained variance. The correlation coefficients (not shown) for the LR method are by construction identical to those of the raw WRF output, and are also not changed by the QM.

One notes that variance-preserving, deterministic methods such as QM do not take into account the fact that not all of the predictand variability can be explained by the predictor (Maraun, 2013; von Storch, 1999). In contrast LR accounts only for the explained variability if the unexplained, random variability is not added. Following standard practice it was not added the random component to LR, which keeps application simple but leads to the well-known underrepresentation of variability. As it is considered a realistic representation of the entire PDF essential for applications in solar resource assessment, it will be employed QM in the following section, despite the lower BIASP for LR compared to QM.

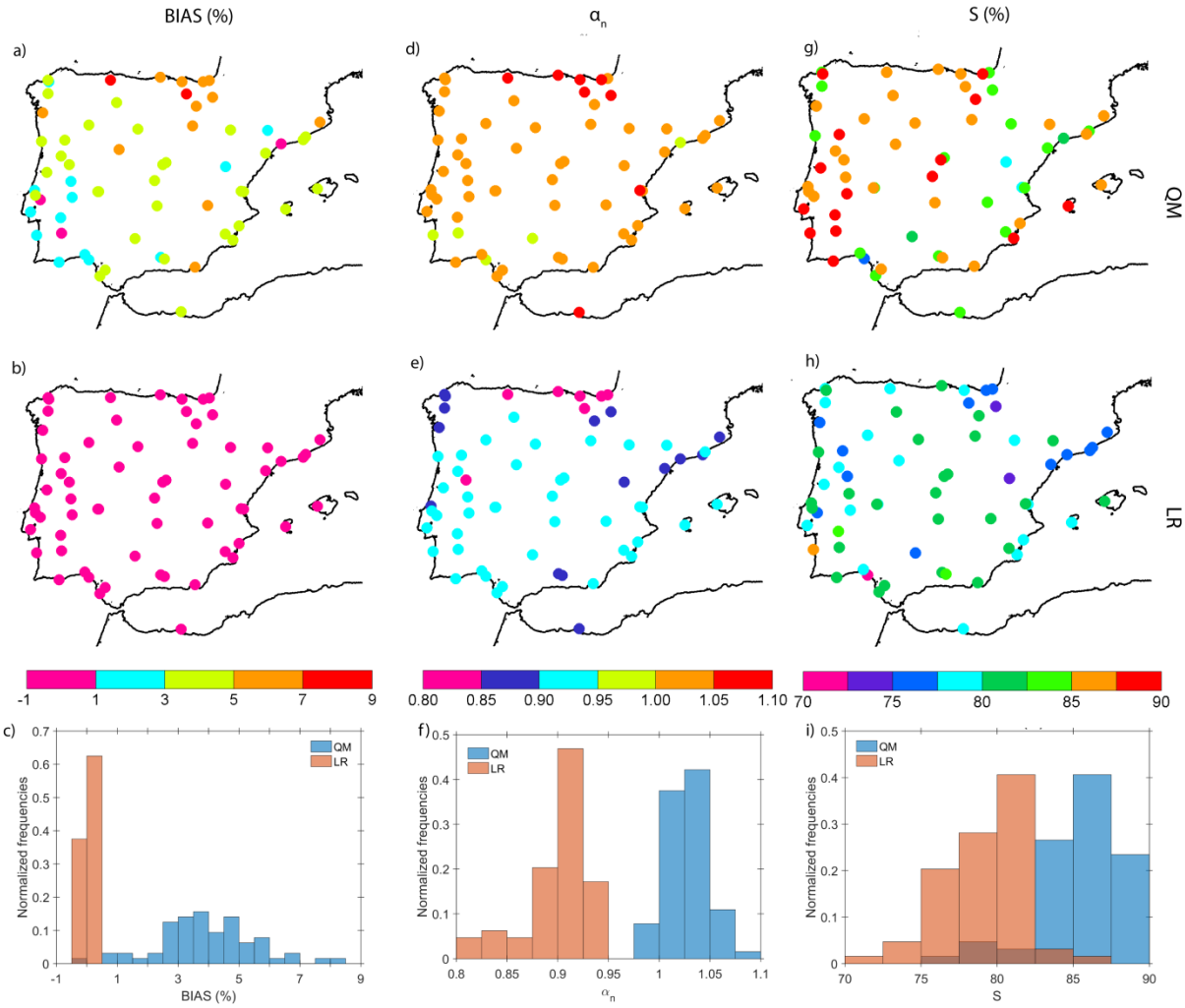

Figure 4.3 From left to right columns: relative BIAS, normalized standard deviation ($\boldsymbol{\sigma_n}$) and skill score (S) for the MOS-corrected WRF: quantile mapping (QM, top row), linear regression (LR, middle row), and normalized frequencies of the values at the stations (bottom row).

Spatial and temporal distribution of solar radiation in Iberian Peninsula

The bias corrected global solar radiation derived from the WRF simulation for the period 1989-2012 is shown in Figure 4.4. The annual mean values vary spatially from approximately 140 W/m^2 to 225 W/m^2, but solar radiation values goes up to maximum 330 W/m^2 in summer. During at least half of the year (spring and summer), solar radiation has values higher than 150W/m^2. The solar radiation has a well-marked annual cycle, where the summer maximum is more than double of the winter maximum value. The north-south gradient along Iberia is in agreement with not only the latitude gradient but also with the typical climate variations of the region. The spatial distribution and range of the annual means are similar to those presented within the Photovoltaic Geographic Information System (PVGIS) from the European Commission, Joint Research Centre (Šúri et al., 2007; Huld et el., 2012). The PVGIS is a free access solar radiation database containing two subsets of data, one derived from spatially interpolated solar radiation information from

meteorological stations and another derived from satellite images with monthly and yearly averages of global solar radiation and often used in assessments of photovoltaic potential (Hofierka and Kanuk, 2009; Brito et al., 2012; Lopez et al., 2011; Kenny et al., 2006) and solar radiation (Pagola et al., 2010).

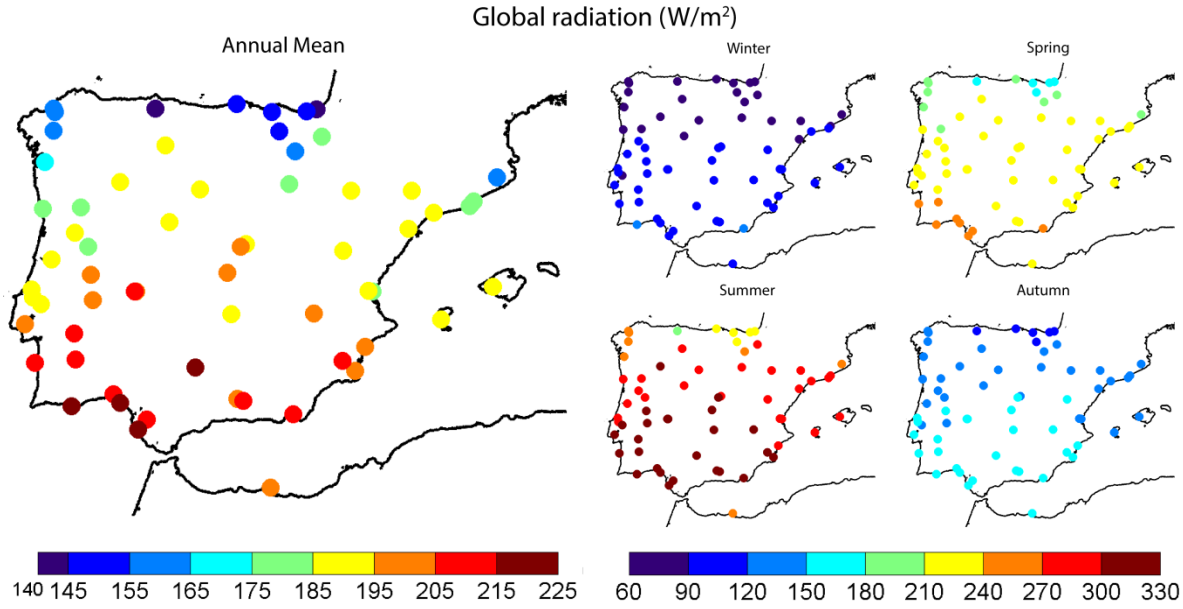

Figure 4.4 Annual and seasonal averages of daily simulated WRF solar radiation for present climate combined with MOS on the analysed locations.

4.4 Iberian Peninsula solar resource map

As presented in Section 3.3, the QM methodology requires observations for fitting. To expand the local results and obtain a solar resource map for the entire Iberian Peninsula it is interpolated the local QM corrections derived from the station-wise analysis across the WRF domain. For that a gridded probability-dependent correction function was developed to obtain corrected solar radiation values at each WRF gridpoint. The methodology consists of: 1) determine for every percentile the difference between the raw simulated WRF values and the bias corrected ones at each of the individual station; 2) each set of percentile-dependent corrections was used to obtain interpolated surfaces (a surface per percentile) equivalent to the WRF Iberian Peninsula domain and 3) subtract from each raw solar radiation simulated value its correspondent probability-dependent correction. The interpolated surfaces are obtained with ordinary kriging.

Kriging is a stochastic method that relies on the knowledge of the spatial structure of the sample points (or observations) to predict values of a variable at locations where no measures are available through, in a way, a sophisticated weighted average of the neighbouring samples, distributing the weights accordingly to their spatial variability

(Alsamamra et al., 2009). The weights are obtained with the help of the semivariogram of the available data (a statistical model which represents how the data vary spatially across the area of interest). So a fundamental step of the kriging process is then the analysis of the spatial structure of the sample points – the semivariogram. This statistical model is modelled to a theoretical semivariogram to allow the inference of values at any arbitrary location of interest (Alsamamra et al., 2009; Ruiz-Arias et al., 2011; Hengl, 2007). Several theoretical models, for example, spherical, exponential, and logarithmic are available for fitting a semivariogram (Hengl, 2007). In this study, a spherical model has been used to fit the observed semivariograms. The same model has been used also in the works of Rehman & Ghori (2000) and Ertekin & Evrendilek (2007). Although it might be pointed out that the present work does not apply interpolation to a climate variable but rather to a correction made to one of such variables it is still relevant to mention that kriging is a geostatistical method widely used in interpolation of climate data such as temperature (Jarvis et al., 2001; Hudson et al., 1994; Holdaway 1996; Hofstra et al., 2008; Haylock et al., 2008), precipitation (Hofstra et al., 2008; Haylock et al., 2008) and also solar radiation (Rehman & Ghori, 2000; Šúri & Hofierka, 2004; Ertekin & Evrendilek 2007; Alsamamra et al., 2009; Journée & Bertran, 2010; Ruiz-Arias et al., 2011). It is not purpose of the present study to discuss the mathematic formulation of the ordinary kriging, which can be found in the aforesaid literature, but to spatially expand the survey of the Iberian solar radiation in order to illustrate the continuous Iberian Peninsula domain and also to allow an elementary comparison to the spatial distribution of the uncorrected WRF solar radiation output.

Figure 4.5 displays the solar radiation maps (W/m^2) obtained for the 1989-2012 period based on the interpolated QM-corrected WRF values at the station locations. The QM methodology not only reduces the solar radiation values in comparison to the WRF raw output (Appendix A, Fig. A3), by removing the model overestimation, but it also influences the spatial distribution of its maximum values. In the raw simulated solar radiation the higher values are concentrated in the Southeast while after QM the maximum shifts slightly to the west, to the Iberia Southwest region (Appendix A, Fig. A3).

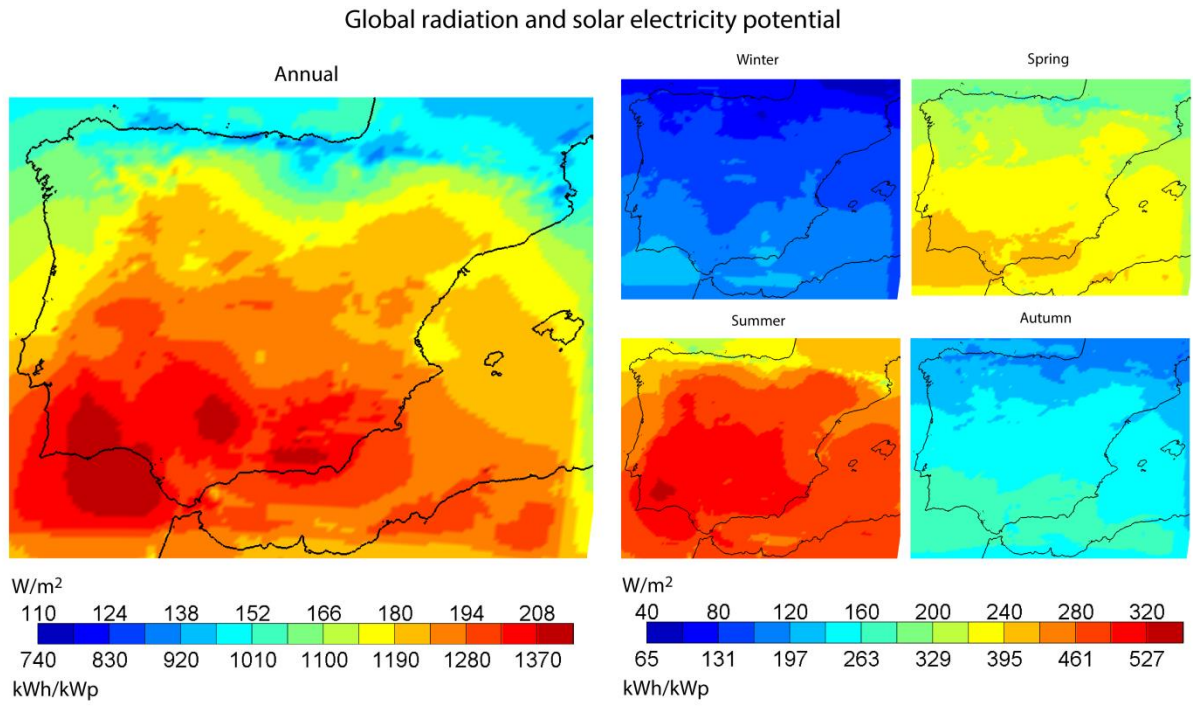

Figure 4.5 Annual and seasonal corrected WRF global solar radiation and solar electricity potential for the Iberian Peninsula present climate. Values are shown in W/m^2 indicating the mean (annual and seasonal) global solar radiation and in kWh/kWp for the sum (annual and seasonal) of solar electricity generated by a 1kWp system with performance ratio 0.75.

After obtaining the appropriate information on the average global solar radiation one can determine the expected annual generation of a photovoltaic (PV) system. However, to suitably obtain the total production of a PV system one should account not only the incident solar radiation but also its technical efficiency and the efficiency of the components to which the system is associated, i.e., inverters; cables and load regulators, etc. It is used the method applied by Šúri et al. (2007) to obtain the annual total of electricity (E) generated from a 1 kWp PV system (P_k):

$$E = P_k P_R G \qquad (9)$$

were P_R is the system performance ratio (assumed to be 0.75) and G the yearly sum of global solar radiation on a horizontal plane of a PV module (kWh/m^2). P_k represents the nominal power output of a PV system operating at Standard Test Conditions (IEC/TS 61836, 1997); temperature of the modules is 25°C while exposed to 1 kW/m2 of irradiance) which due to system losses (cables and inverters) and non-standard real operating conditions (temperature is typically higher than 25°C) has to be multiplied by the performance ratio to reflect the actual output of the system.

Applying the formulation to the solar radiation values obtained in the present study it is concluded that the average sum of annual electricity generated by a 1 kWp PV system in the Iberian Peninsula would range from approximately 740 to 1410 kWh/year (see kWh/kWp in

Fig.4.5). The spatial distribution of these values is as expected in agreement with those portrayed in Fig.4.5 for annual mean solar radiation.

4.5 Conclusions

Atmospheric models can add value to solar energy applications by enabling solar resource assessments and are not only able to study the present climate but also the past and future which is very important in today's changing climate.

The work in this chapter evaluates a long simulation produced using the regional climate model WRF in terms of its ability to simulate global solar radiation values for the Iberian Peninsula and found substantial biases, which were then statistically corrected. This allowed generating an improved quality solar radiation data.

The quality of daily solar radiation simulated by WRF was firstly assessed using ground measurements collected at 64 meteorological stations spread across the whole region during the time period 2000-2011 by means of standard statistical errors and PDF matching scores. The correlations between the simulation and observations are above 0.88 at all locations, which is very high, given the daily resolution. However, a systematic overestimation of solar radiation by WRF throughout the Iberian domain was also found with values up to 40%.

The link between global solar radiation and cloud conditions in the WRF model has also been confirmed in the present study: the systematic overestimation of solar radiation was found to be associated with a systematic underestimation of cloud fractional coverage. The cloud fractional coverage was assessed by comparison between the WRF and satellite observations.

To correct the solar radiation overestimation, the WRF output was combined with a statistical approach. Two methods, a linear regression and a quantile mapping were used and compared. Both methods successfully reduced the biases but quantile mapping also led to realistic variances in contrast to linear regression, which showed the well-known underestimation of variance.

The combination of WRF-simulated global solar radiation and QM enabled the characterization of the spatial distribution and seasonal dependency of the solar resource in the Iberian Peninsula. The annual averages vary from approximately 110 W/m^2 to 215 W/m^2 with a positive gradient from North to South, however with predominance of higher values in the Iberian Southwest. During summer, the average values of solar radiation reach their maximum and can amount to 340 W/m^2. Winter is, as expected, the season with the lowest solar resource available (40 to 140 W/m^2).

To obtain a solar resource map with a complete spatial coverage for the Iberian Peninsula, the station-based corrections were interpolated and applied to the simulated values. The interpolated surfaces have been obtained with ordinary kriging. The corrections made to the entire WRF domain showed that, in comparison to the model uncorrected

output, the location of the solar radiation maximum values shifts slightly to the west, from Iberia Southeast region to Southwest. From these results the annual total electricity generated from a 1 kWp PV system has been calculated and found to range from 740 to 1410 kWh.

It has been shown that numerical atmospheric models such as WRF combined with bias correction techniques such as QM can be a useful tool for solar resource assessment by providing data without missing values for periods longer than the periods of radiation measurements. The final estimates for solar radiation are not strictly zonal, which reflects that meteorological effects have a substantial influence on solar radiation, in addition to the solar angle.

Chapter 5

Combining high resolution dynamical downscaling and quantile mapping for future projections of the Iberian Solar Resource

The planning, production and maximization conditions of solar energy systems rely on accurate climate information, therefore climate change projections are fundamental. In this chapter, the Iberian Peninsula solar radiation resource for future climate obtained from the regional climate model WRF under the RCP8.5 scenario driven by the EC-EARTH climate model is investigated. Since the model output data have systematic errors when compared to observed values, the high resolution (9km) dynamical downscaled data is combined with model output statistics. A quantile mapping methodology which accounts for distribution changes between the projection and the baseline period is used to obtain mean solar radiation for the period 2070-2100.

The results of this Chapter were submitted to *International Journal of Climatology* in March 2016 and were under review when the thesis was printed.

5.1 Background

As far as future projections for solar resources are concerned, Crook et al. (2011) examined how projected changes in temperature and solar radiation over the 21st century would affect photovoltaic and concentrated solar power (CSP) output using two GCMs for the entire globe and for some focal regions. Referring only to Europe, the authors found that PV and CSP output is likely to increase. Spain and Germany presented the highest positive percentage change from 2010 to 2080 in both PV and CSP systems: Spain up to approximately 3.5% and 11%, respectively, and Germany up to approximately 3% and 13%. A similar line of work was developed by Wild et al. (2015). The authors surveyed the potential changes in surface solar radiation over future decades from a set of 39 GCMs used for the 5th IPCC report projects. The models were analysed for the period 2006-2049; the 2006-2015 decade was defined as the reference period representing present day conditions. Solar radiation trends for future climate were evaluated globally wise and its lower values are mainly found in high latitudes and higher values are found in Southeast of North America, wide parts of Europe and China, South Africa and Australia. The variation range of trends obtained from the models projections is between -0.5 to 0.5 (W/m^2)/year. These values are obtained by determining the median of all linear trends applied to the individual model time series of annual quantities between 2006 and 2049 from the set of GCMs analysed. Hence the solar radiation annual mean values were projected to have variations in the range -6 to 6 W/m^2 by the end of 2049. From the regional areas explored, Spain exhibited the most positive projected trend: 0.12 (W/m^2)/year (approximately 6 W/m^2 increase by 2049). The impact of climate change on PV production showed a 0.05-0.1%/year increase trend (approximately 2-4% increase by 2049) for areas with higher solar radiation trends. The areas of Germany and Spain are reported as those with higher values of change of PV between present day and 2049 – median of 0.03%/year (1.3% increase by 2049) and 0.04%/year (1.8% increase by 2049) respectively.

Also with a GCM, Gaetani et al. (2014) focused on assessing the global impact of different anthropogenic aerosol concentration scenarios on surface solar radiation and PV output for Europe and Africa from 2000 to 2030. The extension and intensity of solar radiation simulated changes was found to be increasing as the aerosols emissions decrease and also a significant response in PV output was observed in 2030 with the strength of the climate change signal directly related to the abatement of anthropogenic aerosols.

Burnett et al. (2014) investigated the UK solar radiation resource for the present and future climate. The latter was assessed with the UKCP09 probabilistic downscaled climate change scenario on the periods 2040-2069 and 2070-2099 using as baseline the period 1961-1990. A 3.6% overall annual increase by the 2050s and 4.4% by the 2080s was obtained.

The approach of Panagea et al. (2014) is based on RCMs instead of GCMs which are regarded as more adequate to describe local climatic processes (Giorgi and Mearns 1999; Rummukainen 2010). Five RCMs from the ENSEMBLES project (van der Linden and Mitchell,

2009) were used to address the climate change impact on PV energy output over Greece. Regarding the irradiance projections, the authors reported an increase of +2 to 3W/m^2 by 2050 and another +5W/m^2 until 2100. They also explore the relative contributions of temperature and irradiance on PV output due to the known fact that higher temperatures lead to lower performances on PV energy conversion, however, despite this fact, the results showed an overall increase in available PV energy. The use of RCMs was also followed in the study of Jerez et al. (2015) on the impact of climate change on PV power generation in Europe. Ten different model settings (involving six different RCMs and five GCMs under two climate scenarios – RCP4.5 and RCP8.5 (Riahi et al., 2011) – from the high resolution (12 km) climate projections EURO-CORDEX (Jacob et al., 2014) ensemble are used in this work. Also, solar radiation, temperature and wind speed projection for the period 2070-2099 are analysed. In the case of solar radiation, and focusing only on RCP8.5 climate scenario, its mean annual value, compared to the baseline period 1970-1999 showed increased values of around 5 W/m^2 in Southern Mediterranean regions and decreases between 10 and 20 W/m^2 in the northernmost areas of Europe. The ensemble mean projected changes for the PV power showed negative values in the majority of the domain studied – around -10% - but some areas such as Southwestern Iberia display negligible or uncertain values.

Studies using simulated solar radiation related to future climate scenarios or short-term forecasts often employ also MOS methods that handle bias corrections, although more common in the latter. Panagea et al. (2014) used an empirical correction to adjust the mean and variance of the modelled solar radiation data. Lorenz et al. (2009) developed a stepwise fourth-order regression as function of clear sky index and solar position (cosine of the solar zenith angle) to model the bias between modelled and measured solar radiation data which is then subtracted from the forecast values. Mathiesen and Kleissl (2011) used this same MOS correction in their work which focuses on the analysis and MOS correction of global horizontal solar irradiation short term forecasts from three operational numerical models (two GCMs and one RCM) within the continental United States. Pelland et al. (2013) investigated in their study the use of a Kalman filter to be used as bias removal. The Kalman filter uses recursive equations to extract a signal from noisy data. The authors explored slightly different sets of this approach and found that the most satisfactory was the one where bias depended linearly on the forecasted irradiance. Diagne et al. (2014) also used the Kalman filtering method to improve short term forecasts results from the RCM Weather Research and Forecasting (WRF) model.

The present work is focused on assessing the future projections of solar radiation resource in the Iberian Peninsula. In chapter 4 it was characterized the performance of the model WRF in describing the distribution of solar irradiance in present climate. The high resolution model succeeded in representing the large variability of the climate gradients which are characteristic of the region, but the model biases (systematic overestimation of solar radiation) were shown to be not negligible. The correlations obtained between the daily mean of WRF-simulated solar radiation and observations were everywhere higher than 0.8, which shows that the temporal variability is satisfactorily simulated and MOS correction

can thus be justified (Eden et al., 2012). To limit the model biases a MOS methodology was then applied in order to correct the present climate simulated values. In line with the approach presented in chapter 4, in the present chapter an analysis of the WRF future climate solar radiation projections with a quantile mapping type method (Li et al., 2010).

Although the current study presents only results from a one emission scenario (RCP8.5) and RCM (rather than an ensemble of models), it refers to output of a high resolution simulation (9 km) that does not only focus on the climate change signal but also on the improvement of the model values by considering a bias correction MOS approach.

Section 5.2 describes the WRF model data and the observational dataset followed by the assessment of the main aspects of the distribution errors of the historical reference model simulations in Section 5.3. The MOS methodology applied to the WRF solar radiation output is presented in Section 5.4 and the projected Iberian solar resource in a changing climate is given in Section 5.5. Finally, conclusions are drawn in Section 5.6.

5.2 Model data and observations

WRF climate simulation

The WRF simulations used in this chapter are regional climate simulations forced by the free-running EC-EARTH global model (Hazeleger et al., 2010). Hereafter designated for present climate as historical run, ranging from 1970-2000, and for future run for the period 2070-2100, also forced by EC-EARTH but in agreement with the RCP8.5 (Riahi et al., 2011) (see Section 2.2).

Observations

The observations used to evaluate the solar radiation of WRF historical reference simulation are the same than the ones used in Chapter 4 (see also Section 2.1). They represent measures obtained across Iberian Peninsula (64 locations) between the years 2000-2010 (Fig. 2.1b).

5.3 Biases in mean and variance of the historical reference model simulations

Before QM is applied to the simulated solar radiation to investigate the climate change signal, it is discussed in this section the main aspects of the distribution errors of the historical simulation, i.e. the bias in mean and standard deviation, including their spatial distribution. Figure 5.1 left panel shows the relative model bias in comparison with observations (Fig. 5.1a) and the normalized standard deviation (σ_n, Fig. 5.1b) – ratio of

standard deviation from historical simulation values and observations. The model shows an overestimation of solar radiation throughout the whole region. The highest values predominate in the Northeast region (relative bias of 37 to 40%) and lowest error value predominates in the Southwest (relative bias of about 8.5%). This feature can be attributed to an imperfect representation of the clouds in the model: cloudy skies are typical of the Northern climate of the Basque country (see "País Vasco" in Fig. B1, Appendix B - Tardío et al., 2006), Cantabria and Asturias, which have a high frequency of rainy conditions while a lower frequency of cloudy conditions is characteristic of the South (Cardoso et al. 2013). These results agree with those obtained by Magarreiro et al. (2016) where a hindcast WRF simulation was shown to underestimate the cloud fractional coverage (CFC). This latter run was forced by ERA-Interim (Dee et al., 2011). The underestimation found in this study was present in all the Iberian Peninsula especially in the Northeast region and in the Southeast coast. The overestimation of solar radiation in the Iberian Peninsula and an equivalent spatial distribution of its values was also reported in the same study. A study made by García-Díez et al. (2015) which used a multi-variable analysis of a set of ERA-Interim driven WRF simulations also found a relation between solar radiation and cloud cover biases. The authors analysed their biases in the summer season and found that an overestimation of solar radiation was in agreement with an underestimation of cloud cover. The similarity of the results indicates that the differences between the observed distributions and those in the GCM-driven WRF simulation may be mainly caused by WRF rather than by systematic errors in the driving GCM circulation.

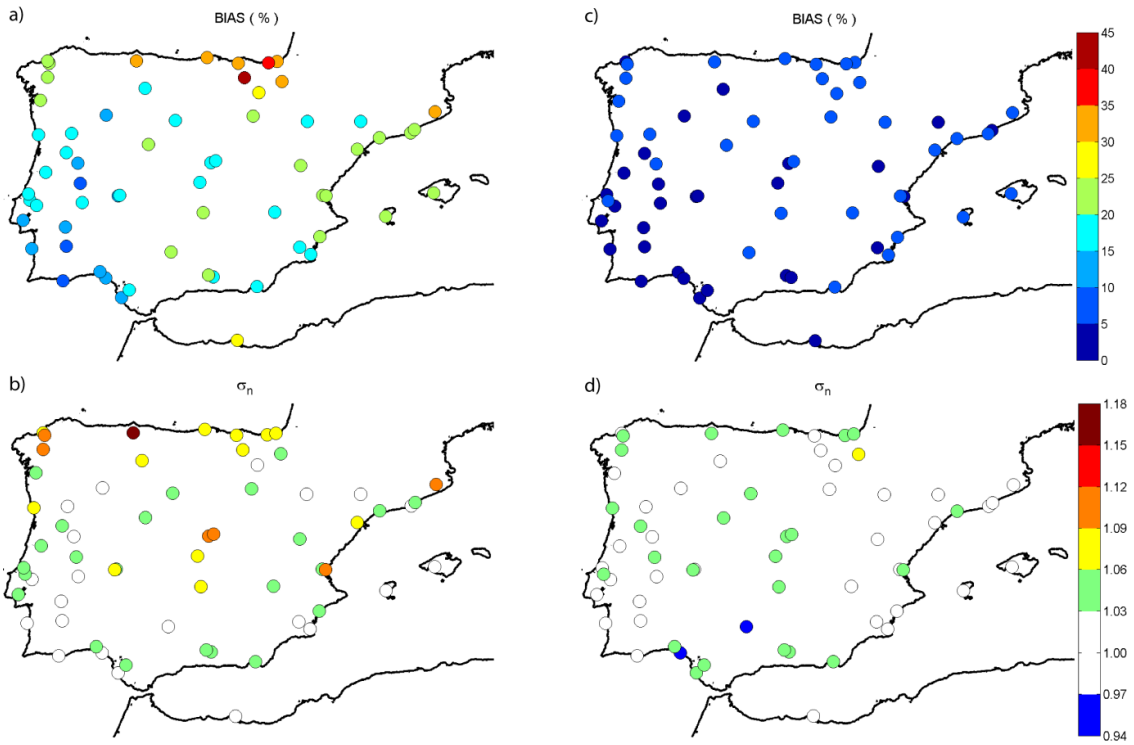

Figure 5.1 Relative BIAS and normalized standard deviation (ratio of standard deviation from historical simulation values and observations, σ_n) between historical simulation and observations: (left panel: a and b) uncorrected historical data and (right panel: c and d) corrected historical data.

The more accurate variability of simulated solar radiation values – $\sigma_n \approx 1$ – are more frequent in Iberian Peninsula Southwest, mainly in the area of South Portugal but also in some regions of the Mediterranean coast of Spain (Fig. 5.1b).

The statistical results of the assessment of the historical reference simulation emphasize the need for using MOS on the model data in order to minimize the systematic errors encountered and to perform a more accurate analysis of the influence of climate change in the future solar radiation levels.

5.4 Combining high resolution dynamical downscaling and quantile mapping: MOS on WRF solar radiation

Chapter 4 presented an extensive validation of WRF ability to describe the Iberian solar irradiance. The WRF 9km resolution simulation forced by the ERA-Interim reanalysis for the period 1989-2012 was evaluated with observed solar radiation data measured at several stations across the Iberian Peninsula through synchronized statistics and probability density function (PDF) matching scores. This study showed the model's suitability to characterize the present climate solar resource for Iberia but also identified systematic biases when compared to observation data. A standard QM method was performed for bias correction of daily data and it was found that this approach constitutes a valuable option. Given this, and considering the results of the previous section, in the present analysis, the WRF solar radiation output from the historical and future simulations are also corrected using QM (Section 3.3), but a more suitable method for analyzing climate change will be employed.

The original method is relatively simple; for a given variable, the cumulative density function (CDF) of a simulation is matched with the CDF of the observations generating a correction function depending on the quantile. This correction function is used to obtain the corrected estimate of the simulated variable quantile by quantile (Section 3.3). When applying this method to future simulations the assumption is made that the bias for a given value in the future is the same as it is in the past. It has been argued by Li et al. (2010) that this might not be the case if the past and future simulations are very different. In order to address this problem Li et al. (2010) have suggested the 'equidistant CDF mapping'. In this method corrections are made not only through the assumption that the difference between the model and observed value during the training period are applicable to the future period but also by taking into account the difference between modelled CDFs for the future and historical periods and can be written as

$$\tilde{x}_{WRF\_p} = x_{WRF\_p} + {F_{obs}}^{-1}(F_{WRF_{fut}}(x_{WRF\_p})) - {F_{WRF_{hist}}}^{-1}(F_{WRF_{fut}}(x_{WRF\_p})) \qquad (10)$$

where F and F^{-1} is the empirical CDF and its inverse, subscripts indicate observed (obs); future (WRF_{fut}) and historical (WRF_{hist}) solar radiation data, $\tilde{x}_{WRF\_p}$ is the corrected estimate of WRF solar radiation future projection and x_{WRF_p} is the raw output of future projection of the model. In the equidistant CDF method a value "a" in a future projection series and its corresponding cumulative distribution is found. Then, the CDFs of the baseline simulations and observations are located in that cumulative probability. The difference between the model historical simulation and observations is subtracted from the model future projection to obtain the corrected value. If after correction, in lower quantiles, a negative value of solar radiation occur it is attributed to it the value zero.

The equidistant CDF method is used for correcting the future simulations; for the historical simulations the two methods (equidistant CDF and standard QM) are, by construction, identical.

The statistical scores relative bias and σ_n from the quantile mapping corrected values of the historical simulation are displayed in Figure 5.1 right panel, together with those for the uncorrected values. In order to avoid artificial skill (Von Storch et al., 2001; Wilks, 2006), a five-fold cross-validation approach is used (Section 3.4).

The relative biases for the daily WRF solar radiation are successfully corrected with quantile mapping (Fig. 5.1c). In the domain analysed, the values vary between approximately 1 and 10% (Fig. B2, Appendix B). These values are still well below the bias levels determined from the uncorrected historical simulation data (Fig. 5.1a) already presented in Section 5.3. All the stations data sets analysed lowered their individual biases, as a result of the correction applied, by at least 70%. The σ_n scores obtained from the uncorrected WRF data although not too different from 1 (varying from 0.97 to 1.18) are closer to that value in a larger number of locations when assessing the model solar radiation corrected data using the quantile mapping correction method (Fig. 5.1d).

5.5 Iberian solar resource in a changing climate

5.5.1 Iberian solar resource for future climate: station-wise evaluation results

Annual mean

The projected Iberian solar resource for the end of the century – 2070-2100 – was assessed considering the 1970-2000 historical climate simulation as baseline. In Figure 5.2 are the future yearly mean values (a) and the relative differences anomalies between future and present climates (b) of daily projected WRF solar radiation corrected with the equidistant CDF mapping method.

The corrected projections show a predominance of increasing mean values of solar radiation for the end of the century in the Iberian Peninsula central and Northwest region. West, South and East coastal regions of Iberian Peninsula are associated to future projections of decreases in mean annual solar radiation. The future projected mean values

for the decades 2070-2100 on the Iberian Peninsula would range from approximately 142 W/m2 to 223 W/m2. The distribution of these mean values would be dominated by a positive gradient from the Northeast to the Southwest. The highest positive anomalies (from 1% to 1.75%) are located in the North-Northwest, along the coast, and in the center-North of Portugal. Relative anomalies close to zero are predominantly located in the Iberian Peninsula center-East while negative values are mainly distributed along the East and Northeast Iberian Peninsula and Mediterranean, South and East Atlantic coasts.

The relative anomalies spatial distribution (Fig. 5.2b) shows some opposite values geographically close to one another. This occurs in the region of Catalonia and Andalusia (Fig B1, Appendix B). One relate these features to the characteristics of their individual locations, since as can be seen in the topography of the WRF model (Fig. 2.1) the opposite values referred above are also located in distinct settings. For instance, in the Andalusia area the opposite anomalies refer to one location in a high altitude setting (≈1000 meters) and another in a contiguous valley (≈100 meters).

The most appropriate comparison between the results here presented and the published literature is to the work developed by Jerez et al. (2015). This work addresses an analysis of an ensemble mean projection of different RCM models with different GCM forcing, while the present one only considers one RCM driven by one GCM. However, in spite of the different analysis setting, it is also based on RCM solar radiation data for the RCP8.5 scenario. The magnitude of the absolute positive anomalies (Fig. B4, Appendix B) projected for the Iberian Peninsula in the present study is in agreement with the one reported in Jerez et al. (2015). They showed increased values of solar radiation of around 0-10 W/m2 in the Iberian Peninsula region. In Jerez et al. (2015) no negative anomalies were reported in Iberian Peninsula but, some of its area is related to values considered as negligible or uncertain for analysis. However, the former authors did not perform MOS on the models data. In the Iberian Peninsula region, the determined bias ranged from -10 to 20% being the overestimation located predominantly in the East and the underestimation in the West. These values may not be in total agreement with those determined in the present study which showed a systematic overestimation of the solar radiation historical data in all the Iberian Peninsula, but also expose the shortcomings of the models and consequently stress the need for combining high resolution dynamical downscaling with MOS methodologies.

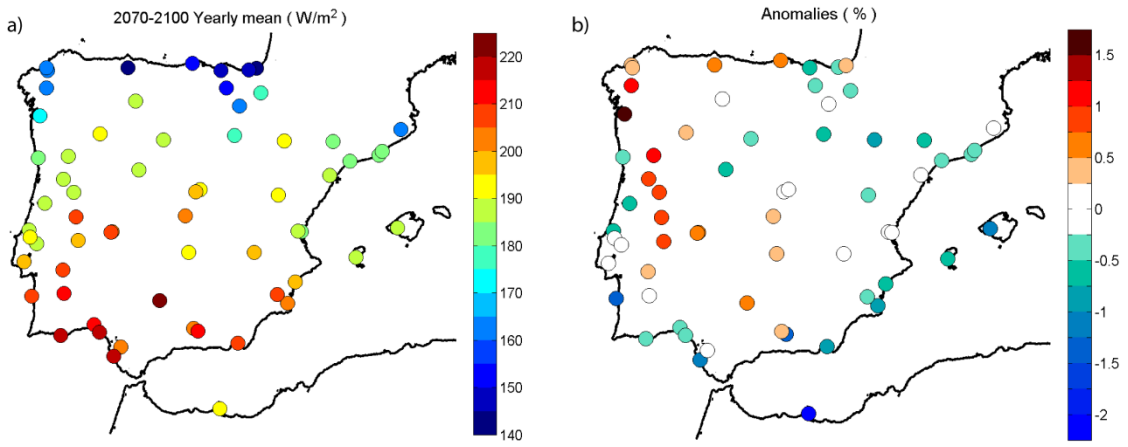

Figure 5.2 Yearly mean of (a) projected WRF solar radiation for the end of the century (2070-2100) after correction and (b) respective anomalies considering historical climate run (1970-2000) as baseline.

Monthly means

Figure 5.3 presents the monthly mean values (a) and the relative anomalies projected for the 2070-2100 decades (b). The monthly plots in Figure 5.3 are displayed in way that each column represents a given season: Winter; Spring; Summer and Autumn from left to right. The monthly mean relative anomalies projected for the 2070-2100 decades shown in Figure 5.3 b) portraits the projected climate change signal at a monthly scale and its annual cycle.

The mean solar radiation in future climate feature maximum values in the summer months, June and July, with highest values of about 340 W/m2. Nevertheless, the projections for August are of much lower values, from 198 to 298 W/m2.It is also interesting to notice that the mean solar radiation projections for May (a spring month) are higher than those for August, ranging from 207 to 322 W/m2. As expected the winter months exhibit the lowest levels of mean solar radiation: projected mean in the winter months December-January-February ranges from 47 to 150 W/m2.

The most noteworthy result is the duration of the summer season: the projections indicate higher positive anomalies in April, May, October and November. The solar radiation projection for May and April are almost entirely dominated by positive anomalies with values that reach, respectively, almost 7% and 5% increases with respect to current solar radiation levels for those months. For November and October the future projected anomalies comprehend also negative anomalies presenting values that range, respectively, from approximately -5% to 6.5% and -7.4% to 6%. These negative anomalies occur along the Mediterranean coast line and in the Northeast (October).

A large central area of the Iberian Peninsula show small changes (between -1 and 1%) on the solar radiation future projected values in the summer months. However, there is a well-marked mild decrease (-3 to -4.5% anomalies) of solar radiation in the Southwest and an increase (3.5 to 4.5%) in the North-Northwest coast for July and August. In the winter

months, January and February, results show an intense decrease in solar radiation which may extend to around -10 to -13% below current levels in some regions, particularly in Northeast. For December, on the other hand, projections indicate the presence of positive anomalies in some areas of the North-center and Southeast regions.

The seasonal changes, although presented here individually for each of their months, are in good agreement with those presented in Jerez et al. (2015). The projected changes of the mean for winter in Jerez et al. (2015) are not significant in most of the Iberian Peninsula area with exception of the Northern region with decreases of solar radiation values (changes of around 10-5 W/m2), which is comparable to the values obtained in the present study (Fig. B4, Appendix B). An analogous comparison is also possible for the spring, summer and autumn. Jerez et al. (2015) found high positive changes of the solar radiation values in the Iberian Peninsula Northern region in the summer (from 10 to 20 W/m2) and non-significant changes in the South-Southwest and some of the central region. For spring, the pattern of the distribution of values was found to be opposite to the summer results, i.e., higher positive changes in the South-Southwest (from 5 to 20 W/m2). In the autumn the mean changes projected are between 5 to 10 W/m2 but slightly more intense in the central-Northwest region. In some extent, although using corrected values, these set of characteristics was also determined in this work (Fig. B4, Appendix B).

Considering the validity of the climate change scenario used, the present analysis shows strong evidences that the intra-annual variability will be enhanced in the future which may indicate that more extreme records of solar radiation will occur. The overall assessment of the Iberian Peninsula solar resource in the future climate suggest that in the region will prevail favourable conditions for further deployment of solar energy systems.

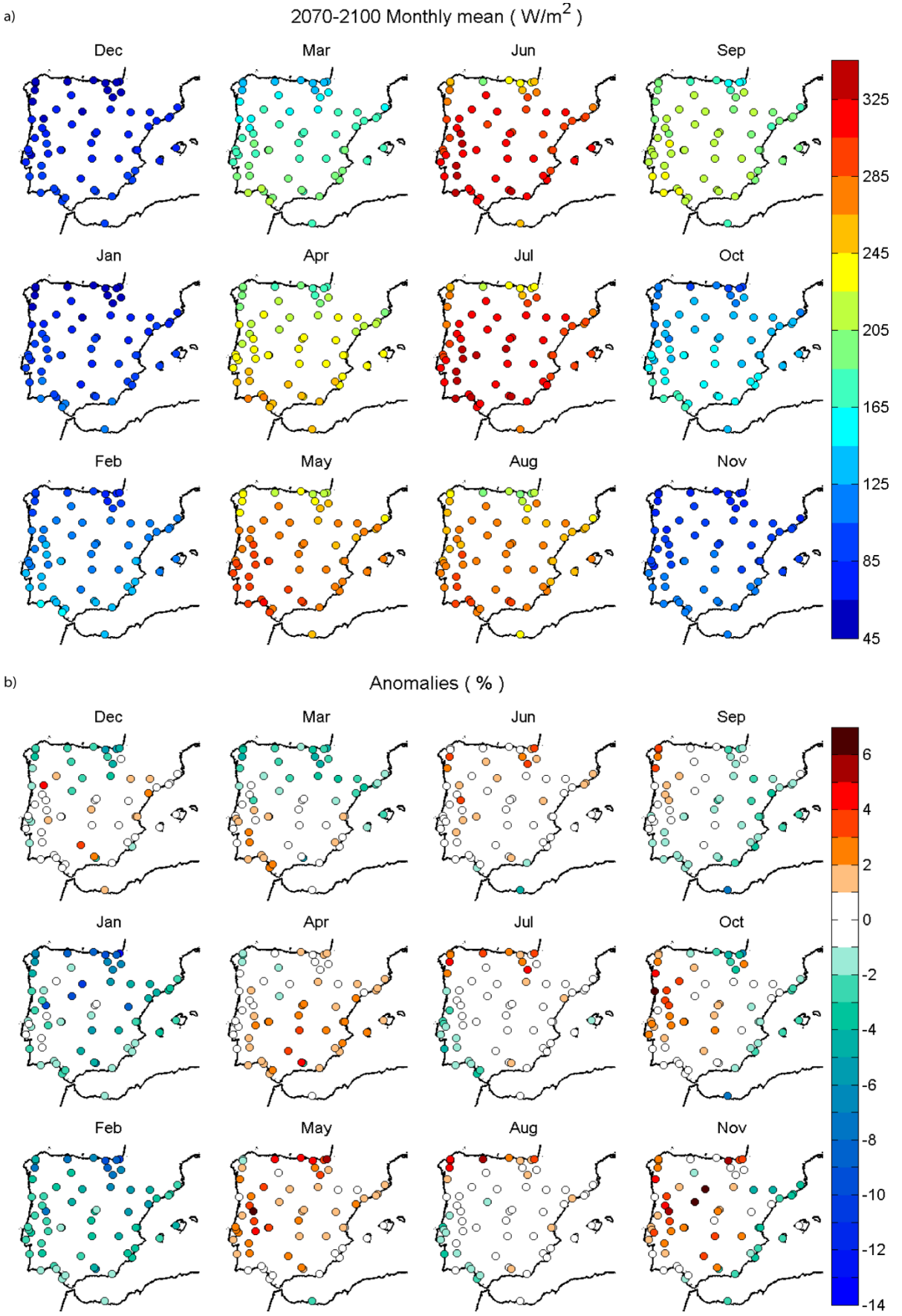

Figure 5.3 Monthly mean of (a)projected WRF solar radiation for the end of the century (2070-2100) after correction and (b) respective anomalies using historical climate simulation as baseline.

5.5.2 Iberian solar resource for future climate: broadening station-wise results to a gridded evaluation

To complement the information of the station-wise future bias corrected projections of Iberian solar radiation presented in the previous section it is used a gridded probability-dependent correction function to obtain the corresponding solar radiation values in all the individual grid points of the WRF Iberian Peninsula domain and thus enabling the expansion of the localized results to solar resource maps.

The methodology follows the one already presented in Chapter 4 (Section 4.4). Considering the station-wise future bias corrected projection it is calculated, for every cumulative probability (discrete values of 1 on 1) i.e. for each percentile, the difference between the raw simulated WRF values and the bias corrected one. This set of percentile dependent corrections acquired from the station-wise analysis is used to obtain interpolated surfaces (one for each percentile) equivalent to the WRF Iberian Peninsula domain. To get then the final corrected values at each individual WRF grid point it is subtracted from the raw solar radiation simulated value its correspondent probability correction. This final step is applied to every time step of the WRF simulated data and only after are the annual and monthly means determined.

As presented in Chapter 4, the interpolated surfaces were also obtained with ordinary kriging (see Section 4.4).

Figure 5.4 displays the yearly mean map (a) and relative anomalies (b) of projected WRF solar radiation corrected with the equidistant CDF mapping method in the entire WRF Iberian Peninsula domain for the end of the century (2070-2100) and, as before, considering the 1970-2000 historical climate simulation as baseline. As expected the Southeast presents the higher mean yearly values of solar radiation (from around 200 to 220 W/m2) and the North the lower ones (130 to 175 W/m2). However the projections indicate that it would be in the North, especially Northwest, region that higher positive anomalies take place, ranging from 1 to 3 %. Large areas of the central region show little variation of solar radiation mean values, experiencing near zero anomalies. The higher negative anomalies are registered for the high altitude Pyrenees region.

The uncorrected anomalies, i.e. the difference between 2070-2100 and 1970-2000 WRF uncorrected output solar radiation data were determined and it was found that the spatial pattern is similar with the one obtained from the corrected data. Nevertheless the anomalies values are slightly accentuated with the quantile mapping corrected data (Fig B5, Appendix B d and e) i.e., the range between maximum and minimum values is somewhat increased. This feature might result from the influence of the interpolation method used to expand the station-wise analysis. Only 19% of the locations (stations flagged with a cross in Fig. B5f, Appendix B) analysed reject the hypothesis, at 90% significance level, that the annual means between baseline and future values are equal. This is true for both uncorrected and corrected data. Thus, it is reasonable to conclude that the MOS used in this study does not have a clear influence on the climate change signal. The influence of the

correction methodology in the final results is however evident in the yearly mean solar radiation maps: the localization of the higher values (in the Southeast, c.f. Fig. 5.4 a) has shifted slightly to the west when comparing to the yearly mean values determined with the uncorrected WRF data (Fig B5 a and b, Appendix B, plotted side by side with equivalent colour scheme). In the monthly analysis, the anomalies maps determined with corrected WRF data also feature values slightly more amplified than those determined with uncorrected WRF output (Fig B6, Appendix B). This intensification of more positive and more negative anomalies is particularly noticeable in areas where the projections obtained for the uncorrected WRF data show values with near zero anomalies. Once again, this feature might be associated to the influence of the interpolation method used and not only due to the correction method.

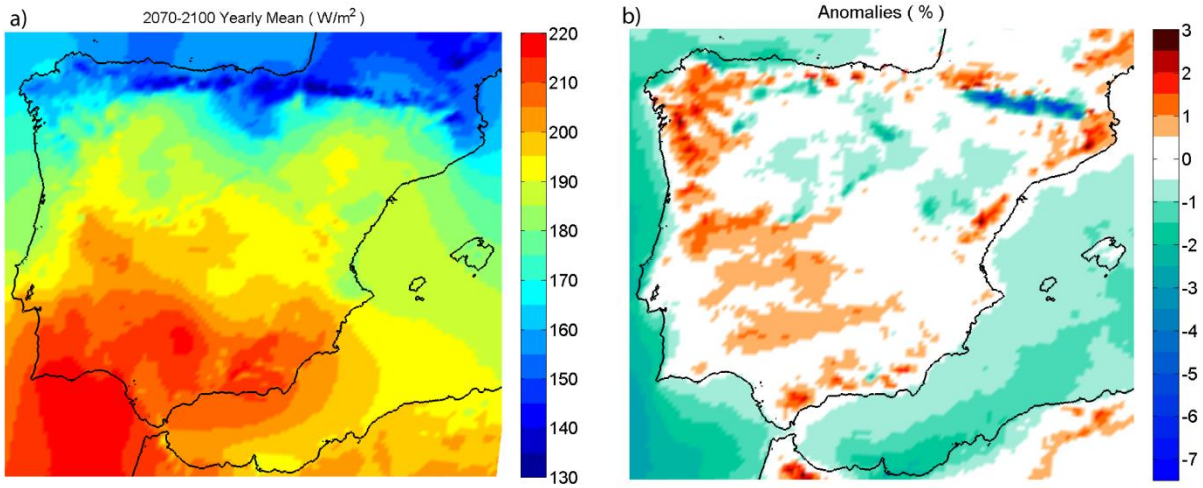

Figure 5.4 (a) Yearly mean map of projected WRF solar radiation for the end of the century (2070-2100) with interpolated probability-dependent correction function and (b) respective anomalies considering historical climate run (1970-2000) as baseline.

5.6 Conclusions

Future projections for the end of the 21st century of the Iberian solar resource were analysed using WRF high resolution (9km) simulations from the periods 2070-2100 and 1970-2000. The RCP8.5 scenario is used in this climate change assessment.

The evaluation analysis is focused in 64 locations in the Iberian Peninsula and the WRF high resolution dynamical downscaling was combined with model output statistics. The WRF solar radiation output systematic errors were corrected using quantile mapping and were successfully minimized from values that ranged from approximately 9 to 41% to values between 1 and 10% in all the locations analysed.

For future projections, bias correction was introduced using the equidistant CDF mapping method as described by Li et al. (2010). The future projected mean values for the

period 2070-2100 ranges from approximately 142 W/m2 and 224 W/m2. The distribution of these mean values is dominated by a positive gradient from the Northeast to the Southwest. Comparing to the baseline climate, the increases on solar radiation mean values may reach +1.5%. Monthly-wise, the mean solar radiation in future climate has maximum values in the summer months June and July (highest values of approximately 340 W/m2). The annual cycle is enhanced which may indicate more extreme records of solar radiation. Projections indicate higher positive anomalies in April, May, October and November which indicates the elongation of the summer season. These projected anomalies obtained for the Iberian Peninsula are however lower than the ones reported in the referenced literature.

The analysis for the 64 locations was generalized to the model grid using interpolated surfaces of the data distribution corrections to allow the use of the equidistant CDF mapping method in all the individual grid points of the WRF Iberian Peninsula domain. The interpolated surfaces were obtained with ordinary kriging. This step also allowed a comparison of the spatial distribution of the uncorrected to the corrected WRF solar radiation output. When compared to the results obtained with MOS, the uncorrected WRF data lead to generally higher mean values of solar radiation for the decades 2070-2100 in the Iberian Peninsula domain but shows smoother fields of relative anomalies.

The corrected WRF data yields slightly higher positive anomalies and slightly lower negative anomalies. The results however do not support that the MOS method used has a definitive influence on the climate change signal. This comparison also showed that the location of the higher yearly mean values of solar radiation is shifted slightly to the west. From this, it is clear that the MOS has clearly impacted the conclusions obtained. Thus, the favourable conditions in the Iberian Peninsula for the deployment of solar energy systems are expected to remain in the future climate.

One should underline that the present study considers only a single RCM driven by a specific GCM and climate projection scenario which does not fully addresses the associated uncertainties of the analysis. It should also be pointed out that the analysis depends to some extent on reliable measures of global solar radiation which may be a limitation. A sensitivity analysis to the spatial density of in situ measurement, and their optimum temporal span, should also be considered in future work. Nevertheless the analysis in the present work constitutes a necessary and valuable step in the field of bias correction of projected RCM global solar radiation.

Chapter 6

Azores solar energy resource from bias-corrected regional climate simulation: present climate and future projections

The Azores region is often neglected in solar resource assessments and solar resource maps of the world or even Europe. However, considering its location, the Azores islands can be faced as a privileged location for potential study of integration of all sorts of renewable energy aiming the self-sustainability of the region in terms of energy consumption.

Following the methods previously presented in the analysis of the WRF simulation for Iberia, in this chapter the solar resource of the Azores archipelago is addressed. The simulated values for present climate and future projections for the mid and end of the 21st century are combined with bias correction methods to obtain a solar resource map for both future periods according to the future scenario RCP8.5.

6.1 Background

The Azores archipelago, a group of 9 islands in the Atlantic North, uses, in its majority, fossil fuels as its primary energy source. Nonetheless, the use of renewable energy sources such as geothermal and wind have been increasing in the last years.

The Azores islands can be faced as a privileged location for potential study of integration of all sorts of renewable energy aiming the self-sustainability of the region in terms of energy consumption. Having this in mind an innovative project was conceived within the MIT-Portugal Program – the Green Islands Project (Green Islands Azores Project, 2015). It is a research project which aims at the development of new energy planning tools to assist the government and people of the Azores in identifying strategies to meet their energy needs with indigenous energy resources.

The privileged richness of the solar resource in the Iberian Peninsula drives the promotion for the adoption and development of solar thermal and photovoltaic systems. However, in the Azores archipelago the solar resource is often regarded as being low and therefore not worth of being seriously considered for renewable energy systems. This is mainly due to the fact that, when compared to the typical weather conditions of for instance Portugal, the Azores islands experience greater amounts of cloud cover. Nevertheless, solar is a renewable resource that cannot be ignored.

In the present chapter the main goal is to contribute to characterize the solar resource of Azores in present and future climate. Since the methodology used for Iberian Peninsula in Chapter 4 and 5 was proven to be suitable for the study of solar resource, the same approach for the analysis of the solar radiation will be followed for the Azores archipelago. The WRF model is used for the simulation of solar radiation data but at a 6km resolution, higher than the one used for the Iberia Peninsula due to the reduced size of the islands. Besides reanalysis driven present climate (1989-2010), the analysis will consider two instances of the future climate: the mid (2040-2059) and end (2080-2099) of the 21st century by comparing them to the historical simulation (1989-2010). The solar resource maps for these three periods are provided. In this chapter, unlike what was presented for the Iberia Peninsula, there will not be made a comparison between the simulations of solar radiation data and its link to cloud cover. The conclusions obtained in that particular analysis are considered to represent the model behavior in both Iberia Peninsula and Azores region by taking into consideration the conclusions obtained by Tomé (2013) in its study of the precipitation simulated values of the WRF model.

This chapter is organized as follows: Section 6.2 the data used and methods followed are described. The results of the assessment of the WRF solar radiation simulations; the MOS results and the solar resource map for the Azores present climate are presented in Section 6.3. In Section 6.4 the focus of the analysis results is the future projections of the solar radiation for the region by considering two instances in time, the mid and end of the 21st century. The conclusions and the summary are then given in Section 6.5.

6.2 Data and methods

Observations

The global solar radiation measurements datasets available and used in the assessment of the Azores solar resource for present and future climate are multi-year daily mean data for the islands Faial; Terceira; Graciosa; Pico; Flores; Corvo; S^{ta} Maria and two locations in São Miguel, Ponta Delgada and Nordeste (Fig. 2.2b). The multi-year daily mean data is available at the Green Islands Project website (Green Islands Azores Project, 2015) and was constructed from measurements made by the Azores delegation of the Portuguese Weather Service (IPMA) during the period 1999-2009. An average daily value was determined for a given day of the year according to the available measurements of that same day at the correspondent site (further details see section 2.1).

WRF climate simulations

The Azores WRF simulation firstly used in this chapter to assess the solar resource in present climate has been driven, at the lateral boundaries, by the ERA-Interim reanalysis (Dee et al., 2011) and refers to a 6km horizontal resolution for the period 1989-2010 (Section 2.2).

For the future climate analysis, a present climate simulation forced by the free-running EC-EARTH global model (Hazeleger et al., 2010), hereafter designated as historical reference baseline simulation, ranging also from 1989-2010 which is compared with a set of two simulations for future climate also forced by EC-EARTH. The latter represent the 21st mid century conditions in 2040-2059 and at the end of the century in 2080-2099. The future simulations follow the future emission scenario RCP8.5 (Riahi et al., 2011) (see Section 2.2).

Accordingly with the available observations the WRF simulated data is aggregated into multi-year daily mean values of solar radiation.

Model Output Statistics

Following the methodology presented in Chapter 3 and used in Chapter 4, in the present chapter linear regression and quantile mapping are used in the analysis of the solar resource for present climate (Section 6.3). Recalling that for an event-wise method a pairwise time series is needed, for the analysis on future projections of solar radiation only quantile mapping based method can be used. Therefore the methodology used in Chapter 5 is followed to obtain the Azores solar resource for future climate (Section 6.4). Once again, as in Chapter 4 and 5, in order to avoid artificial skill (Von Storch et al., 2001; Wilks, 2006), a five-fold cross-validation approach is used (Section 3.4).

6.3 Present Climate

6.3.1 Evaluation of WRF simulation in present climate conditions

First and foremost, it is important to acknowledge that the nature of observations (multi-year daily means) constitute a limitation on the study presented throughout this chapter. The variability of this observational data is a conditioned one when in comparison to long-term records of solar radiation. Nevertheless, given the lack of data availability the analysis is carried on with this dataset.

The statistical indicators (Section 3.1) of the comparison made between the multi-year daily mean data of observations and WRF data for the locations analysed in the Azores islands, are listed including absolute and relative magnitudes in Table 6.1.

Table 6.1 Statistical performance results for **multi-year daily mean** data obtained for Azores islands and WRF 6km resolution. MAE, RMSE and BIAS are shown in absolute (W/m^2) and in relative magnitude (%). Correlation coefficient (r), skill score (S) and normalized standard deviation ($\boldsymbol{\sigma_n}$) are also presented. (The superscripts C; W and E indicate Cental; Western or Eastern Group.)

	MAE		RMSE		BIAS		r	S	$\boldsymbol{\sigma_n}$
	W/m^2	*%*	*W/m^2*	*%*	*W/m^2*	*%*		*%*	
Faial^C	29.65	17.06	38.98	22.43	24.28	13.97	0.93	62.19	1.04
Terceira^C	27.61	16.43	36.82	21.90	11.88	7.07	0.90	66.03	1.12
Graciosa^C	26.39	13.74	34.94	18.20	0.23	0.12	0.93	57.81	0.82
Pico^C	35.82	22.22	44.66	27.71	19.19	11.91	0.89	60.44	0.84
Flores^W	54.66	37.58	63.10	43.38	54.38	37.38	0.93	46.58	1.20
Corvo^W	31.37	18.97	40.08	24.24	22.58	13.65	0.91	60.00	0.92
Ponta Delgada^E	29.22	16.38	39.46	22.12	22.43	12.58	0.91	63.84	1.10
Nordeste^E	46.24	30.18	55.92	36.50	44.61	29.12	0.89	57.53	1.03
S^{ta} Maria^E	25.85	12.34	33.37	15.93	-5.54	-2.65	0.93	60.16	0.86

As expected, given the nature of the datasets (multi-year daily means) the correlation coefficient between model values and observations are high in all locations, ranging from 0.89 to 0.93. Regarding BIAS, with exception to S^{ta} Maria Island, the results show an overestimation by the WRF model in all locations. Flores and Nordeste (in São Miguel Northeast region) exhibit the highest BIAS with magnitudes of, respectively, 37% and 29%. Graciosa shows a negligible BIAS value (0.12%) and Terceira; Pico; Ponta Delgada (in São Miguel Southern region); Corvo and Faial fall, in ascending order, in the 7 to 14% interval of BIAS results. In S^{ta} Maria however, a BIAS of -2.7% indicates an underestimation of the WRF solar radiation values. The distribution of higher to lower values of MAPE along the locations analysed is consistent with the BIAS results: Flores and Nordeste exhibit the higher ones (37% and 30% respectively) and S^{ta} Maria the lowest (12%). The RMSE errors, ranging from 16% to 43%, present also the same distribution pattern of its values.

It is shown through the skill score results that the ability of the predicted global radiation to represent the PDFs of the measured values is not very high. The values range from 46% in Flores to 66% in Terceira. The normalized standard deviation, which ideally would approach unity by reflecting the matching of standard deviations of simulated and observed solar radiation values, is closer to that result in Nordeste and Faial (respectively 1.03 and 1.04). Graciosa, which stood out by presenting negligible BIAS is associated to one of the poorest normalized standard deviation results – 0.82 – showing that the model despite characterizing well enough the mean value of solar radiation in this location does not perform as well in terms of representing the spread of the data values. This result obtained in Graciosa is only topped by the one corresponding to Terceira which exhibits a normalized standard deviation of 1.2.

Given the lack of bibliography on numerical model's simulated solar radiation on islands such as Azores it is not possible to compare the obtained results with others. Tomé (2013) analysed the outcome of variables such as precipitation and temperature from the same model simulations and found that the model underestimated precipitation in the Western, Central and Eastern groups. This underestimation in precipitation may be considered indirectly in line with the overestimation of solar radiation. This consideration sets on the idea that the model would also misrepresent the cloud cover in the areas analysed. Although this issue had been addressed for Iberian Peninsula in Section 4.3 it will not be further explored in the present chapter.

It is worth mentioning that there are considerable differences between the real topography of the Azorean Islands and the topography associated to WRF. Pico, the island with highest mountain peak, has a much lower elevation in WRF than its real topography (Tomé, 2013). Also, giving its small area (approximately 17 km^2) Corvo is not represented in the model 6km resolution (Fig. C1, Supplementary C). The point chosen to conduct the analysis in the present work is in fact considered by the model as ocean and not land. Given the limited size of the islands this factor should not be totally disregarded particularly in the case of the smallest ones. The closest WRF grid point to the location where data was measured may not adequately represent the real local conditions that are associated with the observations points.

6.3.2 Model Output Statistics in present climate conditions

The biases of the simulated solar radiation characterized in section 6.3.1 are here corrected with linear regression (LR) and quantile mapping (QM). As performed in Chapter 4 for Iberia, the comparison between these methods allows us to select the most appropriate to obtain a solar resource map for Azores Archipelago in present climate. Figure 6.1 shows the MOS cross-validated relative BIAS, normalized standard deviation, MAPE, RMSE and skill score. The results of both MOS methods are plotted next to the statistical results obtained from the uncorrected solar radiation WRF values to better illustrate the differences

between them. The BIAS of the WRF solar radiation data is reduced to negligible values (approximately between -1.3 to 1%) by LR (Fig.6.1a See also Table C1, Appendix C). The QM, although reducing significantly the BIAS compared to the uncorrected WRF solar radiation data does not reach such low values which vary between -2% in Terceira to almost 11% in Nordeste. The MAPE (Fig.6.1 c) and RMSE (Fig.6.1 c) results also show that LR leads to a larger reduction of statistical errors than QM. The results of the normalized standard deviation (Fig.6.1 b) reflect the advantage of the QM method once it combines the correction not only of the mean values of the data analysed but also the dispersion of the data around that mean, i.e., the standard deviation. The normalized standard deviation is more close to unity in all locations using QM than LR (Table C1, Appendix C) but the latter still represents an improvement from the uncorrected solar radiation WRF data. This was expected since the observation datasets used in this study are constituted by multi-year daily means, which will naturally reduce the observed variability of the solar radiation, and it is well known that LR is less appropriate than QM to capture the variability of observations. The skill score results were improved with both methods presenting values from 61 to 70%. The difference between skill score results of LR and QM methods is in fact small. Considering these results the LR is favoured over QM to obtain the corrected solar radiation map for present climate.

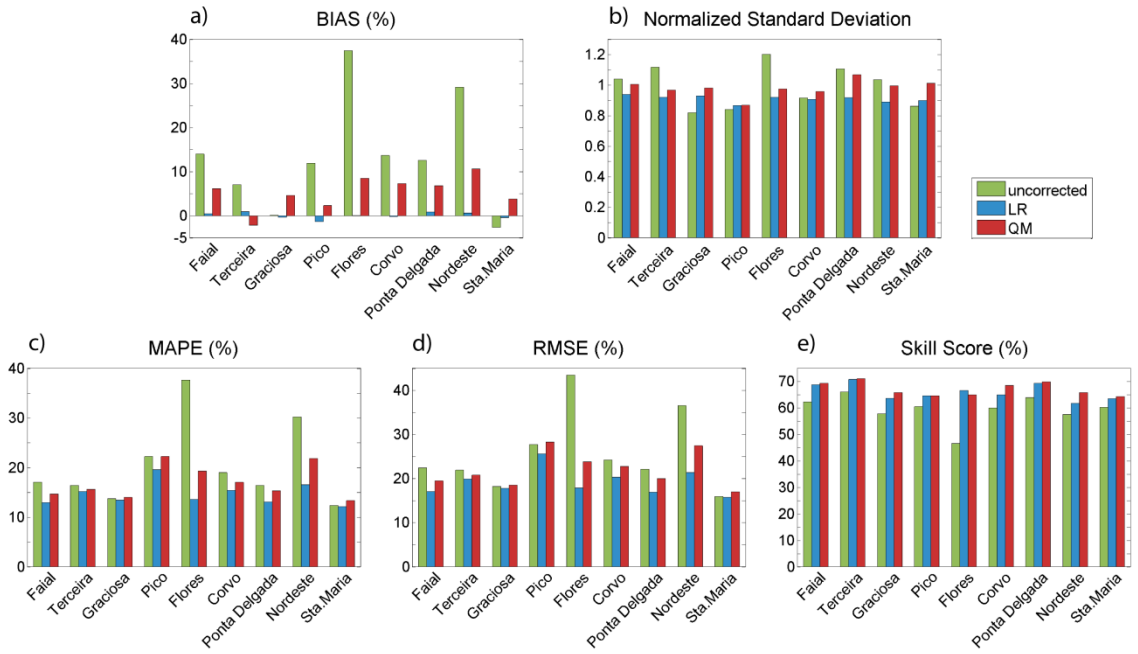

Figure 6.1 Statistical performance results for multi-year daily mean data obtained for Azores islands and the MOS-corrected WRF. (a) BIAS, (c) MAPE and (d) RMSE are shown in relative magnitude (%) for linear regression (LR, blue) and quantile mapping (QM, red). (e) Skill score and (b) normalized standard deviation are also presented. The results of both methods are plotted next to the statistical results obtained from the uncorrected solar radiation WRF values (green).

6.3.3 Azores solar resource maps

Following the methodology used in the Iberian Peninsula analysis (Chapter 4, Section 4.4) the solar radiation map was obtained using a probability-dependent correction function to correct the solar radiation values at each WRF gridpoint for the Azores islands. However, given that only one observation point exist per island (two in the case of São Miguel) it is not possible to develop an interpolated surface for each percentile. An interpolated surface would need information from different locations. Hence, the approach used for the Azores islands consists of assuming that the solar radiation corrections applied to each observation point is valid for the entire area of the respective islands. For São Miguel, where two locations are available (Ponta Delgada and Nordeste), the mean value of the corrections of each individual location was determined. That mean value is then the one assumed to be valid for the entire area of the island. São Jorge, one of the islands of the Central group was not considered throughout the analysis because no observations were available for that particular island. Nonetheless for illustrative purpose the WRF solar radiation values for São Jorge are adjusted with the correction values used in Faial.

Annual mean

Figure 6.2 illustrates the present climate solar radiation annual mean for the 1989-2010 period. For illustrative purpose, and given the limited size of the islands, the figure is presented with different zoom levels between the Western, Central and Eastern group. Throughout the islands the solar radiation mean values range from about 110 W/m^2 to 210 W/m^2. In the Western group, Flores and Corvo present the lower mean values of all the islands while Graciosa and S^{ta} Maria exhibit the higher ones. In the islands Pico; Faial; São Miguel and Terceira it is possible to identify areas with lower solar radiation mean values which correspond to the location of the highest elevations of each island.

Although it was assumed that the correction made to the WRF solar radiation values in only one location of the island is applicable to its entire area it was found that when compared to the uncorrected WRF values (Fig. C2, Appendix C) the results are consistent between them. By consistency one is referring to the spatial distribution of lower and higher solar radiation values. The MOS used, by removing the BIAS of the model output, has obviously limited the range of solar radiation annual mean to values lower than the ones of the uncorrected simulated WRF solar radiation.

The solar radiation mean values may not seem high when compared to typical values found in the majority of the area of Iberia but are definitely comparable to the average solar radiation observed in central Europe countries (Šúri et al., 2007) with well-developed markets of PV applications (Dewald & Truffer, 2011).

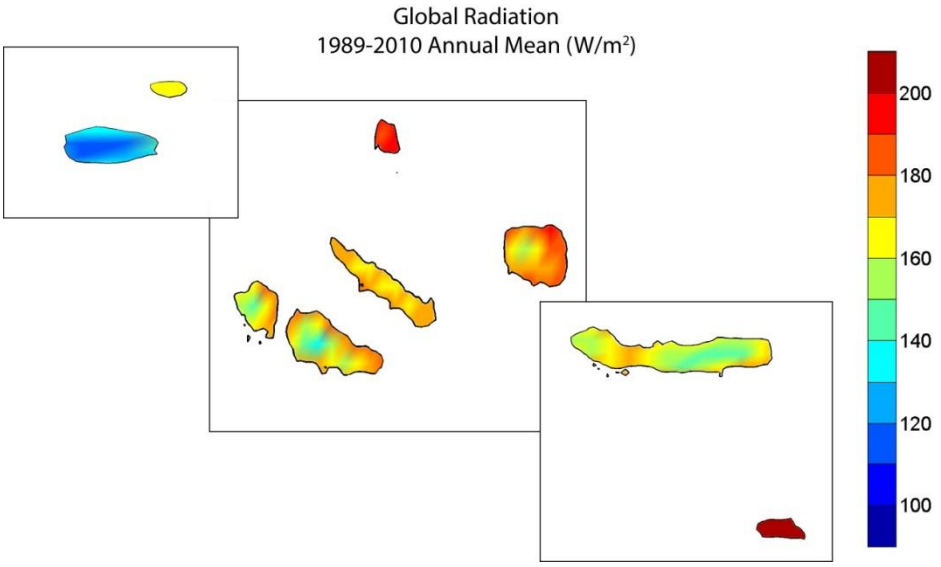

Figure 6.2 Annual corrected WRF global solar radiation for the Azores archipelago in present climate (1989-2010). Values are shown in W/m^2.

Seasonal means

The Azores archipelago is frequently affected by low pressure systems associated to weather fronts that cross the Atlantic Ocean. The polar front leads to low pressure systems which make the typical Azores weather to be considered as rainy between September to March. In the remaining months the impact of the Azores High influences the weather to be typically less rainy (Tome, 2013). Generally, the Azores climate is characterized as having mild annual oscillations. Regarding solar radiation it was found that a clear seasonal pattern is patent. The Western group, Flores and Corvo island, is the one which exhibit less variability between Winter and Summer months. Considering all the islands, the seasonal solar radiation means vary between 45 W/m^2 in Winter to 315 W/m^2 in Summer and as already found in the annual analysis are Graciosa and S^{ta} Maria the islands which present the higher values in any of the seasons.

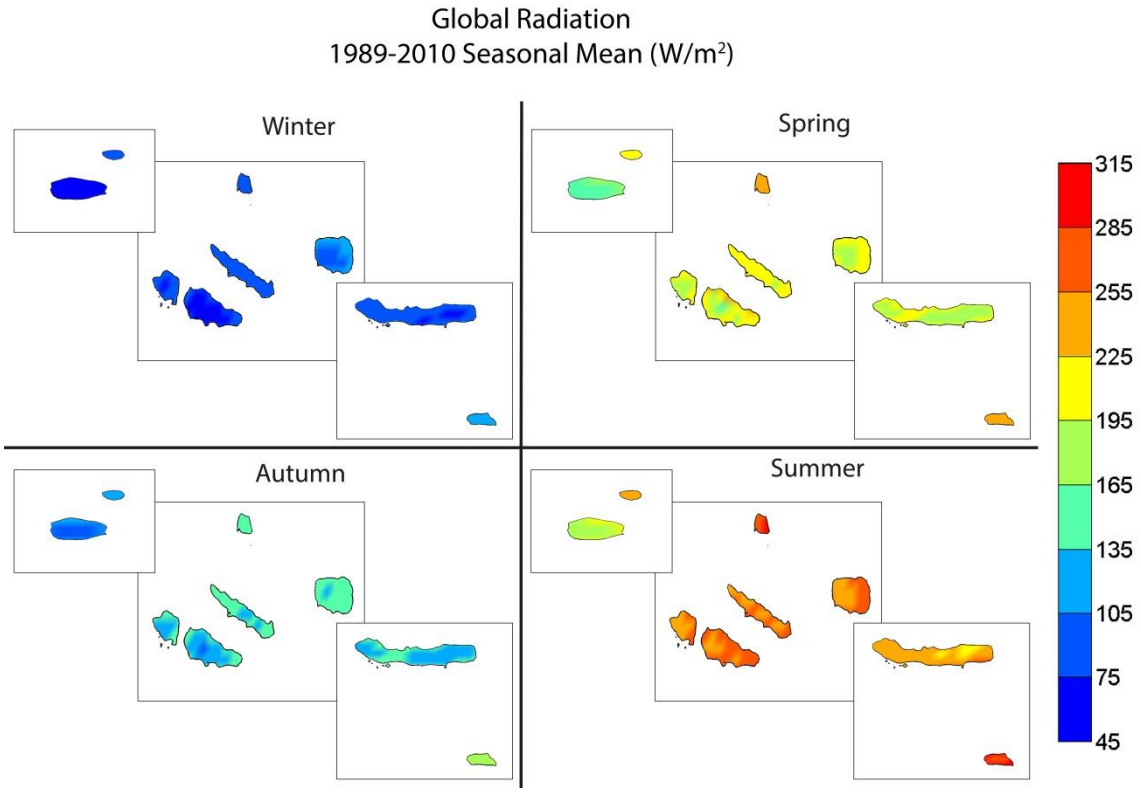

Figure 6.3 Seasonal corrected WRF global solar radiation for the Azores archipelago 1989-2010 present climate. Values are shown in W/m^2.

6.4 Future Climate

As already presented in Section 3.3, when RCMs are driven by GCMs used for analysis of climate change scenarios a fitting of its output using a pairwise MOS is not possible. So, the linear regression method used for bias correction of the present climate is not adequate for correction of the future climate WRF simulations. Thus the equidistant CDF method presented in Chapter 5 (Section 5.4) is used. The Li et al. (2010) 'equidistant CDF method' was used in the Iberian Peninsula future climate analysis in order to account the possibility of modification of the simulations climate change signal. This signal is often assumed to be stationary in time when MOS is applied to future simulations, as for example when it is used standard quantile mapping. Through the analysis of the Iberia Peninsula future climate it was found that the Li et al. (2010) method did not lead to a considerable impact on the climate change signal of the simulated solar radiation. However, since the climate conditions of the Azores islands are different from those of the Iberia Peninsula the same method is used in the current analysis ensuring in that way the opportunity to address the modification of the solar radiation climate change signal. One should also recall that albeit the equidistant CDF method is used for correcting the future simulations, for the historical simulations the method is, by construction, identical to the standard quantile mapping.

6.4.1 Biases in mean and variance of the historical reference WRF simulation

Before the MOS is applied the main aspects of the distribution errors of the historical simulation are examined: the bias in mean and standard deviation. Table 6.2 shows the BIAS in absolute (W/m^2) and relative magnitude (%) and normalized standard deviation results of the multi-year daily mean data of observations and WRF 1989-2010 historical simulation data for the locations analysed in the Azores islands.

Table 6.2. BIAS, shown in absolute (W/m^2) and relative magnitude (%), and normalized standard deviation ($\boldsymbol{\sigma_n}$) results for **multi-year daily mean** data obtained for Azores islands and WRF 1989-2010 historical reference simulation. (The superscripts C; W and E indicate Cental; Western or Eastern Group.)

	BIAS		$\boldsymbol{\sigma_n}$
	W/m^2	%	
Faial^{C}	29.35	16.89	1.11
Terceira^{C}	16.08	9.56	1.20
Graciosa^{C}	0.90	0.47	0.83
Pico^{C}	21.22	13.16	0.89
Flores^{W}	52.62	36.17	1.19
Corvo^{W}	20.89	12.64	0.93
Ponta Delgada^{E}	26.04	14.60	1.21
Nordeste^{E}	44.41	28.99	1.01
S^{ta} Maria^{E}	-1.53	-0.73	0.90

The model shows an overestimation of the solar radiation values in the historical simulation in all locations with exception to S^{ta} Maria Island. The spatial distribution pattern of the lowest and highest BIAS results is similar to the one observed in the analysis of the reanalysis driven climate (Section 6.3.1): Graciosa shows a negligible BIAS value (0.47%), Flores and Nordeste exhibit the highest BIAS of respectively 36% and 29% and Terceira, Corvo, Pico, Ponta Delgada and Faial present, in ascending order, BIAS values between 9.5% and 17%. In S^{ta} Maria is found an underestimation of the model however the BIAS magnitude determined, -0.73%, may be considered as negligible. The more accurate variability of simulated solar radiation values $-\sigma_n \approx 1 -$ is found in Nordeste. Ponta Delgada; Flores and Graciosa are the ones which present higher deviation between the observed and simulated solar radiation variability.

6.4.2 Model Output Statistics in future climate conditions

The relative biases of the solar radiation WRF historical simulation are well corrected with quantile mapping (Fig. 6.4a). The BIAS values which were, for uncorrected simulation (Fig. 6.4a, green bars), comprised between approximately -1 to 36% are now limited to values of -3 to 10% (Fig. 6.4a, red bars). The normalized standard deviation scores are after

quantile mapping correction closer to 1 in all locations. In Graciosa and S^{ta} Maria, the locations which presented negligible BIAS for the uncorrected data, the quantile mapping induced an increase in the BIAS scores. These locations, besides exhibiting such low BIAS, presented also a considerable underestimation of variability, i.e., a difference between the observed and simulated standard deviation (σ_n of respectively 0.83 and 0.9). Since quantile mapping corrects for errors in the shape of the distribution, the adjustment to all the quantiles led to an increase in the mean of the corrected simulated values, and consequently to the resulting BIAS. Graciosa and S^{ta} Maria show normalized standard deviation that reaches a perfect value after QM correction (0.98 and 1 respectively) and a BIAS that although higher than the one found for the uncorrected results are still small (3% and 2% respectively). Nevertheless it is carried out the same analysis for the assessment of the solar radiation future climate for these locations than the one for the remaining ones, i.e., including the bias correction methodology.

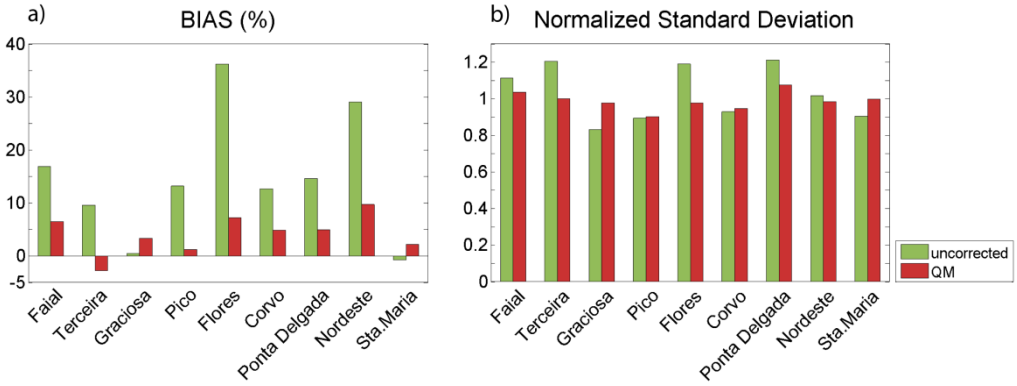

Figure 6.4 a) Relative BIAS and (b) normalized standard deviation results for multi-year daily mean data obtained for Azores islands and the QM-corrected (red) WRF historical reference. The results are plotted next to the statistical results obtained from the uncorrected solar radiation WRF historical reference values (green).

6.4.3 Azores solar resource for future climate

As presented in Section 6.3.3 a solar radiation map for future climate at the Azores archipelago is obtained using a probability-dependent correction function applied at each WRF gridpoint. The considerations and assumptions disclosed in Section 6.3.3 are also followed in the present section.

For Azores, the solar resource for future climate is analysed considering two time periods: the mid 21st century, from 2040 to 2059, and end of the century, from 2080 to 2099. Recalling the characteristics of the WRF simulations presented in Section 2.2 and as presented in the Iberia Peninsula assessment, in this section, the future climate WRF simulations are obtained under the RCP8.5 scenario driven by the EC-EARTH climate model.

Annual mean

The projected solar resource of the Azores archipelago for the mid (2040-2059) and end (2080-2099) of the century is shown in Figure 6.5. Future mean annual values of solar radiation (Fig 6.5. a and b) and relative differences (anomalies) between future and present climate (Fig 6.5. c and d) are shown. Here, present climate refers to the 1989-2010 historical climate simulation which constitutes the baseline for the determination of the anomalies. The results obtained from the analysis of the individual locations, may be consulted in Table C2, Appendix C. Given the small amount of locations and the redundancy of the analysis here it is focused the outcome of the solar radiation maps.

The annual means of the Azores archipelago for the mid and end of the century vary between approximately 110 and 210 W/m^2. The difference between the mean results obtained for 2040-2059 and 2080-2099 is not statistically significant. Nevertheless, it is found, in both mid and end of the century (Fig.6.5 a and b), that Flores and Corvo are the islands with lower annual solar radiation means while Graciosa and S^{ta} Maria exhibit the higher values. As was pointed out in Section 6.3.3 in the islands Pico; Faial; São Miguel and Terceira it is possible to identify areas with lower solar radiation means which correspond to the location of the highest elevations of each island. Also, when comparing the uncorrected mean solar radiation values to the ones obtained after MOS (Fig. C3 Appendix C) it is found once again that there is consistency between them being possible to observe that it is the range of solar radiation values that is obviously modified.

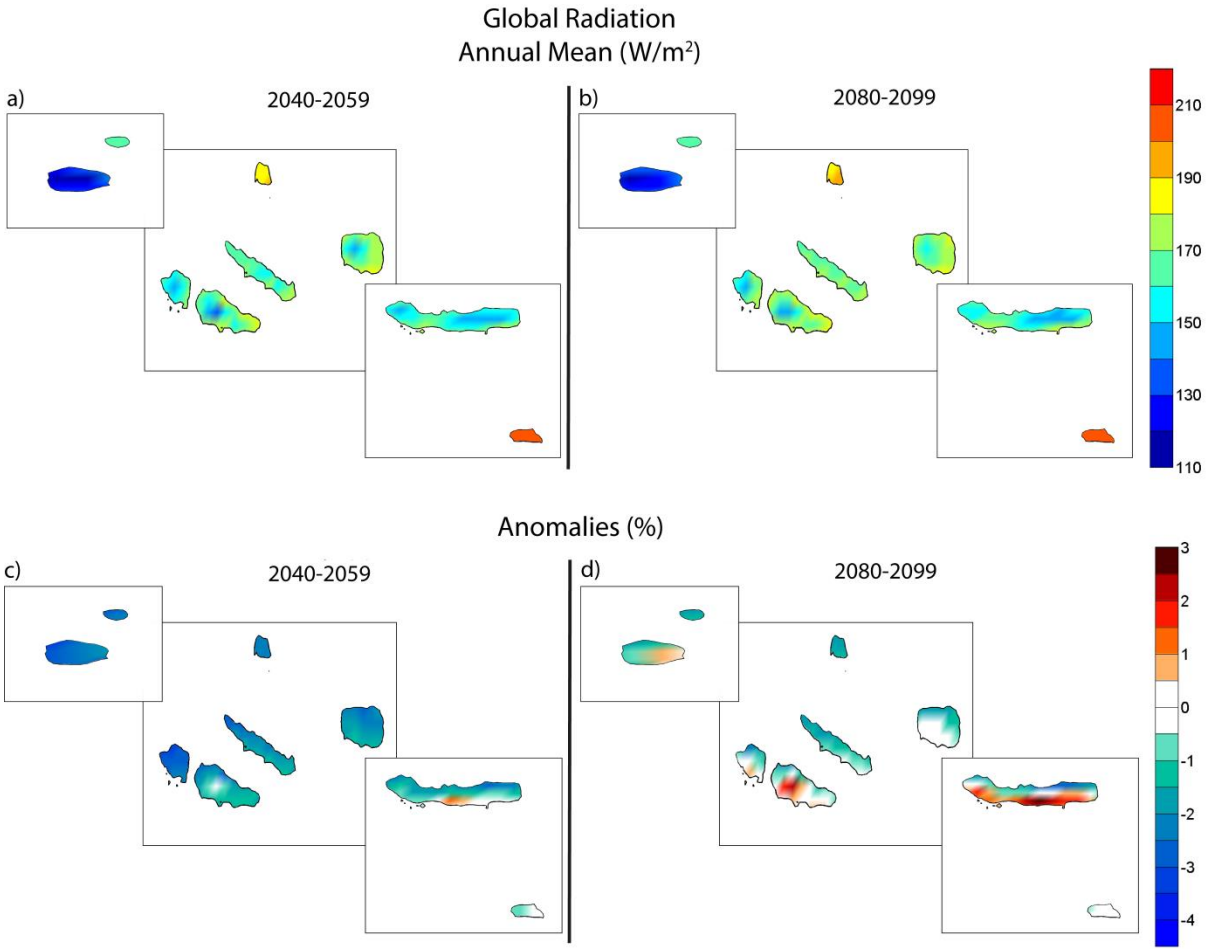

Figure 6.5 (a; b) Annual mean maps (W/m^2) of projected WRF solar radiation for the mid (2040-2059, left panel) and end of the century (2080-2099, right panel) after correction and (c; d) respective anomalies (%) considering the historical climate run (1989-2010) as baseline.

In Section 6.4.1, when discussing the impact of the QM method used to correct the historical reference WRF simulation, Graciosa and S^{ta} Maria were shown to be locations that experienced an increase in the resulting BIAS after correction. Interestingly, it is seen that those two islands show a small difference when compared between the maps of uncorrected mean solar radiation and the one obtained after MOS (Fig. C3, Appendix C). This leads one to infer that the influence of the equidistant CDF mapping in the future simulations for the Graciosa and Sta Maria islands is less noticeable then for the remaining islands. Still, one should mention that, in fact, when comparing the baseline climate with both instances of future climate it is found that, at 90% significance level, the hypothesis that their means are different is not rejected. This was found to be true for both situations of comparing uncorrected or corrected data (not shown here). Nuances of the differences between baseline and future climate are better illustrated in the anomalies maps (Fig. 6.5 c and d).

For the future climate, in the Azores islands, a decrease of solar radiation mean values is predicted for most of the territory for the mid century, which will vary between approximately -3.5% and 0.5%. In this future period, negative anomalies dominate entirely

throughout the islands. In the central-Southern region of the São Miguel Island however a slight increase of approximately 1% surrounded by areas with no distinct anomalies is predicted. In the Eastern part of S^{ta} Maria Island and in the area corresponding to the high altitude mountain in Pico also no distinct anomalies are predicted for the mid-century. For the end of the century, the predicted anomalies exhibit a more accentuated increase of solar radiation in the Southern region of São Miguel, the entire higher altitude mountain region of Pico, Eastern part of Flores and a limited area in Southern Faial. These positive anomalies are projected to vary between 0.5 to 3%. The negative anomalies predicted for the end of the century cover a much smaller area and are also less intense (i.e., closer to zero) when compared to the mid-century results. Also, the areas with no distinct anomaly emerge in wider regions: the Southwestern region of Terceira; large areas in central and South region of Pico; South and Western areas of Faial and almost the entire island of S^{ta} Maria. These results may be used to draw a parallelism to the findings reported by Tomé (2013) concerning the future projections of precipitation amount in the same WRF simulations used in the present analysis. This work showed that the islands Pico, Terceira, São Miguel and S^{ta} Maria are expected to have losses of precipitation amount with values of over 10% at the end of the century. Results for solar radiation and precipitation thus seem to be consistent.

When compared to the anomalies determined using the uncorrected WRF solar radiation data (Fig. C4, Appendix C) it is found that the results do not differ much between them. Considering this and the discussion above, it is reasonable to conclude that the MOS used in the analysis of the solar resource for future climate in the Azores archipelago does not have a clear influence on the climate change signal. As discussed in Chapter 5 this aspect is consistent with the conclusion also made in the analysis of the Iberian Peninsula solar resource for future climate.

Seasonal means

The seasonal annual means of solar radiation for the mid and end of the century are displayed in figure 6.6. It can be seen that the mean values obtained for the period 2040-2059 (Fig.6.6, left panel) do not differ much from the ones of 2080-2099 (Fig.6.6, right panel). The seasonal means vary between 45 W/m^2 in Winter to up to 315 W/m^2 in Summer. In the Summer season, Graciosa; S^{ta} Maria; Pico and Corvo represent the islands with higher solar radiation means, with values above 255 W/m^2, at both the mid and end of the century. In Winter, the islands of Flores and Pico have the lower solar radiation means which values fluctuate approximately between 45 and 105 W/m^2.

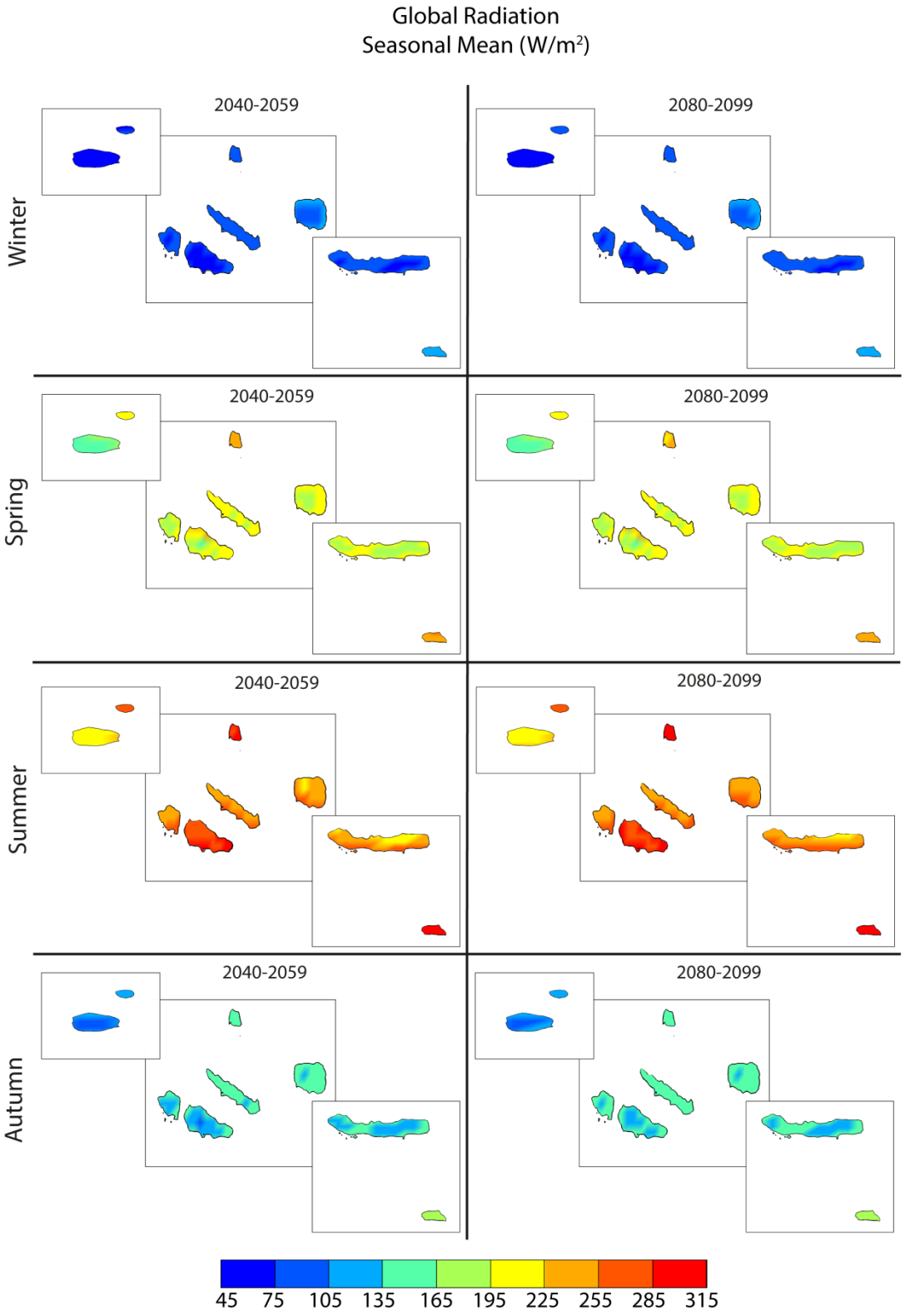

Figure 6.6 Seasonal mean maps (W/m^2) of projected WRF solar radiation for the mid (2040-2059, left panel) and end of the century (2080-2099, right panel) after MOS correction.

In Figure 6.7, the seasonal anomalies of projected solar radiation values for the mid (2040-2059, left panel) and end of the century (2080-2099, right panel) determined after MOS correction and considering the historical climate run (1989-2010) as baseline are shown.

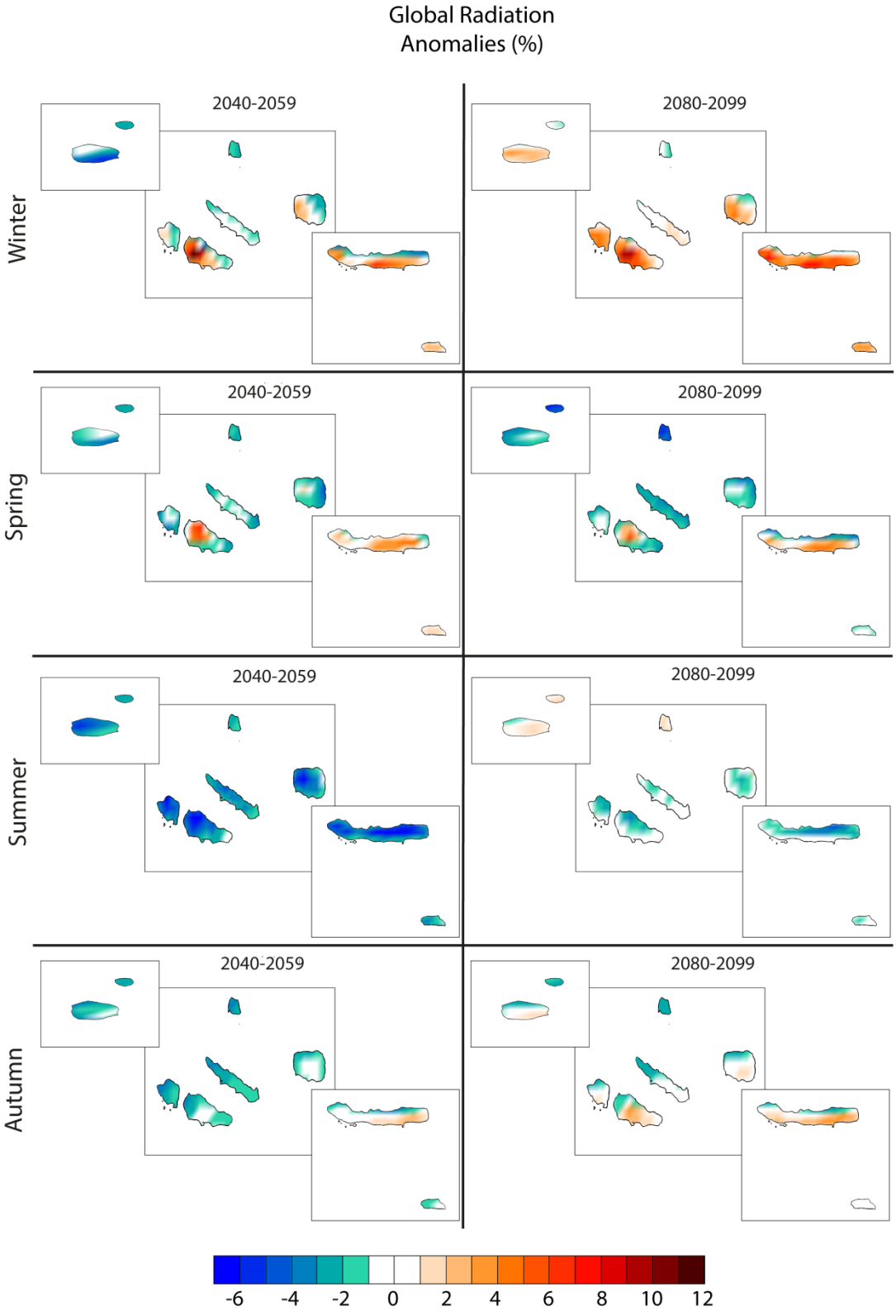

Figure 6.7 Anomalies (%) of projected WRF solar radiation for the mid (2040-2059, left panel) and end of the century (2080-2099, right panel) after MOS correction considering the historical climate run (1989-2010) as baseline.

The subtleties of the differences existent between the solar radiation means are better perceived though the anomalies analysis. One of the issues that stand out on the results obtained is that that Winter shows the larger positive anomalies projections with values that reach up to 10-12%. On the other hand, more negative anomalies are projected for the Summer. At the mid century, in Summer, the anomalies vary mostly between approximately -6% to -1%, while by the end of the century it is projected, for the same season, anomalies between -3% to 2% in the majority of the territory. It is therefore evident, as already perceived in the annual analysis above, that the solar radiation values are expected to experience a slight decrease until the mid century but that it will have the tendency to be reverted by the end of the century. This is found to be valid for all the seasons with exception of Spring. In that season the projections point to the opposite situation when comparing the results of the 2040-2059 and 2080-2099 period. As already mentioned, it is in Winter that the higher positive anomalies are projected with values that reach up to 10-12%. Although it is also valid for this season the inference that the solar radiation values are expected to decrease by the mid century and latter increase by the end of the century, in Pico, in the area correspondent to the higher altitude location this is not accurate. In this location the determined anomaly presents a slight decrease from 10-12% to 7-10%.

Considering the entire seasonal cycle of the projected anomalies the islands of Pico, São Miguel and Faial are those which experience the greatest variability, from Winter to Summer, in each of the periods analyzed.

6.5 Conclusions

A simulation of solar radiation values for present climate produced by the regional climate model WRF (6km) driven by the ERA-Interim reanalysis for the Azores archipelago was evaluated. The model output was assessed by means of standard statistical errors and PDF matching scores and using multi-year daily means of solar radiation observations collected at 9 locations during the years 1999-2009. These locations represent a point per island except São Miguel, which include two points and São Jorge, where no observational data was available.

The correlations found between the simulation and observations are high, ranging from 0.89 to 0.93. Excluding the results of S^{ta} Maria Island, it was also found that WRF systematically overestimated the values of solar radiation in all locations with values ranging from 7% to up to 37%. In S^{ta} Maria it was found an underestimation of solar radiation of around 3%.

To correct the solar radiation WRF biases statistical correction methods were applied. Linear regression and quantile mapping were used and compared. The major advantage of

the quantile mapping approach i.e., the ability to realistic correct the variance of a given data considering not only its mean value, was shown not to be highly relevant for the specific multi-year daily means of solar radiation. Although it was obtained slightly poorer results of corrected variances for linear regression, this approach led not only to negligible BIAS values in all the locations but also to a more accentuated decrease on MAPE and RMSE when compared to the QM approach. The resulting PDF matching scores for both methods were similar. These results lead to the option to use the linear regression method for the correction of the WRF solar radiation output which, combined with a probability-dependent correction function, allowed to obtain an annual and seasonal solar resource map for the present climate with a complete spatial coverage of the entire Azores archipelago.

Additionally, future projections for the mid and end of the 21st century of the Azores solar resource were also performed. EC-Earth driven WRF simulations (6km) considering RCP 8.5 scenario were used for the periods 2040-2059, 2080-2099 and the historical reference 1989-2010 baseline period. When RCM's are driven by GCM's used for analysis of climate change scenarios a fitting of its output using a pairwise MOS is not possible. So, quantile mapping was used for correction of the model biases. For future projections an adaptation of the standard quantile mapping was used following the method presented by Li et al. (2010). As before (Section 6.3.3) the probability-dependent correction function was used to obtain a solar resource map (both annual and seasonal) for the future climate at mid and end of the century.

The annual means obtained for the Azores archipelago for the mid and end of the century vary between approximately 110 and 210 W/m^2. Anomalies maps are also presented for the two instances in time addressed for the future climate. For the future climate, in the Azores islands, it is predicted a decrease of solar radiation mean values in the majority of the territory for the mid century which will fluctuate between approximately -3.5% and 0.5%. The negative anomalies predicted for the end of the century represent a much smaller area and are also less intense (i.e., closer to zero) when comparing to the mid-century results. However, for some regions of São Miguel and Pico were predicted positive anomalies with values between 0.5 to 3%. When comparing the anomalies determined using the uncorrected WRF solar radiation data it was found that the results do not differ much between them, and so it is concluded that the MOS used in the analysis of the solar resource for future climate in the Azores archipelago does not have a clear influence on the climate change signal. However it is still obvious that the methodology impacts the conclusions obtained due to the fact that the range of solar radiation mean values are updated after correction of the WRF output.

It should be stressed that the present study considers only a single RCM driven by a specific GCM and climate projection scenario which does not fully addresses the associated uncertainties of the analysis. One should keep in mind that reliable measures of global solar radiation are fundamental for the success of such an analysis. However, for Azores it was only available multi-year daily means and the consistency of the database in terms of number of years used to derive each individual daily mean is also somewhat deficient.

Because of this, the results here presented should be regarded with some care. Moreover the fact that it is used only one location per island to derive the necessary values for correction of all the WRF grid points correspondent to that same island constitutes also a limitation of the methodology used. Despite these shortcomings this study constitutes a valuable work in the field of not only correction of bias from numerical model's solar radiation output, but especially for providing solar resource maps for the Azores archipelago which, until this date, had not being considered in similar research.

Chapter 7

Assessment of diffuse radiation models for the Azores region

Measurements of diffuse, global and direct solar irradiance are key to a proper assessment of the potential of solar energy technologies. Unfortunately, worldwide measured irradiance databases usually consist of only global solar radiation data, often with limited spatial coverage. The estimation of the diffuse fraction from global radiation is therefore essential. Solar radiation models for prediction of hourly diffuse fraction from global radiation are reviewed in this chapter in order to explore their applicability to the Azorean region. Since models of diffuse fraction exhibit some degree of location dependence, a correction to the best performance model to improve the results for the studied region by considering the solar zenith angle is also presented.

The results of this Chapter have been published in: Magarreiro, C., Brito, M. C. & Soares, P. M. M. (2014) Assessment of diffuse radiation models for cloudy atmospheric conditions in the Azores region, *Solar Energy*, 108, 538-547.

7.1 Background

Throughout the world, measured irradiance databases consist almost entirely of global solar radiation; additionally, its spatial coverage is limited. Driven by these limitations, several solar radiation models have been developed. Estimating the fraction of global radiation which is diffuse is a valuable asset, in particular for the project of solar energy conversion systems which require detailed information of the two components. It is not only the performance of the system which is at stake but also the appropriate selection of solar technology, e.g. the option for concentrated photovoltaics may not be adequate for a location with a significant fraction of diffuse radiation.

Liu and Jordan (1960) work was pioneer in the development of solar radiation models. These authors presented empirical relationships between daily diffuse to daily total radiation and monthly average daily diffuse to monthly average daily total solar radiation. The measurements of global radiation used to develop these methods were collected in Massachusetts, United States of America. Following the work by Liu and Jordan, Orgill and Hollands used the same approach to estimate the diffuse fraction, also using the clearness index as the only variable (Orgil and Hollands, 1997). Hollands and Crha accounted the scattering of radiation between two atmospheric layers and the ground including variables of ground albedo, transmittance of the upper layer of the atmosphere and scattering albedo of the lower layer (Hollands and Crha, 1987). Orgil-Hollands and Hollands-Crha model developments and validation were based in solar radiation values recorded in Canada. The model proposed by Maxwell (1987) also stands out among those based in US data. It is a model developed as a quasi-physical model. It incorporates parametric variables associated to discrete changes in the atmospheric transmittances, rather than to the magnitude of atmospheric transmittances, leading to a simple model in which the effect of those parametric variables is intrinsically accounted.

The applicability of the different models is obviously related to the local atmospheric conditions and its climatic characteristics. Models are not of general validity and can only be applied to where the albedo of the surrounding terrain and the atmospheric contamination by dust are not greatly different from those where the corresponding methods were developed. Driven by this reason an effort to expand the range of diffuse fraction models has been made throughout time by several authors. Models adjusted to data acquired in Europe are mainly linked to Northern, Central or, more recently, Mediterranean areas (e.g.: Skartveit et al. (1998); Reindl et al. (1990); Karatasou et al. (2003); Miguel et al. (2001)). To the authors' knowledge, there are no published studies focused in Azores or in any place with similar climate/cloud characteristics. The existence of mid latitude islands is scarce and, notwithstanding, the typical Atlantic climate of Azores Islands is not very common in other regions. The Azorean climate reveals in its annual cycle an important amount of cloud cover with a variability which is more complex than the common Summer/Winter pattern.

This study explores the applicability of different existing correlation models of diffuse fraction and clearness index or other plain parameters in the Azorean region. Furthermore,

after assessing their performance, a correction of the best performing model is suggested for improving the global solar radiation decomposition for Azores.

7.2 Diffuse fraction models and methods

The diffuse solar radiation models available in literature have been developed for use with hourly, daily and monthly averaged values of global radiation. This work evaluates existing models focusing on hourly data since it is the most widely used time step when estimating the dynamic behavior and performance of solar energy systems.

The selection of hourly models was mainly based on three features: model simplicity, where simplicity stands for the minimum input of meteorological parameters and models' implementation ease of use, the reported model performance and the availability of the required measurement data. Additionally, a broad range of locations from where models derived was also considered.

7.2.1 Diffuse fraction – clearness index regression models

The simplest, practical and most common diffuse radiation models attempt to correlate the diffuse fraction (the ratio of diffuse component (D) from global radiation (G), k_d) with the clearness index (ratio of horizontal extra-terrestrial radiation (G_{ex}) reaching the Earth's surface, $k_t = G/G_{ex}$). They are usually developed through piecewise fitting and divided in three intervals according to the k_t range. The first, second and third intervals represent data for overcast, partly cloudy and clear sky, respectively. The first and second k_t intervals correlations are usually developed using linear and polynomial functions and the most appropriate k_t interval which minimizes the standard error of the final correlation. The clear sky k_t range may also include data from conditions of sky with some cloud cover scattered in a way that there is no shading of the sun itself and, since the scattered clouds will reflect the solar radiation and act as diffuse radiation concentrators, records of instantaneous solar radiation may have a significant portion of diffuse radiation besides the strong beam radiation. As there is generally a limited set of data in this range, and given the unpredictable nature of cloud reflection, it is customary to assume a constant value of the diffusion fraction for this interval (Orgil and Hollands, 1997).

Erbs et al. (1982) used a database from four USA weather stations to develop an estimation of the diffuse fraction of hourly, daily and monthly average global radiation and to determine the degree to which the relationships established were dependent on season and location.

Soares et al. (2004) and Oliveira et al. (2002) developed models for the city of São Paulo, in Brazil, applying slightly different techniques. Using linear regression fitting, Oliveira et al. (2002) were able to model daily and monthly values of diffuse radiation. Soares et al. (2004) improved the estimation by using a neural network synthetic series to develop a polynomial model.

Chandrasekaran and Kumar (1994) also established the relationship between hourly diffuse fraction and k_t for a tropical location, Madras, India.

The model of Reindl et al. (1990) used measurements from Northern Europe and North America to study the influence of climatic and geometric variables on hourly diffuse fraction. These authors intended to determine if other predictor variables, in addition to the clearness index, significantly reduce the standard error of this type of correlations. They established three correlations: taking into account i) clearness index, solar altitude, surface temperature and relative humidity; ii) solar altitude and clearness index; iii) only clearness index. The results showed that, on an overall basis, correlation i) reduces the composite residual sum squares by around 14% when compared to the k_t only correlation.

The studies developed from data of the Mediterranean area considered in this study are the models of Karatasou et al. (2003) and Miguel et al. (2001). Miguel et al. (2001) evaluated existing models with data from the north Mediterranean area and developed new daily and hourly correlations. The locations include sites in Portugal, Spain, France, Italy and Greece. Karatasou et al. (2003) model was derived from Athens data; it only uses k_t and focuses on hourly and daily values. The statistical analysis performed by Karatasou et al. (2003) between their model and Reindl, Erbs, Liu and Jordan and Orgill-Hollands models demonstrated a decrease of 10-20% of the root mean square error (RMSE).

Table 7.1 lists the parameters estimates for the referenced models. Coefficients and k_t intervals are shown.

Table 7.1 Coefficients and k_t intervals of the polynomial models applied.

Models	k_d	Intervals
Erbs et al.	$1.0 - 0.09\ k_t$	$k_t \leq 0.22$
	$0.951 - 0.1604\ k_t + 4.388\ {k_t}^2 - 16.638\ {k_t}^3 + 12.336\ {k_t}^4$	$0.22 < k_t \leq 0.80$
	0.165	$k_t > 0.80$
Soares et al.	1.0	$k_t \leq 0.17$
	$0.90 + 1.1\ k_t - 4.5\ {k_t}^2 + 0.01\ {k_t}^3 + 3.14\ {k_t}^4$	$0.17 < k_t \leq 0.75$
	0.17	$k_t > 0.75$
Chandrasekaran and Kumar	1.0	$k_t \leq 0.24$
	$0.97 + 0.80\ k_t - 3.00\ {k_t}^2 - 3.10\ {k_t}^3 + 5.2\ {k_t}^4$	$0.24 < k_t \leq 0.80$
	0.17	$k_t > 0.80$
Karatasou et al.	$0.9995 - 0.05\ k_t - 2.4156\ {k_t}^2 + 1.4926\ {k_t}^3$	$k_t \leq 0.78$
	0.17	$k_t > 0.78$
Miguel et al.	$0.995 - 0.081\ k_t$	$k_t \leq 0.21$

	$0.724 + 2.738\ k_t - 8.32\ {k_t}^2 + 4.967\ {k_t}^3$	$0.21 < k_t \leq 0.76$
	0.18	$k_t > 0.76$
Reindl et al.	$1.012 - 0.248\ k_t$	$k_t \leq 0.3$
	$1.45 - 1.67\ k_t$	$0.3 < k_t \leq 0.78$
	0.147	$k_t > 0.78$

7.2.2 Diffuse fraction – clearness index and additional parameters regression models

Whenever further information and meteorological parameters are available for the site under study, it may be interesting to improve the diffusion radiation models including those inputs.

Maxwell (1987) used physical principles to develop a model using empirical data-fitting techniques, known as a quasi-physical model. The algorithm – Direct Insolation Simulation Code (DISC) – requires input of global horizontal irradiance, the clearness index and the air mass to assess the discrete changes in atmospheric transmittances. The model estimates the direct beam solar radiation (I) arriving at Earth's surface and then the diffuse component is deduced from its difference to the measured global solar radiation.

Skartveit et al. (1998) presented a model for the diffuse fraction of hourly global radiation involving clearness index, solar elevation, regional surface albedo and an hour-to-hour variability index. The model was tuned for Norway and consists of a snow free terrestrial model with the possibility of including surface albedo. The variability index parameter improves the model while being a rough diagnostic tool to statistically detect the presence of variable and inhomogeneous clouds. In fact, diffuse radiation is highly affected by clouds; scattered clouds on the sky may enhance the diffuse radiation while a break in an extensive cloud deck may boost the global radiation due to higher beam radiation contribution. In an attempt to perceive these effects, the variability index (τ) is defined as the root mean squared deviation between the clear sky index at a time (ρ) and the subsequent (ρ+1) and preceding (ρ-1) hour. For $\tau \approx 0$, representing invariable hours, the diffuse fraction k_d is then separated into four situations, depending on the value of the clearness index: i) $k_t \leq 0.22$, no significant beam irradiance at any solar elevation; ii) $0.22 \leq k_t \leq k_2$, broken clouds which partly obscure the sun; iii) $k_2 \leq k_t \leq k_{max}$, from the assumption that the beam radiation does not exceed a maximum value ($k_{b\,max}$) k_{max} limits the upper bin; iv) $k_t \geq k_{max}$ meaning that k_t may exceeds k_{max} due to diffuse irradiance from clouds not obscuring the sun. The limits k_2 and k_{max} are functions of solar elevation. In cases where τ>0, i.e. variable hours, a term is added to account for the effect of variable and inhomogeneous clouds. High values of τ are associated to broken clouds and low τ is associated to overcast or nearly clear sky.

Driven by the inadequacy of the diffuse models available for southern latitudes, in particular in Australia, Boland et al. (2001) developed a new model. Unlike the usual binning of data according to the different values of clearness index, they proposed a logistic function fitting for the whole range of clearness index Boland et al. (2008). The model was further improved with multiple predictors such as hourly clearness index; daily clearness index; solar altitude; apparent solar time and a measure of persistence of global radiation (Ridley et al., 2010). This model is hereafter referred as BRL, the Boland-Ridley-Lauret model.

The models mentioned above do not directly account for the presence of clouds in the sky. The cloud cover is not an often measured parameter, but since it was available in the database used, an attempt was made to determine how the diffuse solar irradiance prediction could benefit from the application of such models.

The model developed by Kasten (1983), tested under the International Energy Agency Task IX (Davies et al., 1988), is a total cloud based model comprising the calculation of direct beam radiation using

$$I = G_{ex}\, e^{(-T_1 \tau_1 m)}(1 - C) \tag{11}$$

where C is cloud cover and T_1, the Linke turbidity factor can be derived from:

$$\frac{G}{G_0} = 1 - aC^b \quad \text{and} \quad G_0 = G_{ex}\, A\, e^{(-BT_1 m)} \tag{12}$$

where G_0 gives the cloudless sky radiation and, a, b, A, B are fitted coefficients.

7.3 Data

The analysis was performed with data from Graciosa Island obtained through the Atmospheric Radiation Measurements (ARM) Climate Research Facility. It consists of measures of global and diffuse solar radiation retrieved at every 60 seconds between May 2009 to December 2010 (Section 2.1). For the purposes of this chapter the variables are aggregated to hourly mean values. This data is supplied with the option of being previously assessed in a quality control (QCRad, Long and Shi, 2006) to ensure its high quality. Figure 7.1 shows the time series of only global and diffuse irradiance for the full measurement period.

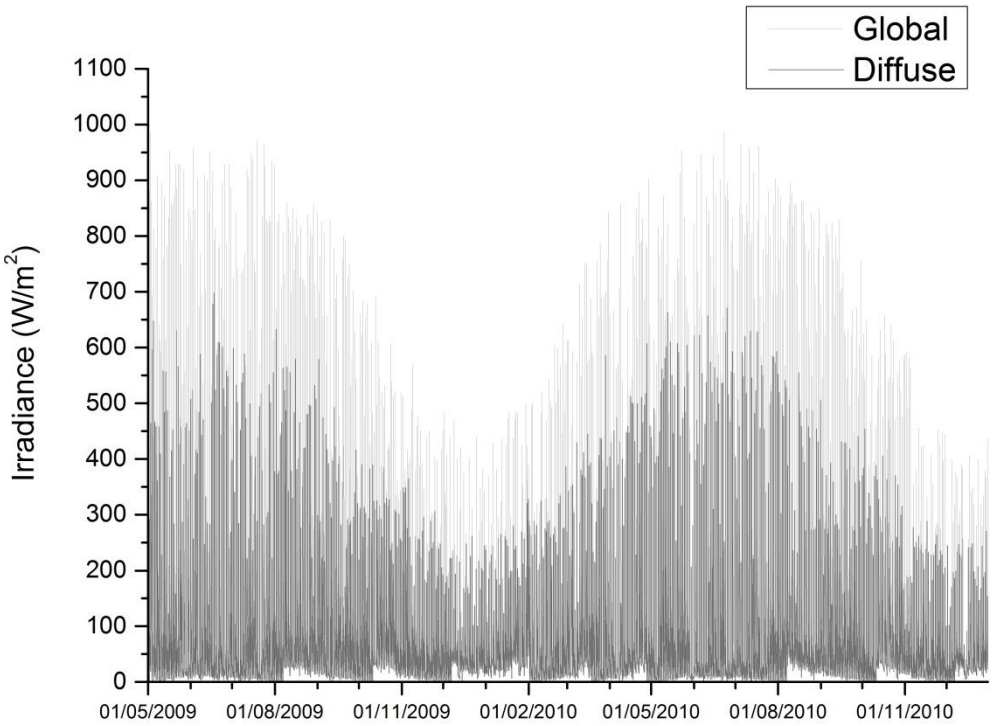

Figure 7.1 Hourly global and diffuse irradiance: values corrected with QCRAD.

The atmospheric conditions of Azores are highly influenced by marine boundary layer clouds which are passive modulators of solar energy. Hence, the link between radiometric variables and information of clouds presence in the sky is crucial to be addressed. However, cloud cover is not a common available measure and, in this work, it was only possible to explore this bond due to the extent of the ARM campaign from which data was acquired.

The cloud cover which is the percentage of cloud presence in the sky used in this chapter was retrieved by a Total Sky Imager (TSI) which captures images of the sky during daylight hours. The raw sky images are then processed to infer fractional sky cover (Section 2.3).

7.4 Performance results and discussion

As previously mentioned models are commonly developed through piecewise or single polynomial regression fittings of the relationship between clearness index and diffuse fraction. The distribution of points depends then on the site (and therefore atmospheric conditions) where data was collected. Unsurprisingly, a low clearness index, related to an overcast weather sky, implies a small portion of radiation reaching the Earth's surface compared to the extra-terrestrial radiation. On the other hand, a high clearness index is associated to clear sky conditions while intermediate values are linked to situations of partially cloudy sky.

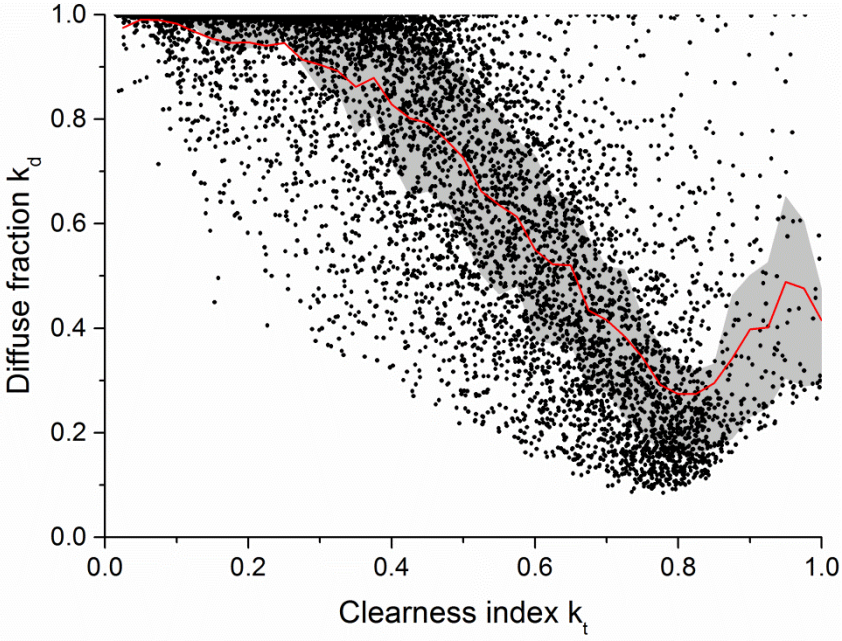

Figure 7.2 The hourly diffuse fraction k_d (measured values) as a function of clearness index k_t. Grey region represents the band between the 25th and 75th quantile and in red is the mean line.

Figure 7.2 shows the dispersion of clearness index values along the experimental range of diffuse fraction from Graciosa data. In cloudy conditions, a high density of k_d high values are present. On the other hand, there is a large variability of measured k_d for each k_t value, in particular in the partially cloudy k_t range, but also extending to the upper limit of k_t. Scattered clouds on the sky dome may enhance the diffuse irradiance through intense forward scattering of solar radiation while the beam irradiance stays unaffected. This effect may be the reason for the presence of high clearness index with high diffuse fraction data records. These high values of k_d with corresponding high k_t values is sometimes labelled as bad data (Boland et al. 2008) but considering the quality check procedures performed, here are not assumed as related to erroneous reading. This is particularly relevant for the Azores location, whose climate is strongly marked by cloudy conditions and high atmospheric turbidity. It is worth mentioning that only 17% of the data points analysed correspond to records below 40% cloud cover and that almost 50% correspond to records above 80% cloud cover.

The accuracy of the models for the period May 2009 – December 2010 was assessed by means of standard statistical errors and by probability density functions (PDFs) matching score (S). The considered error measures are: MAE (Mean Absolute Error) and its normalized value MAPE (Mean Absolute Percentual Error), RMSE (Root Mean Square Error) and BIAS. These indicators are defined in Section 3.1. The overall statistical errors obtained are reported below, in Table 7.2.

The hourly diffuse irradiance predicted with the selected models is represented in Figure 7.3 against the diffuse measured values. The scatter plots analysis gives some insights into the performance of the models.

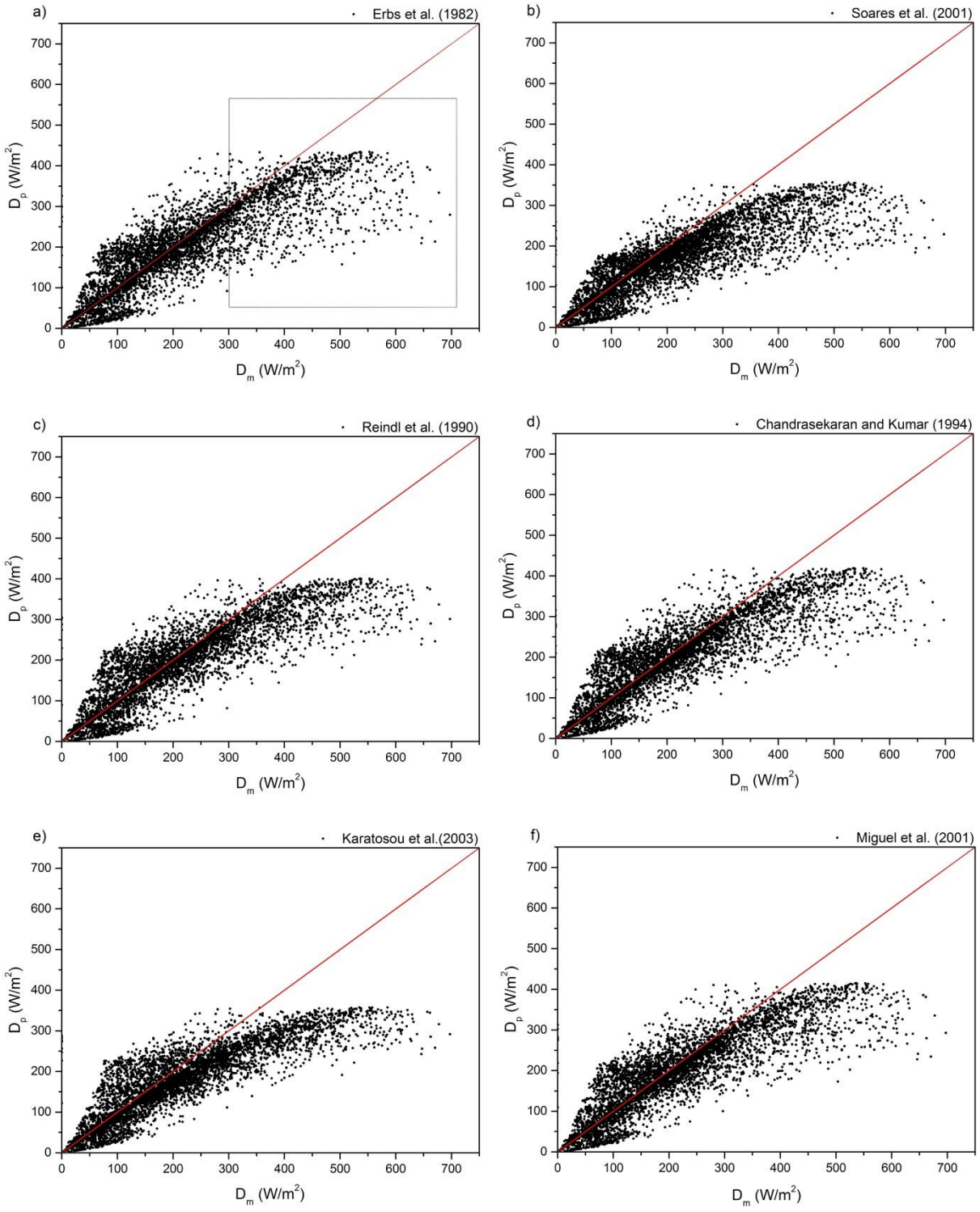

Figure 7.3 Diffuse irradiance measured vs. Diffuse irradiance predicted trough the different models. Straight lines represent diagram diagonal.

Models based on the clearness index, such as those of Erbs, Soares, Chandrasekaran and Kumar, Karatosou, Miguel and Reindl, present a similar pattern. The dispersion of paired values on the scatter plots of Figure 7.3 show clearly an underestimation of diffuse irradiance for high diffuse radiation values. Between 200 and 300 W/m^2, the distribution of points in the scatter plots bends downwards with respect to the approximate 1:1

relationship (the box drawn in Fig.7.3a illustrates this feature). Below this limit, the measured diffuse radiation is well described by the different models, in spite of with large spread.

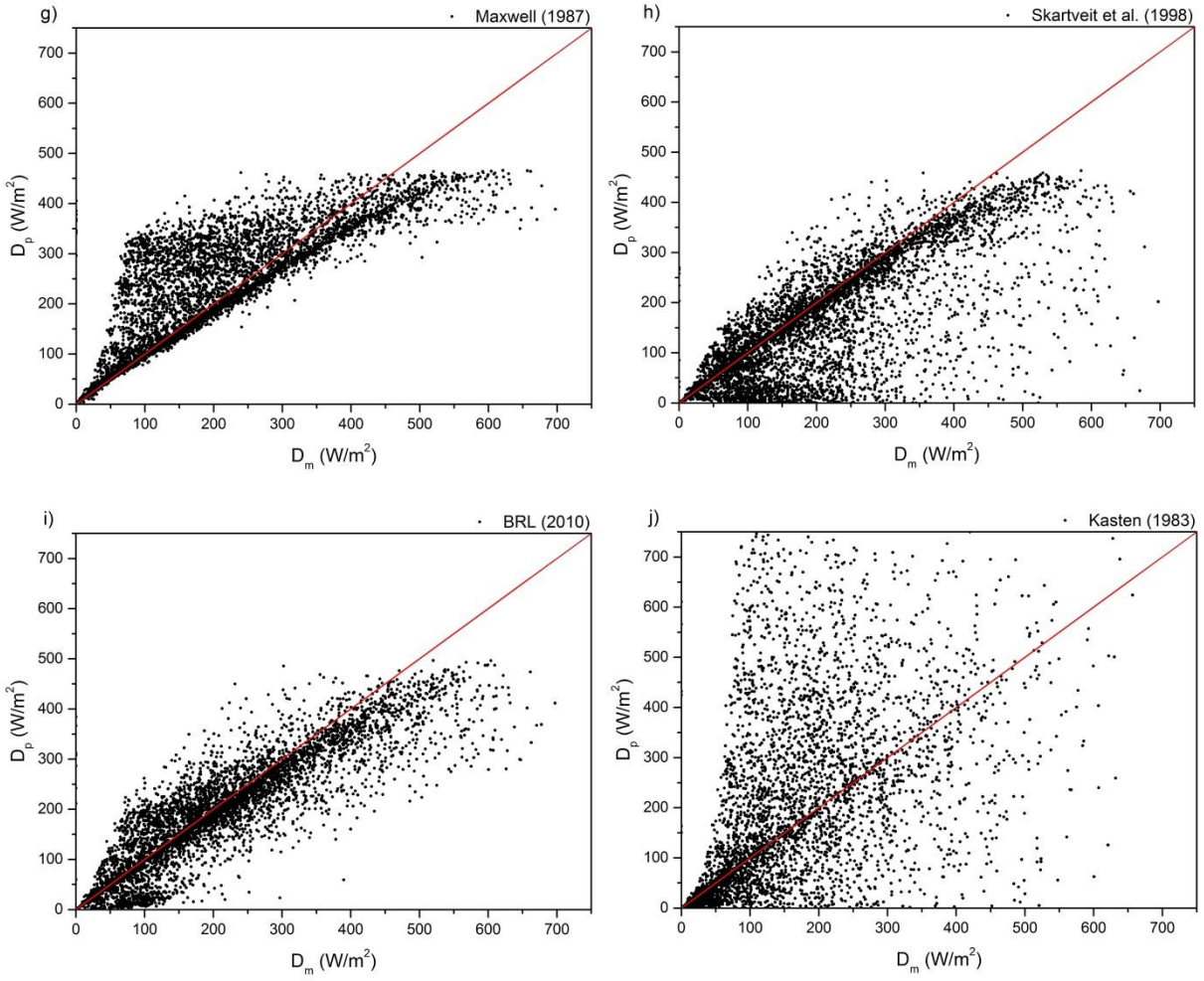

Figure 7.3 (continued)

Figure 7.4 shows where the set of points of measured diffuse radiation above 300 W/m^2 stands in the diffuse fraction-clearness index scatter plot. The corresponding k_t-k_d pairs of these values (red dots) seem to present no particular distribution, i.e., one cannot simply state that there is a certain range of k_d or k_t that is intrinsically related to them.

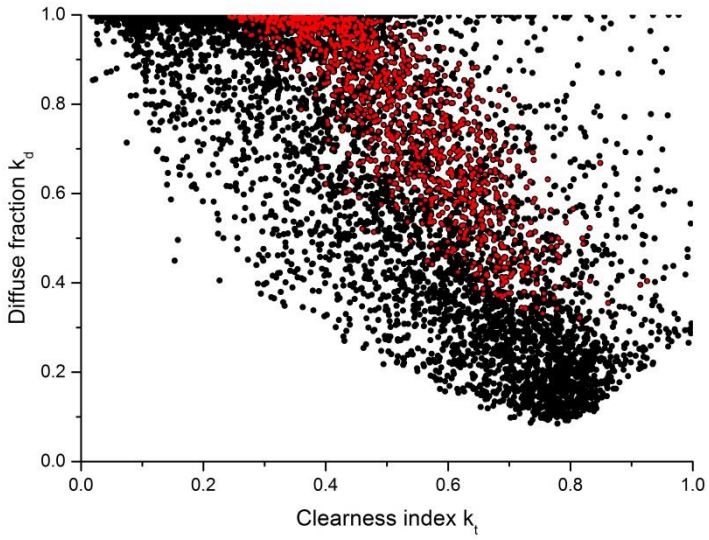

Figure. 7.4 Location of k_t-k_d pair's which correspond to diffuse radiation above 300 W/m^2 (red dots) in the clearness index k_t – diffuse fraction k_d scatter plot.

The underestimation of predicted diffuse irradiance may reflect the inadequate suitability of the models in such conditions. With particular reference to Soares, Chandrasekaran and Kumar and Reindl models it can be said that they were developed with data that do not have the similar concentration of high diffuse fraction values along the k_t range as the one that was found in the data used in this study.

The overall statistical errors obtained (Table 7.2) reveal that the BRL model is the best performing model and Kasten model is the one with worst performance. In general, models present negative mean bias, i.e. underestimation of predicted diffuse radiation, with the exception of Maxwell and Kasten models. Excluding the latter, the systematic errors described by the MAE and normalized MAPE scores are in the 20-30% range for all models.

The Maxwell model, which also takes into consideration the air mass, yields an overestimation of the diffuse radiation in the 50 – 250 W/m^2 range. The distinctive bend pattern for high diffuse radiation discussed above is less noticeable for this model. Despite the smoothing of this bending feature, the frequent overestimated values in the range 0 – 300 W/m^2 make it, in an overall assessment, not the best performing model.

The results obtain by the Skartveit model showed to be not as good as one could expect. It is fair to presume that the model additional parameters would favour the adequate prediction of diffuse radiation, but the error measures did not provide any added value for this more complex model.

Unexpectedly the results of Kasten model does not benefit from the cloud cover input. It was by far the less adequate model.

As already stated, the BRL model, which assumes a non-polynomial fitting to the clearness index, has shown the best results. Although it also underestimates the diffuse radiation for high values, this feature is less dominant then in the other models analysed.

Table 7.2 Statistical performance of the diffuse irradiance models analysed. The new model is presented further on this section.

Models	Extra input	MAE (W/m^2)	MAPE (%)	RMSE (W/m^2)	BIAS (W/m^2)	S (%)
Erbs et al.		42.29	23.46	69.04	-20.84	84.51
Soares et al.		52.43	29.08	83.53	-41.60	82.36
Reindl et al.		43.50	24.13	68.93	-23.51	83.39
Chandrasekaran and Kumar		41.99	23.29	66.92	-18.68	84.63
Karatasou et al.		49.05	27.21	73.82	-30.81	82.76
Miguel et al.		42.41	23.52	67.88	-21.01	84.05
Maxwell	air mass	54.17	29.94	81.58	30.40	79.93
Skartveit et.al.	variability index	52.03	28.76	90.88	-38.18	85.82
BRL	persistence	40.85	22.66	62.85	-19.21	86.21
Kasten	cloud cover; Link turbidity; air mass	117.09	78.96	186.8	65.32	79.15
New model		39.17	21.73	60.39	-6.45	87.87

The skill score (S), which provides an indication of how a model simulates the observed PDF, i.e. the overall observed conditions disregarding the synchronization of predicted-observed occurrence, evidences the ability of a model to predict the whole solar radiation resource, in this case its diffuse component. From the models tested, BRL was again the one that showed the best skill score. The PDFs in Figure 7.5 show the frequency variability of the models and measured data, highlighting an important spread between models, and that some of them overestimate observed frequencies in more than 100%. Additionally, the observed longer tail for high values of diffuse radiation is missing in the large majority of the models.

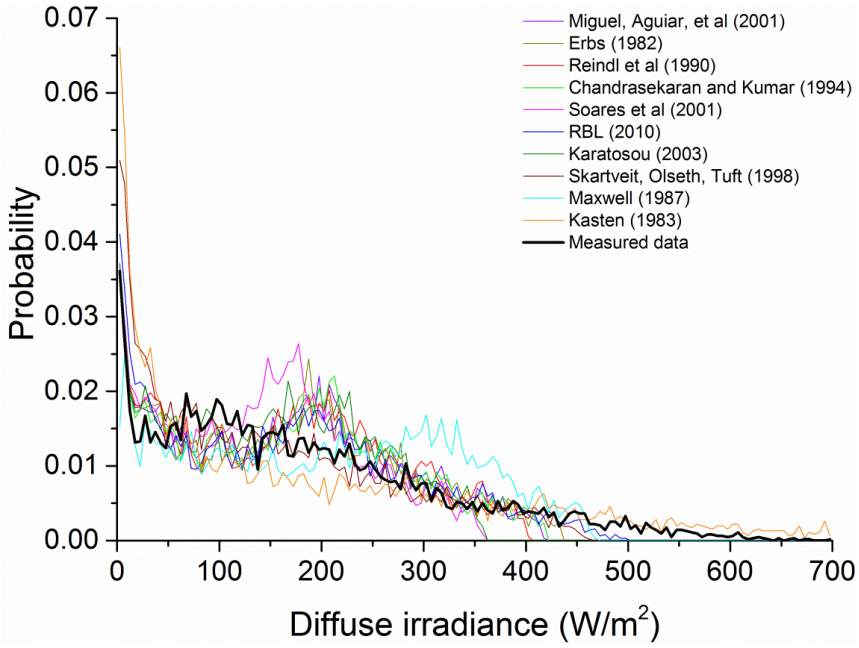

Figure 7.5 Probability density functions for the tested models and the measured data.

Since almost half of the data records correspond to situations with more than 80% cloud cover, it is relevant to assess the impact of the cloud cover on the statistical performance of the different models. Hence, the statistical indicators for individual subsets of data accordingly to their level of cloud cover were determined. The subsets of data correspond to the values of cloud cover from 0 to 100% in intervals of 20%. Figure 7.6 shows the results for RMSE and BIAS for all models, except the Kasten model which has much larger errors than the other models.

The accuracy of the models is higher for partially cloudy and full cloud cover conditions. This effect is not due to the frequency of data in each subset; for example, the subset of 60-80% cloud cover has less than half of the data points of the 80-100% subset but the performance of the models is similar. These results thus show that the models are able to describe the diffuse radiation when there is significant could cover and that the source of mismatch between measured and modelled diffuse radiation is relevant for skies with cloud cover below 40%.

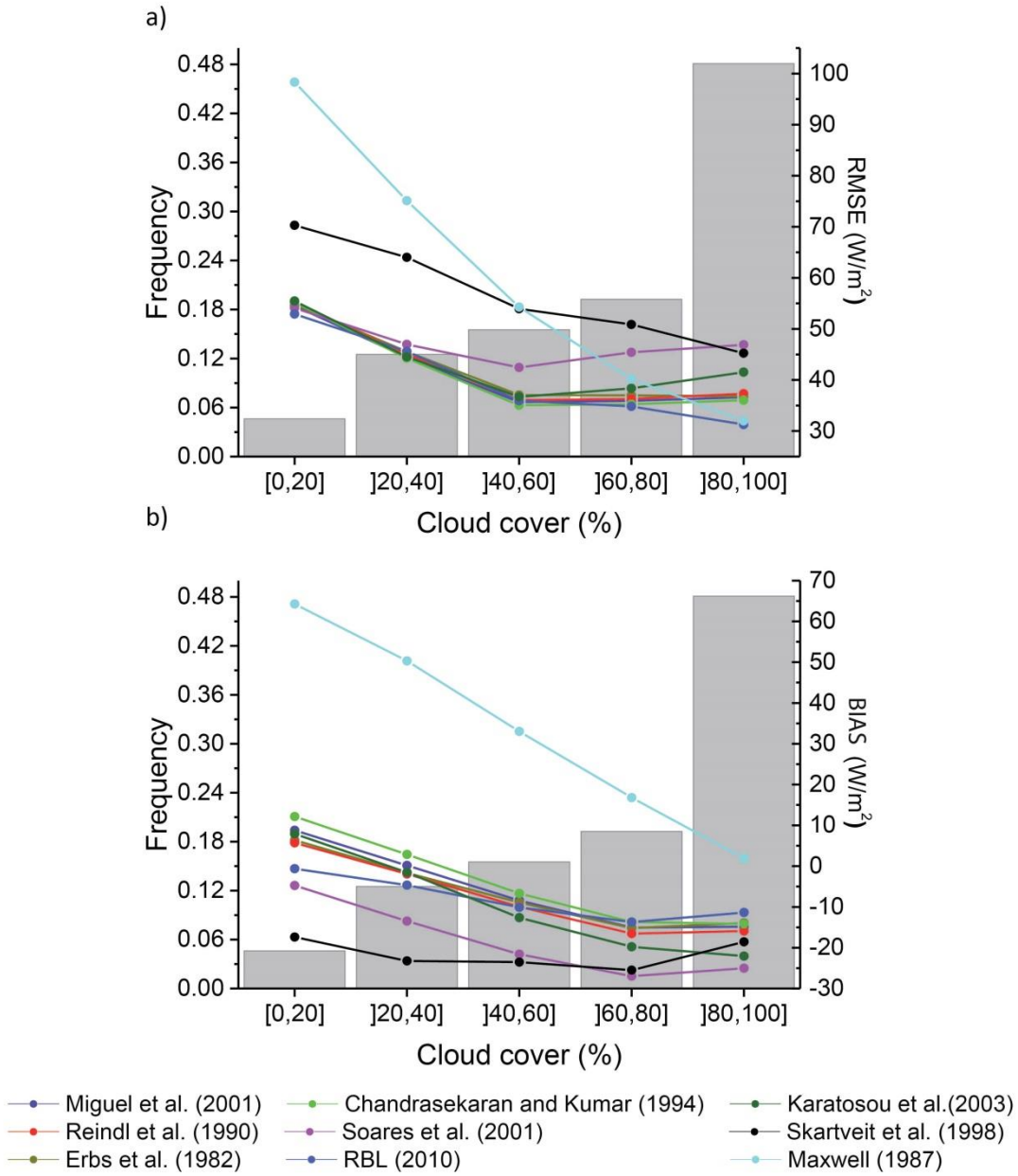

Figure 7.6 Statistical performance of the models for calculating the diffuse irradiance in different bins of cloud cover: a) RMSE and b) MBE.

The results of the evaluated models show room for improvement, in particular in the region with high diffuse radiation, above 300 W/m^2. Thus, the possible relationships among the variables k_t, zenith angle and global radiation, that could enhance the description of the behavior of diffuse radiation values, were analyzed. Thus, the following conditions were applied to the best performing model (the BRL model):

When $\theta \leq -9.895 \times 10^{-4}\, G + 1.615 \;\wedge\; \theta \geq -2.800 \times 10^{-3}\, G + 1.615$

$$k_{d_{This\ work}} = 1.10\, k_{d_{BRL}} \tag{13}$$

Figure 7.7 shows the scatter plot of measured versus predicted diffuse irradiance. The statistical performance errors can be seen in Table 7.2. Figure 7.7 shows an improved relationship between the predicted and measured diffuse radiation. The skill score is improved and the overall statistical scores are reduced, more noticeable in the MBE score. The bending seen in other models above 300 W/m^2 is not only partially corrected but also slightly smoothed when compared to the simple BRL model. The new PDF (Fig. 7.7b) highlights the overall improvement when compared with the measured values, and a slight correction of the PDF tail representation.

Nonetheless and inevitably, it is clear that there is still room for improvement and that different approaches of the ones used on the models here tested should be further explored.

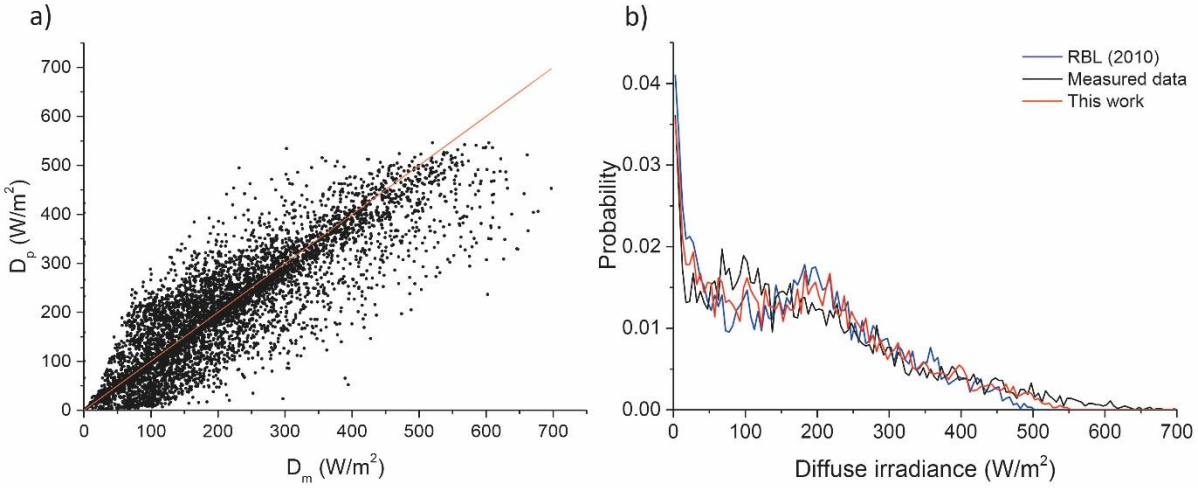

Figure 7.7 a) - Diffuse irradiance measured vs. Diffuse irradiance predicted trough the proposed model. Straight line represent diagram diagonal. b) – Probability density function for the RBL model (blue), measured diffuse irradiance (black) and BRL model with the proposed modification in this work (red).

7.5 Conclusions

The present work describes the analysis and comparison of a selection of diffuse radiation models when applied to the Azorean region for the assessment of the potential of solar energy technologies. The meteorological conditions of the Azores are characterized, throughout its annual cycle, by large amount of cloud cover. For the promotion of the energy sustainability of the region, and the exploration of its natural energy resources, the solar radiation resource should be characterized as detailed as possible, because that information is crucial to determine the best solar technology to adopt. It is thus important to understand not only the global behavior of the solar radiation but also its components, diffuse and beam irradiance.

The analysis was conducted using data from Graciosa Island acquired through the Atmospheric Radiation Measurements (ARM) Climate Research Facility from its 2009/2010 Mobile Facility deployment. In addition to the radiometric variables it was also possible to access measurements of cloud cover. It was observed that almost 50% of the data points

correspond to values above 80% cloud cover while only 17% correspond to records below 40%.

The selection of diffuse solar radiation models was based on model simplicity and reported performance. A systematic underestimation of diffuse irradiance above 300 W/m^2 was found for all models correlating diffuse fraction to clearness index.

The Boland-Ridley-Lauret (BRL) model was shown to be the most adequate. Even so, the statistical performance was far from satisfactory, featuring a MAPE of 23%; a RMSE of 63 W/m^2 and BIAS of -19 W/m^2; it is thus clear that a more suitable model for the Azores region is required. To overcome this and considering the underestimation of diffuse irradiance above 300 W/m^2 a correction to the BRL model targeting these values is presented. Model results lead to an improvement in all the statistical scores evaluated.

The re-calibration of the BRL model and the exploration of new predictors should be addressed in future work in order to enhance the robustness of a new model even more suitable for the studied region.

Chapter 8

Final conclusions and future work

In the current thesis the solar radiation resource provided by the combination of dynamical and statistical downscaling methods is used to provide quality solar resource maps for the Iberian Peninsula and the Azores archipelago for both present and future climate. The climate change impact on solar resource of the two regions is also targeted.

Given that specific conclusions are expressed throughout the thesis according to the respective topic addressed, an overview of the main highlights of each chapter and future work are here presented.

One goal of this thesis is to show that atmospheric numerical models are an added value to solar resource assessments. Indeed, they can overcome the limited temporal and spatial coverage of global radiation measures available throughout the world. The consistency of the output of such models discards issues such as missing values and non-uniformity of the available databases of solar radiation measured at meteorological stations. In addition, besides simulating values for present climate they also enable the investigation of the impact of future climate conditions.

The work developed in the thesis focused firstly on the solar resource of the Iberian Peninsula. It is a region with large climate gradients which are representative of diverse meteorological conditions, and may enable therefore the adaptation of the methods used in the proposed study to other regions of the globe.

The atmospheric numerical models simulate the climate system and quantify the climate response of the interactions among its constituents. GCMs are able to reproduce the main features of the climate system but given that they are too coarse to adequately describe the mesoscale processes, for regional applications it is appropriate to use RCMs. The RCMs which numerically solve the governing equations of the atmosphere in a limited

spatial domain are subjected to initial boundary conditions taken from GCMs. This dynamical downscaling process is represented in the scope of this thesis by the WRF model.

The first fundamental step is to benchmark the WRF model in terms of solar radiation simulated values in order to understand its usefulness (Chapter 4). For that, a WRF long simulation of global solar radiation values for Iberian Peninsula was evaluated through comparison against measured values obtained from meteorological stations across the region. The results showed a good correlation (above 0.88) between the datasets but substantial biases were found. This confirmed the known shortcomings of the dynamical downscaling process as well as of the RCM itself. The present climate solar radiation was systematically overestimated by the WRF model (values up to 40%). The misrepresentation of cloudy conditions in numerical models is often suggested as a major source of inaccuracy in the simulated solar radiation and it was confirmed that, in fact, the systematic overestimation of solar radiation was found to be related with a systematic underestimation of cloud fractional coverage. To improve the model's output and obtain a more rigorous solar radiation data, the WRF simulated values were statistically processed in order to correct the determined biases. In this stage, statistical downscaling comes into play. In this thesis this approach is used in its simplest form: as a bias correction MOS. The predictor is established to be solely the solar radiation WRF simulated data and the predictand is the solar radiation corrected value. The MOS methods used considered an event-wise (LR) and a distributional one (QM). LR and QM were both combined with the reanalysis driven WRF simulated solar radiation data to address the bias correction of the model's output for the Iberian present climate (Chapter 4). The LR and the QM results were compared and although both successfully reduce the biases (below 5% in the majority of the locations analysed), QM led to better modelled realistic variances than LR. Given this results QM was selected to derive the solar resource map for Iberia by considering a probability-dependent correction function for all WRF grid points. This methodology, although still dependent of solar radiation measures, showed to be a valid and valuable approach to provide spatially complete realistic solar radiation data without missing values and for periods longer than the periods that measurements are available.

Reaching this conclusion, the analysis of the present thesis progressed to the evaluation of the impact of future climate (end of 21st century) in solar resource over Iberia (Chapter 5). For that the RCP8.5 climate scenario which is in general, from the total set of RCPs, the least favored scenario especially in terms of greenhouse gas emission. The representation of the mean solar radiation values from the WRF historical simulation, for present climate, showed once more a systematic overestimation. For the future projections of solar radiation bias correction was also used. Since bias correction methods assume in its essence that the correction algorithm and its parameterization for current climate are also valid for future climate, here it was introduced the 'equidistant CDF mapping' developed by Li et al. (2010) which is a variant of the standard QM and designed to be more flexible in this stationarity issue. The results showed that the equidistant CDF mapping method does not have a strong influence on the climate change signal of the solar radiation projections. However, although

the method might have not impacted considerably the anomalies results it led to a slight shift on the geographic location of the higher mean values of solar radiation when compared to the raw simulations. For Iberia the climate change will have a small impact on solar resource which in spite of some spatial heterogeneity confirms that the region will remain favorable for the deployment of solar systems. Comparing to the baseline climate, the increases on solar radiation mean values may reach +3%. In some Iberia regions though, a decrease of approximately -3% is also projected.

The study conducted for the Iberian Peninsula, on the solar resource assessment for present and future climate paved the way to extend the application of the same methodology in the Azores archipelago (Chapter 6). This is motivated by the fact that the Azores region is often neglected in solar resource assessments and solar resource maps of the world or even Europe. Moreover, the Azores islands can be faced as a privileged location for potential study of integration of all sorts of renewable energy aiming the self-sustainability of the region in terms of energy consumption and although solar resource is often faced as being low and not worth of being seriously considered for renewable energy systems in that region, it should not be ignored.

For Azores, instead of continuous measured records of solar radiation values, only multi-year daily means of observations where available. Also, the dataset refers to only one location per island with exception to S. Miguel island which had two locations and S. Jorge which had no data. The nature of these observations (multi-year daily means) constitute a limitation on the analysis since the variability of the solar radiation data is to some extent conditioned. Despite this, the methods used in the analysis of the Iberian Peninsula solar resource for the present and the future projections are employed in the same manner.

In present climate conditions it was also found a high correlation (above 0.89) between the simulated and the observations of Azores solar radiation. The systematic overestimation was also present for all islands (up to 37%) except S^{ta} Maria where it was determined an underestimation (approximately 3%) of the solar radiation by the WRF model. The bias correction method selected to derive the solar resource map of the Azores archipelago was LR. Unlike what was used for the Iberia Peninsula (QM), in this situation, LR decreased the biases to negligible values (approximately between -1.3 to 1%) and the corrected variances were only slightly poorer than the ones obtained with QM results.

The solar resource of Azores may not be comparable to typical values found in the majority of the area of Iberia but it is definitely similar to the ones encountered in central Europe countries with well-developed markets of solar systems.

For future climate conditions the Azores solar resource was assessed for two periods, the mid and end of the 21st century. Here, the equidistant CDF method led to the same conclusion that it was found for Iberia Peninsula: it does not bring a clear influence on the climate change signal on the Azores' solar radiation future projections. However, as obviously, the range of solar radiation mean values are updated after bias correction of the WRF output. The climate change impact on the solar resource of the Azores archipelago is small, as it was already found in Iberia. However, given that this analysis was performed for

two instances of the future, mid and end of the 21st century, it was possible to identify a slight decrease of the solar radiation mean values by the mid century (values ranging from -4% to -1% in the majority of the islands) with a subsequent rise by the end of the century (values ranging from -2% to +3%).

For the technical and economic viability of any solar energy harnessing technology it is mandatory to have a complete knowledge about the resource availability i.e., its variability in space in time. Depending on the technology to be considered not only global solar radiation but also its diffuse and direct component must be part of the analysis. In atmospheric numerical models the direct and diffuse components are not common outputs to the user and only global solar radiation is available. So, given that one aims to show that combination of dynamical and statistical downscaling is a skillful approach to solar resource assessments, the separation of global radiation into its diffuse and direct components is analysed in this thesis through models of diffuse solar radiation fraction in order to address this limitation of the atmospheric models.

One important characteristic of diffuse fraction models is that they are empirically derived from site-specific measurements and a model developed and validated in a very specific climate type region may not hold its suitability to other regions. So, since the Iberian Peninsula has already been considered in several studies which developed and validated diffuse fraction models, this work was performed only for the Azores region which has not been object of this type of analysis before (Chapter 7). The typical Atlantic climate of Azores Islands is not very common in other regions and is also known to have a distinct weather pattern than the Iberian Peninsula, characterized by a higher amount of cloud cover. A set of diffuse fraction models available in literature were chosen based on their performance and simplicity and tested for the Azores region. The statistical results showed however large bias for all the selected diffuse fraction models (ranging from approximately -40% to 65%) tested for the Azores region. From these models it was also found a tendency for systematic underestimation of the diffuse radiation on its higher values (approximately above 300 W/m^2). It is found in literature that most separation models are not properly designed to operate correctly under high clearness index conditions but, in this work, the underestimation found is not related to any specific range of clearness index or even diffuse fraction. Based on the results, a correction to the best performance model (which presented a BIAS of approximately -20%) was developed to improve the modelling of diffuse fraction in the Azores region. The proposed diffuse fraction model for the Azores region reduced substantially the bias found for the former best performance model (BIAS of approximately -6%).

The work developed in the present thesis constitutes a necessary and valuable step in the field of bias correction of simulated global solar radiation by atmospheric numerical models. The solar radiation maps provided are of great importance for resource assessment not only for the Iberia Peninsula but especially for the Azores archipelago which solar resource was here thoroughly analyzed in first hand.

The thesis also paves the way to other complementary lines of work which are listed below. Although being considered as limitations of the respective analysis presented, they can also be seen as an opportunity for future work:

- For climate change projection is common practice to consider a multi-model ensemble approach which allows accounting for the uncertainty of different global projections. Since the present work considers only a single RCM driven by a specific GCM and climate projection scenario, the sensitivity of the solar radiation projections for Iberia Peninsula and Azores archipelago should be explored by considering a multi-model ensemble.
- The bias correction methods depend to some extent on reliable measures of global solar radiation. A sensitivity analysis to the spatial density of *in situ* measurement, and their optimum temporal span, should also be considered in future work.
- The diffuse solar fraction model proposed in Chapter 7 should be further enhanced with the exploration of new predictors and/or combination with bias correction methods.

Appendix A

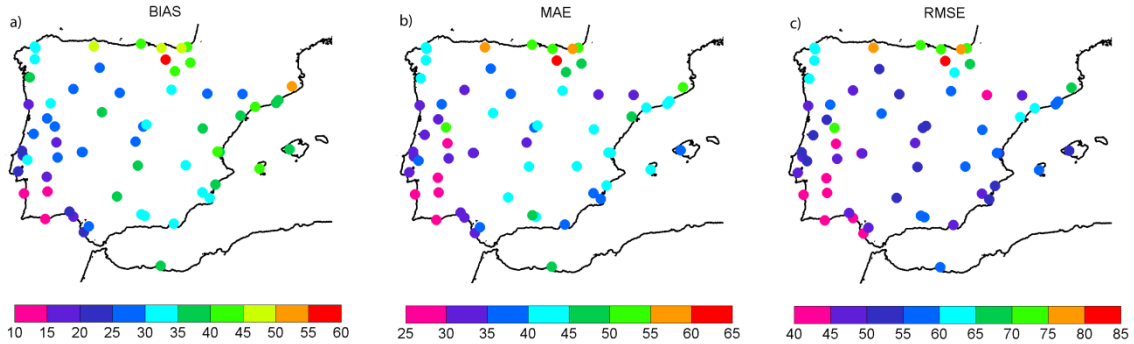

Figure A1. Statistical performance results for daily data obtained for the Iberian Peninsula: BIAS (a), MAE (c) and RMSE (e) are shown in absolute magnitude (W/m^2).

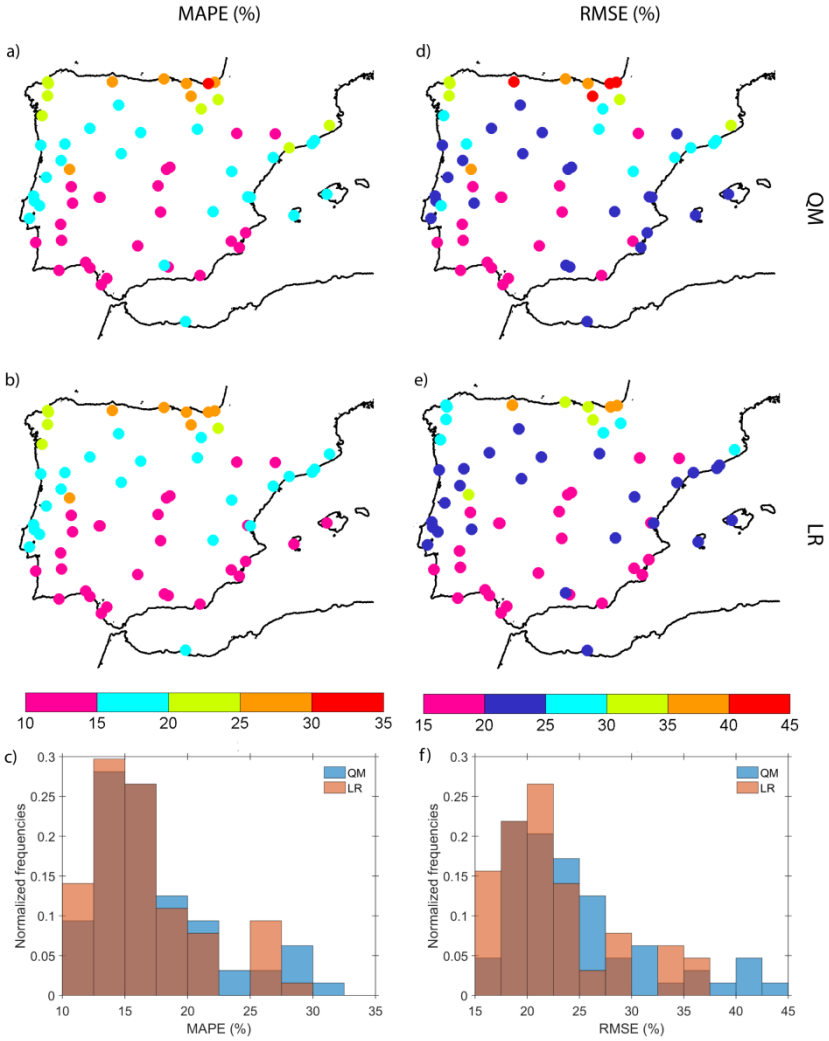

Figure A2. MAPE (left column) and relative RMSE (right column) after implementation of the MOS methods: quantile mapping (QM, top row) and linear regression (LR, middle row). Normalized frequencies of the respective statistical values with overlapping of the LR (orange) and QM (blue) results (bottom row).

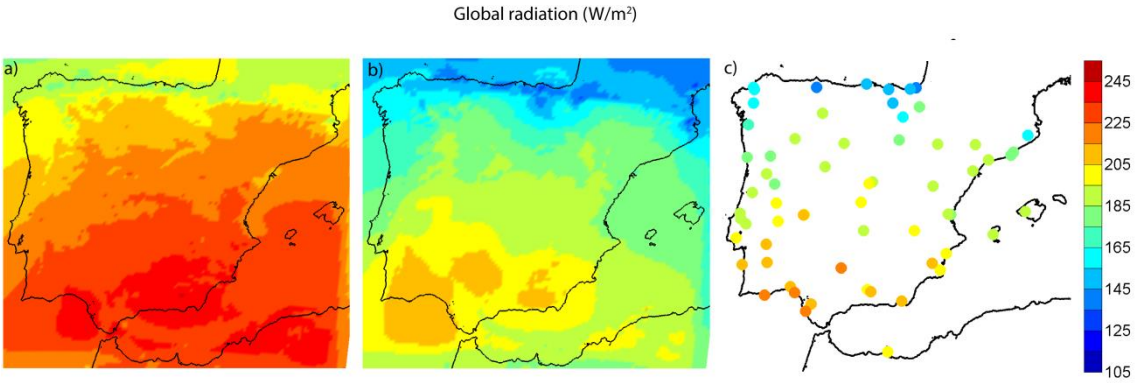

Figure A3. Annual average of (a) simulated uncorrected WRF solar radiation and (b) corrected with MOS for the Iberian Peninsula present climate. a) and b) were determined using interpolated probability-dependent correction function in all the individual grid points of the WRF IP domain obtained from the station-wise QM method. c) represents the localized analysis and is plotted side by side the solar radiation maps with equivalent colour scheme for illustration purposes.

Appendix B

Figure B1. Spanish provinces and regions (Tardío et al. 2006).

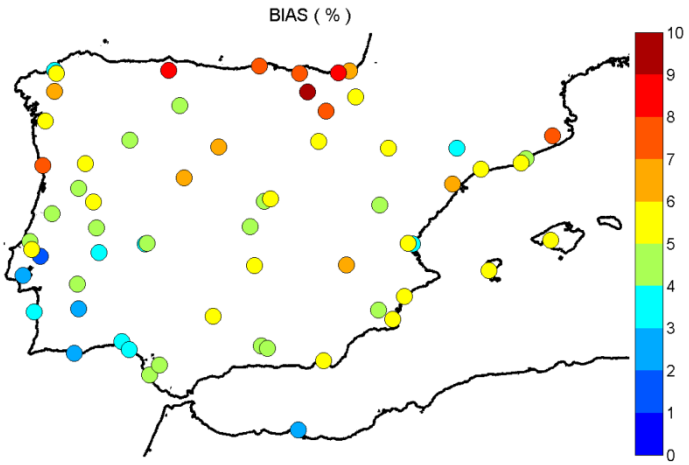

Figure B2. Relative BIAS between corrected historical simulation and observations.

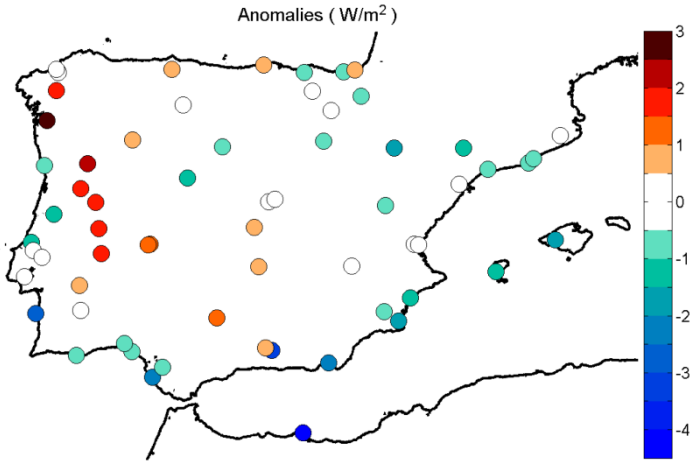

Figure B3. Yearly anomalies (W/m2) of corrected WRF solar radiation projections for the end of the century (2070-2100) using historical climate simulation as baseline.

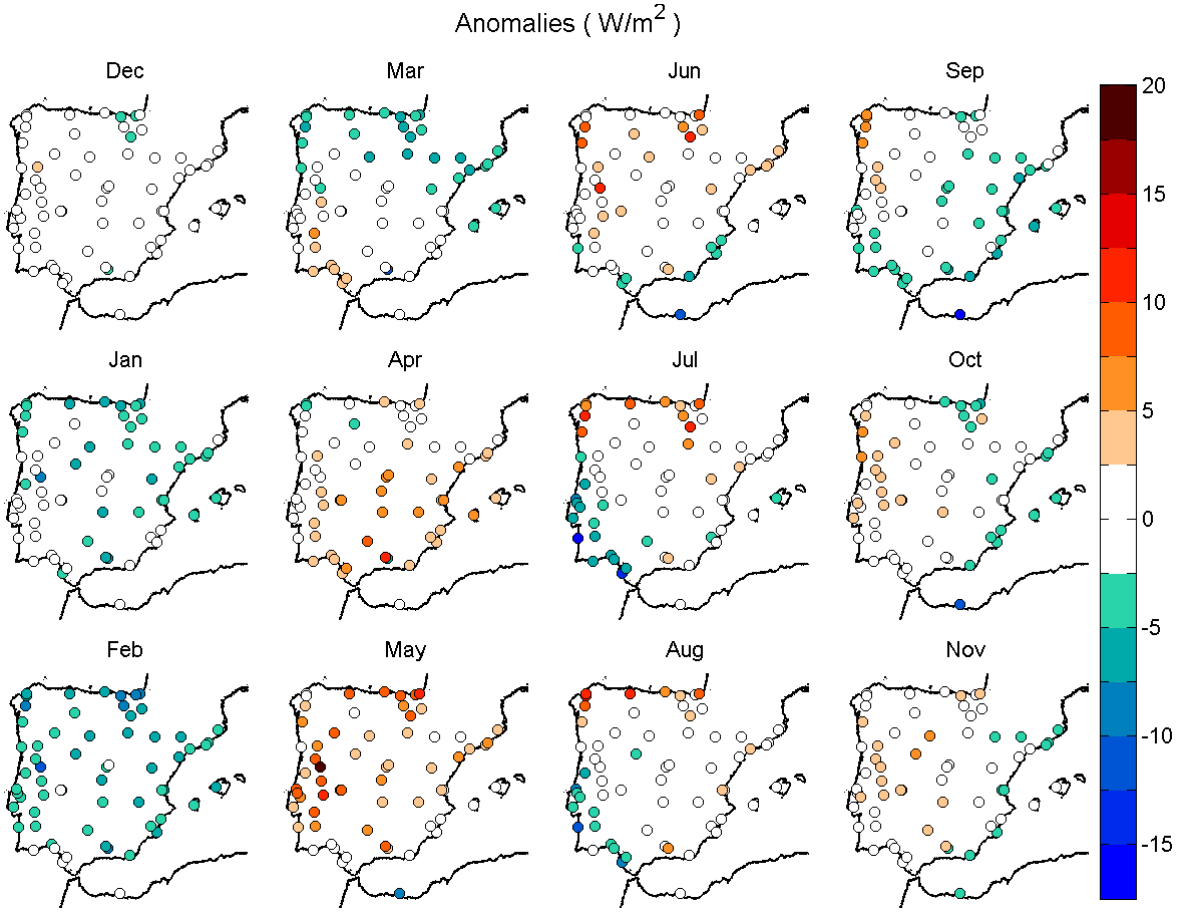

Figure B4. Monthly anomalies (W/m^2) of corrected WRF solar radiation projections for the end of the century (2070-2100) using historical climate simulation as baseline (b).

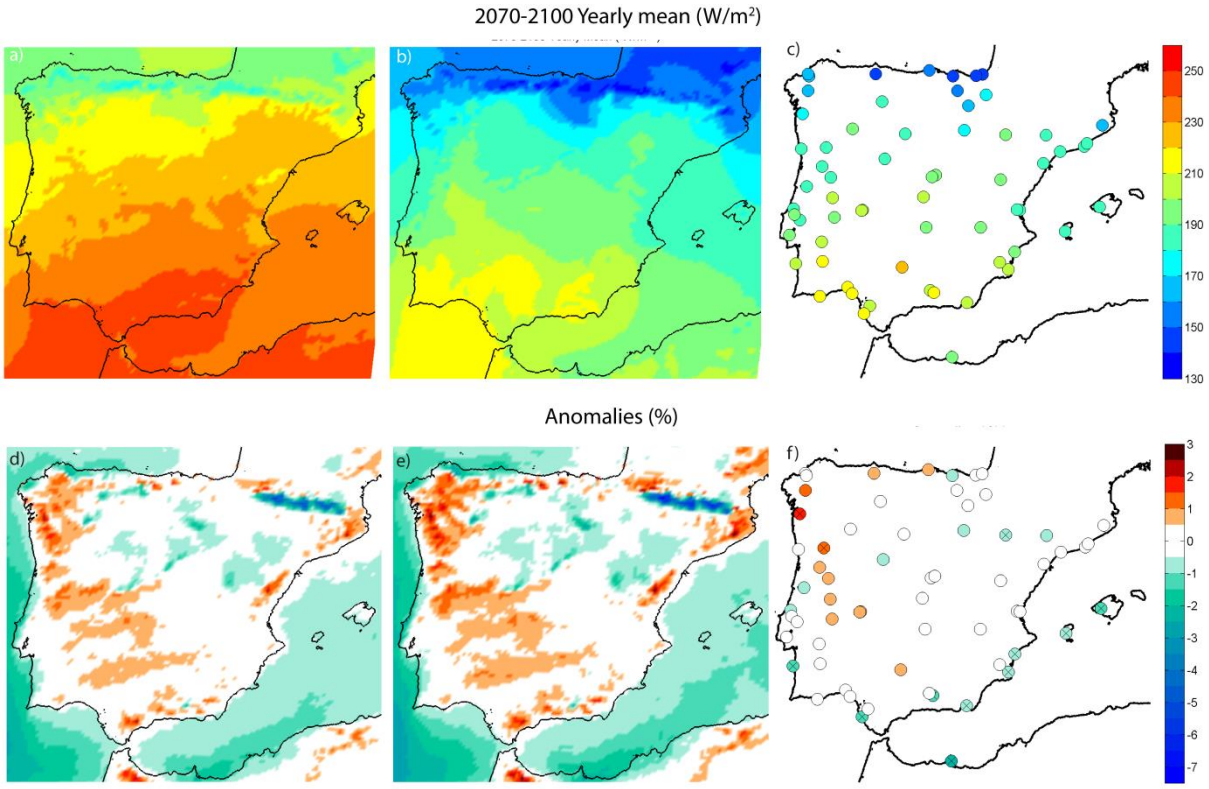

Figure B5. (top panel) Yearly mean solar radiation map and (bottom panel) anomalies of projected WRF (a and d) uncorrected and (b; e; c and f) corrected data in the WRF IP domain for the end of the century (2070-2100). b) and e) were determined using interpolated probability-dependent correction function obtained from the station-wise equidistant CDF mapping method in all the individual grid points of the WRF IP domain. c) and f) represent the localized analysis and are plotted side by side the solar radiation maps for illustration purposes. In f) stations flagged with a cross indicate the locations where baseline and future annual means are, at 90% significance level, not equal in both corrected and uncorrected WRF data.

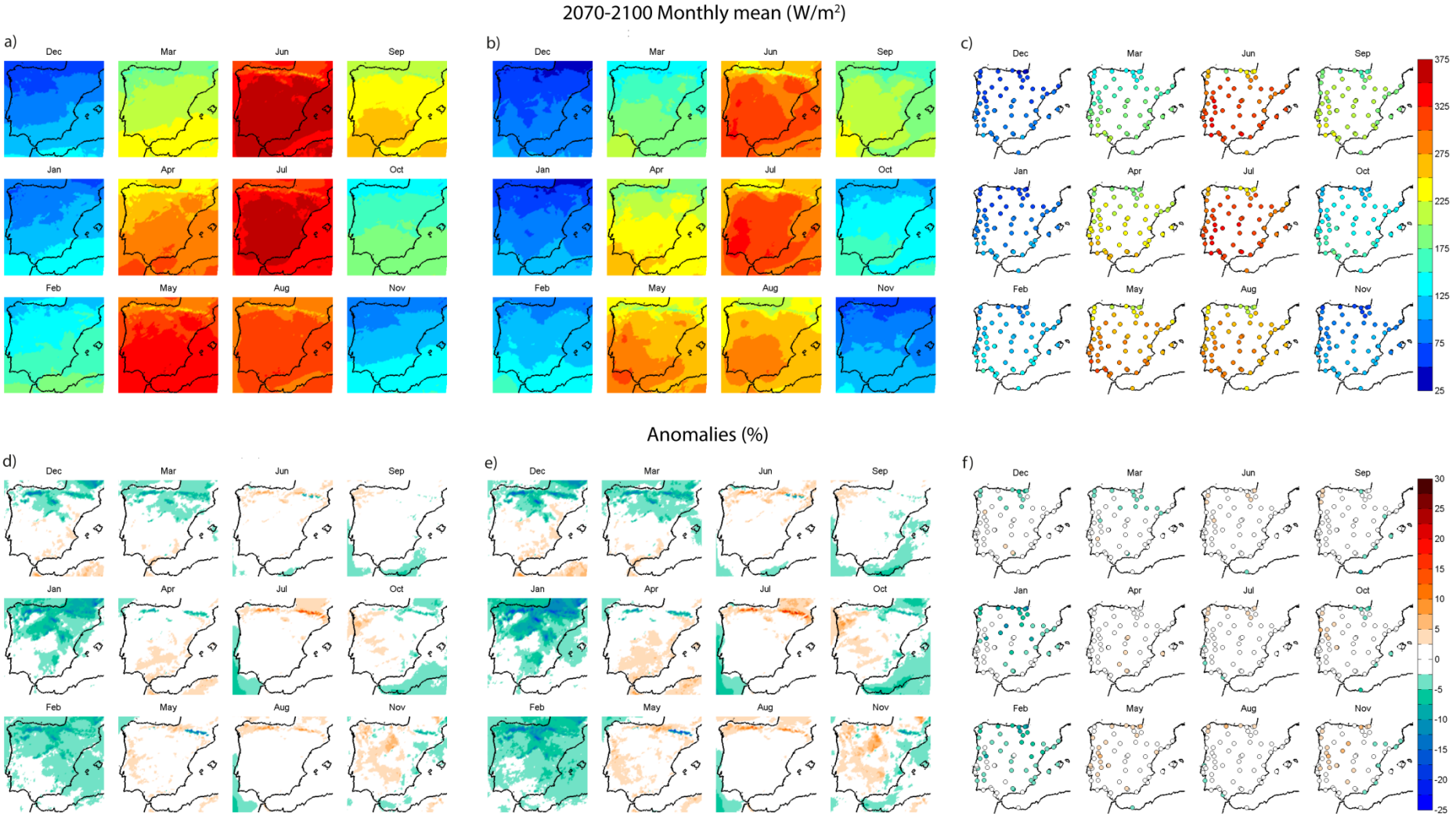

Figure B6. (top panel) Monthly means solar radiation map and (bottom panel) anomalies of projected WRF (a and d) uncorrected and (b; e; c and f) corrected data in the WRF IP domain for the end of the century (2070-2100). b) and e) were determined using interpolated probability-dependent correction function obtained from the station-wise equidistant CDF mapping method in all the individual grid points of the WRF IP domain. c) and f) represent the localized analysis and are plotted side by side the solar radiation maps for illustration purposes. The monthly plots are displayed in way to each column represent a given season: Winter; Spring; Summer and Autumn from left to right.

Appendix C

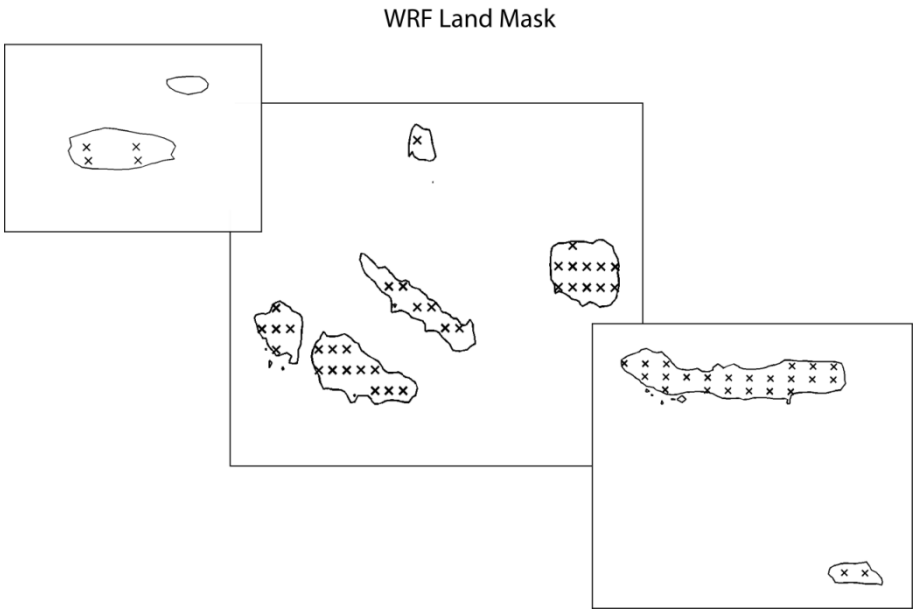

Figure C1. Land mask of WRF 6km resolution. Cross signs represent the points that the model considers as land.

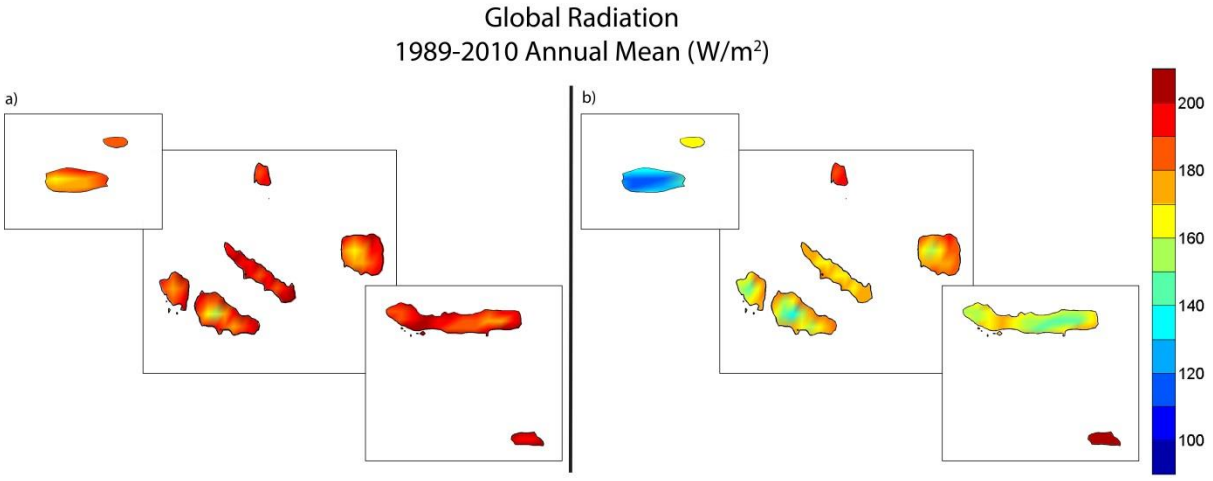

Figure C2. Annual (a) uncorrected and (b) MOS corrected WRF global solar radiation for the Azores archipelago 1989-2010 present climate. Values are shown in W/m^2.

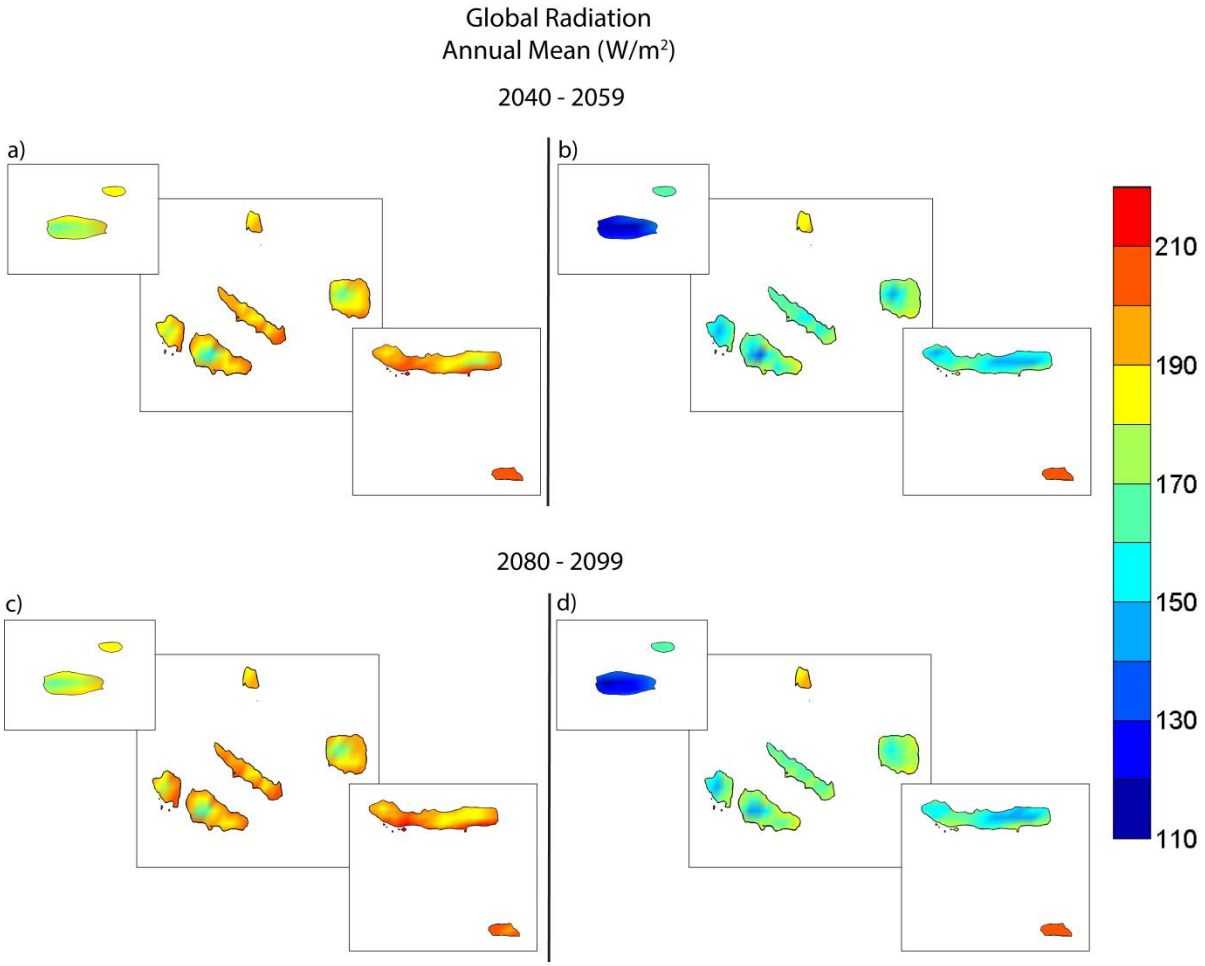

Figure C3. Annual (a; b) uncorrected and (b; d) MOS corrected WRF global solar radiation for the Azores archipelago at the mid (2040-2059, top panel) and end of the century (2080-2099, bottom panel). Values are shown in W/m^2.

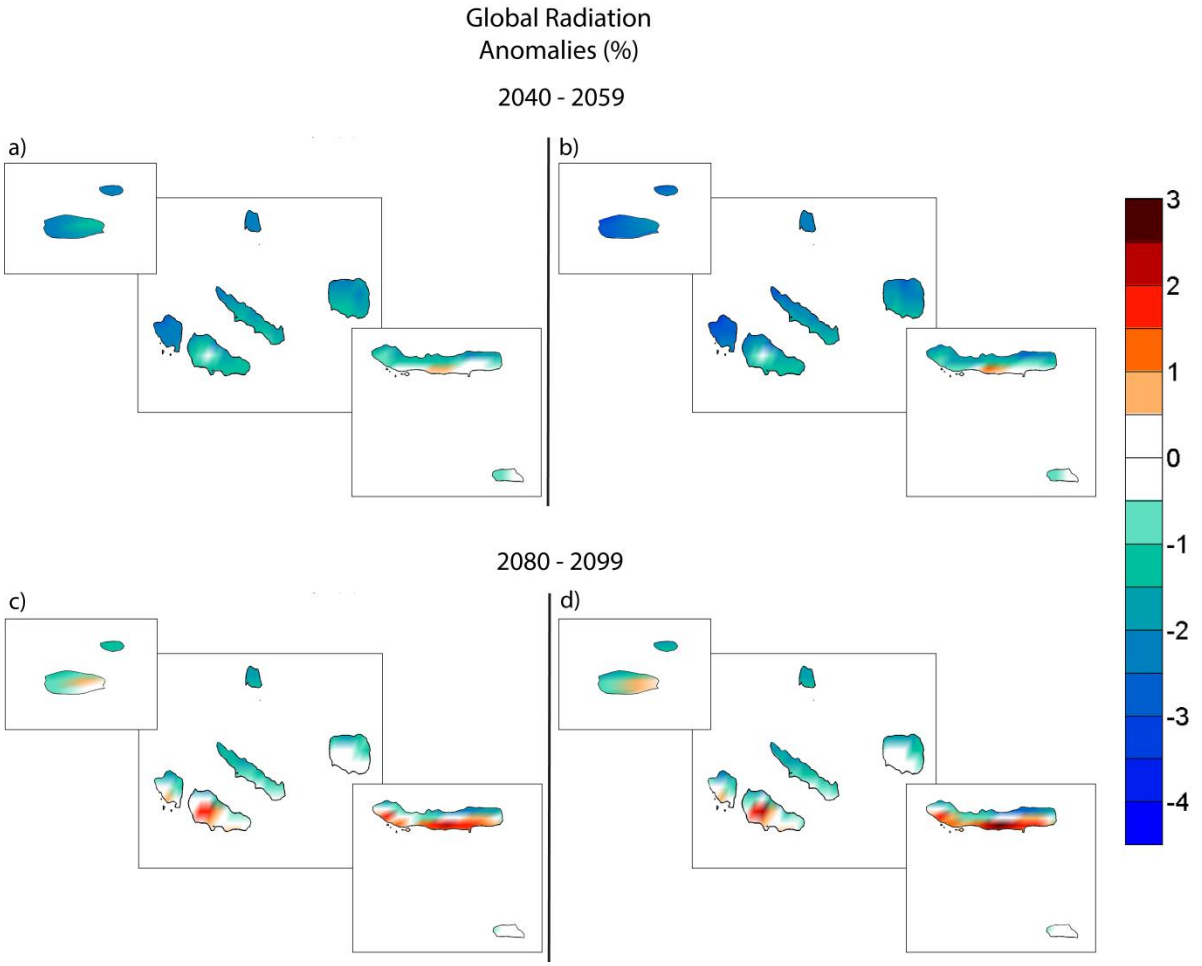

Figure C4. (a; c) uncorrected and (b; d) MOS corrected WRF solar radiation anomalies (%) for the mid (2040-2059, top panel) and end of the century (2080-2099, bottom panel) considering the historical climate run (1989-2010) as baseline.

Table C1. Statistical performance results for **multi-year daily mean** data obtained for Azores islands and the **MOS-corrected** WRF. MAPE, RMSE and BIAS are shown in relative magnitude (%) for linear regression (LR) and quantile mapping (QM). Skill score (S) and normalized standard deviation (σ_n) are also presented. (The superscripts C; W and E indicate Cental; Western or Eastern Group.)

	MAPE (%)		RMSE (%)		BIAS (%)		S (%)		σ_n	
	LR	*QM*	*LR*	*QM*	*LR*	*QM*	*LR*	*QM*	*LR*	*QM*
Faial^{C}	12.93	14.69	17.07	19.47	0.45	6.16	68.77	69.32	0.94	1.00
Terceira^{C}	15.17	15.61	19.9	20.77	0.92	-2.12	70.68	70.96	0.92	0.97
Graciosa^{C}	13.42	13.98	17.77	18.54	-0.37	4.59	63.56	65.75	0.93	0.98
Pico^{C}	19.53	22.21	25.55	28.29	-1.34	2.30	64.56	64.56	0.87	0.87
Flores^{W}	13.56	19.27	17.9	23.82	0.06	8.47	66.58	64.93	0.92	0.97
Corvo^{W}	15.41	17.03	20.29	22.78	-0.15	7.29	64.93	68.49	0.91	0.96
Ponta Delgada^{E}	13.11	15.29	16.9	20.02	0.85	6.79	69.32	69.86	0.92	1.07
Nordeste^{E}	16.55	21.79	21.36	27.43	0.65	10.63	61.64	65.75	0.89	0.99
S^{ta} Maria^{E}	12.17	13.35	15.78	17.01	-0.41	3.81	63.46	64.29	0.90	1.01

Table C2. Annual mean (W/m^2) of projected WRF solar radiation for the mid (2040-2059) and end of the century (2080-2099) after correction and respective anomalies (%) considering the historical climate run (1989-2010) as baseline. (The superscripts C; W and E indicate Cental; Western or Eastern Group.)

WRF 6km	Annual Mean		Anomalies (%)	
	2040-2059	*2080-2099*	*2040-2059*	*2080-2099*
Faial^{C}	169	174	-2.51	0.04
Terceira^{C}	165	167	-1.66	-0.41
Graciosa^{C}	187	189	-2.5	-1.73
Pico^{C}	158	160	-1.53	-0.57
Flores^{W}	143	146	-1.74	0.11
Corvo^{W}	161	163	-2.37	-1.51
Ponta Delgada^{E}	177	181	-0.54	1.28
Nordeste^{E}	150	150	-2.56	-2.04
S^{ta} Maria^{E}	207	208	-0.93	-0.59

Bibliography

Alexandri, G., Georgoulias, A. K., Zanis, P., Katragkou, E., Tsikerdekis, A., Kourtidis, K., & Meleti, C. (2015) On the ability of RegCM4 regional climate model to simulate surface solar radiation patterns over Europe: an assessment using satellite-based observations, Atmospheric Chemistry and Physics, 15(22), 13195-13216.

Alsamamra, H., Ruiz-Arias, J. A., Pozo-Vázquez, D., & Tovar-Pescador, J. (2009) A comparative study of ordinary and residual kriging techniques for mapping global solar radiation over southern Spain, Agricultural and Forest meteorology, 149(8), 1343-1357.

Amengual, A., Homar, V., Romero, R., Alonso, S., & Ramis, C. (2012) A statistical adjustment of regional climate model outputs to local scales: application to Platja de Palma, Spain, Journal of Climate, 25(3), 939-957.

Badescu, V., (2008) Modeling Solar Radiation at the Earth's Surface, Recent Advances. Springer

Barnston, A. G., and van den Dool, H. M. (1993) A degeneracy in cross-validated skill in regression-based forecasts, Journal of Climate, 6(5), 963-977.

Betts, A. K. (1986) A new convective adjustment scheme Part I: Observational and theoretical basis, Quarterly Journal of the Royal Meteorological Society, 112(473), 677-691.

Betts, A. K., & Miller, M. J. (1986) A new convective adjustment scheme Part II: Single column tests using GATE wave, BOMEX, ATEX and arctic air-mass data sets, Quarterly Journal of the Royal Meteorological Society, 112(473), 693-709.

Boé, J., Terray, L., Habets, F., & Martin, E. (2007) Statistical and dynamical downscaling of the Seine basin climate for hydro-meteorological studies, International Journal of Climatology, 27(12), 1643-1656.

Boland, J., Scott, L., Luther, M., (2001) Modelling the diffuse fraction of global solar radiation on a horizontal surface. Environmetrics, 12, 103–116

Boland J., Ridley B., Brown B.,(2008) Models of diffuse solar radiation, Renewable Energy 33 (4), 575-584

Brito, M. C., Gomes, N., Santos, T., & Tenedório, J. A. (2012) Photovoltaic potential in a Lisbon suburb using LiDAR data. Solar Energy, 86(1), 283-288.

Burnett, D., Barbour, E., & Harrison, G. P. (2014) The UK solar energy resource and the impact of climate change, Renewable Energy, 71, 333-343.

Chandrasekaran J., Kumar S., (1994) Hourly diffuse fraction correlation at a tropical location, Solar Energy 53 (6), 505-510

Campaniço, H., Soares, P. M., Hollmuller, P., & Cardoso, R. M. (2016) Climatic cooling potential and building cooling demand savings: High resolution spatiotemporal analysis of direct ventilation and evaporative cooling for the Iberian Peninsula, Renewable Energy, 85, 766-776.

Cardoso, R. M., Soares, P. M. M., Miranda, P. M. A., & Belo ‐ Pereira, M. (2013) WRF high resolution simulation of Iberian mean and extreme precipitation climate, International Journal of Climatology, 33(11), 2591-2608.

Che, H. Z., Shi, G. Y., Zhang, X. Y., Arimoto, R., Zhao, J. Q., Xu, L., ... & Chen, Z. H. (2005) Analysis of 40 years of solar radiation data from China, 1961–2000, Geophysical Research Letters, 32(6).

Chen F, Dudhia J (2001) Coupling an advanced land surface-hydrology model with the Penn State–NCAR MM5 modeling system Part I: model implementation and sensitivity, Mon Weather Rev 129:569–585.

Chiacchio, M., Solmon, F., Giorgi, F., Stackhouse, P., & Wild, M. (2015) Evaluation of the radiation budget with a regional climate model over Europe and inspection of dimming and brightening, Journal of Geophysical Research: Atmospheres, 120(5), 1951-1971.

Christensen, J.H., B. Hewitson, A. Busuioc, A. Chen, X. Gao, I. Held, R. Jones, R.K. Kolli, W.-T. Kwon, R. Laprise, V. Magaña Rueda, L. Mearns, C.G. Menéndez, J. Räisänen, A. Rinke, A. Sarr and P. Whetton (2007) Regional Climate Projections. In: Climate Change 2007: The Physical Science Basis, Contribution of Working Group I to the Fourth Assessment Report of the Intergovernmental Panel on Climate Change [Solomon, S., D. Qin, M. Manning, Z. Chen, M. Marquis, K.B. Averyt, M. Tignor and H.L. Miller (eds.)], Cambridge University Press, Cambridge, United Kingdom and New York, NY, USA

Clark, A. J., Gallus Jr, W. A., Xue, M., & Kong, F. (2009) A comparison of precipitation forecast skill between small convection-allowing and large convection-parameterizing ensembles, Weather and forecasting, 24(4), 1121-1140.

Collins, W. D., Rasch, P. J., Boville, B. A., Hack, J. J., McCaa, J. R., Williamson, D. L., ... & Dai, Y. (2004) Description of the NCAR community atmosphere model (CAM 3.0).

Crook, J. A., Jones, L. A., Forster, P. M., and Crook, R. (2011) Climate change impacts on future photovoltaic and concentrated solar power energy output, Energy & Environmental Science, 4(9), 3101-3109.

Davies J.A., McKay D.C.m Luciani G., Abdel-Wahab M., (1988) Validation of models for estimating solar radiation on horizontal surfaces, volume 1, IEA Task IX, Final Report, Atmospheric Environment Service of Canada, Canada.

Dee, D. P., Uppala, S. M., Simmons, A. J., Berrisford, P., Poli, P., Kobayashi, S., ... & Bechtold, P. (2011) The ERA‐Interim reanalysis: Configuration and performance of the data assimilation system. Quarterly Journal of the Royal Meteorological Society, 137(656), 553-597.

Déqué, M. (2007) Frequency of precipitation and temperature extremes over France in an anthropogenic scenario: model results and statistical correction according to observed values, Global and Planetary Change, 57(1), 16-26.

Dewald, U., & Truffer, B. (2011) Market formation in technological innovation systems – diffusion of photovoltaic applications in Germany, Industry and Innovation, 18(03), 285-300.

Diagne, M., David, M., Boland, J., Schmutz, N., & Lauret, P. (2014) Post-processing of solar irradiance forecasts from WRF model at Reunion Island, Solar Energy, 105, 99-108

Eden, J. M., Widmann, M., Grawe, D., & Rast, S. (2012) Skill, correction, and downscaling of GCM-simulated precipitation, Journal of Climate, 25(11), 3970-3984.

Eden, J. M., Widmann, M., Maraun, D., & Vrac, M. (2014) Comparison of GCM-and RCM-simulated precipitation following stochastic postprocessing, Journal of Geophysical Research: Atmospheres, 119(19).

Engerer, N. A. (2015) Minute resolution estimates of the diffuse fraction of global irradiance for southeastern Australia, Solar Energy, 116, 215-237

Erbs D.G., Klein S.A., Duffie J.A., (1982) Estimation of the diffuse radiation fraction for hourly, daily and monthly-average global radiation, Solar Energy 28 (4), 293-302

Ertekin, C., & Evrendilek, F. (2007) Spatio-temporal modeling of global solar radiation dynamics as a function of sunshine duration for Turkey, Agricultural and Forest Meteorology, 145(1), 36-47.

Gaetani, M., Huld, T., Vignati, E., Monforti-Ferrario, F., Dosio, A., & Raes, F. (2014) The near future availability of photovoltaic energy in Europe and Africa in climate-aerosol modelling experiments, Renewable and Sustainable Energy Reviews, 38, 706-716.

García-Díez, M., Fernández, J., & Vautard, R. (2015) An RCM multi-physics ensemble over Europe: multi-variable evaluation to avoid error compensation, Climate Dynamics, 45(11-12), 3141-3156.

Gilgen H., Wild M., and Ohmura A., (1998) Means and Trends of Shortwave Irradiance at the Surface Estimated from Global Energy Balance Archive Data. J. Climate, 11, 2042–2061.

Giorgi, F., & Mearns, L. O. (1999) Introduction to special section: Regional climate modeling revisited, Journal of Geophysical Research: Atmospheres, 104(D6), 6335-6352.

Giorgi, F. (2006) Climate change hot-spots, Geophysical research letters, 33(8).

Giorgi, F., Coppola, E., Solmon, F., Mariotti, L., Sylla, M. B., Bi, X., ... & Turuncoglu, U. U. (2012) RegCM4: model description and preliminary tests over multiple CORDEX domains, Climate Research, 2(7).

Green Islands Azores Project (2015) [ONLINE] Available at: http://www.green-islands-azores.uac.pt/grupos/detalhegrupo.php?projecto=9. [Accessed 05 May 2015]

Grell, G. A., & Devenyi, D. J. Dudhia, and DR Stauffer, (1994) A description of the fifth-generation Penn State/NCAR mesoscale model (MM5), NCAR Tech. Note NCAR/TN-398STR

Gueymard, C. A., & Ruiz-Arias, J. A. (2016) Extensive worldwide validation and climate sensitivity analysis of direct irradiance predictions from 1-min global irradiance, Solar Energy, 128, 1-30.

Gutiérrez, J. M., San-Martín, D., Brands, S., Manzanas, R., & Herrera, S. (2013) Reassessing statistical downscaling techniques for their robust application under climate change conditions, Journal of Climate, 26(1), 171-188.

Haylock, M. R., Hofstra, N., Klein Tank, A. M. G., Klok, E. J., Jones, P. D., & New, M. (2008) A European daily high ‐ resolution gridded data set of surface temperature and precipitation for 1950 ‐ 2006, Journal of Geophysical Research: Atmospheres, 113(D20).

Hazeleger, W., Severijns, C., Semmler, T., Stefanescu, S., Yang, S., Wang, X., ... & Willén, U. (2010) EC-Earth: a seamless earth-system prediction approach in action, Bulletin of the American Meteorological Society, 91(10), 1357-1363.

Hempel, S., Frieler, K., Warszawski, L., Schewe, J., & Piontek, F. (2013) A trend-preserving bias correction–the ISI-MIP approach, Earth System Dynamics, 4(2), 219-236.

Hengl, T., (2007) A Practical Guide to Geostatistical Mapping of Environmental Variables, EUR 22904 EN. Office for Official Publications of the European Communities, Luxembourg

Herrera, S., Fita, L., Fernández, J., & Gutiérrez, J. M. (2010) Evaluation of the mean and extreme precipitation regimes from the ENSEMBLES regional climate multimodel simulations over Spain, Journal of Geophysical Research: Atmospheres, 115(D21).

Hofierka, J., & Kaňuk, J. (2009) Assessment of photovoltaic potential in urban areas using open-source solar radiation tools. Renewable Energy, 34(10), 2206-2214.

Hofstra, N., Haylock, M., New, M., Jones, P., & Frei, C. (2008) Comparison of six methods for the interpolation of daily European climate data, Journal of Geophysical Research: Atmospheres (1984–2012), 113(D21).

Holdaway, M. R. (1996) Spatial modeling and interpolation of monthly temperature using kriging, Climate Research, 6(3), 215-225.

Hollands K.G.T., Crha S.J., (1987) An improved model for diffuse radiation: Correction for atmospheric back-scattering, Solar Energy, 38 (4), 233-236

Hong, S. Y., & Lim, J. O. J. (2006) The WRF single-moment 6-class microphysics scheme (WSM6), J. Korean Meteor. Soc, 42(2), 129-151.

Hudson, G., & Wackernagel, H. (1994) Mapping temperature using kriging with external drift: theory and an example from Scotland, International journal of Climatology, 14(1), 77-91.

Huld, T., Müller, R., & Gambardella, A. (2012) A new solar radiation database for estimating PV performance in Europe and Africa, Solar Energy, 86(6), 1803-1815.

IEC/TS 61836 (1997) Solar Photovoltaic Energy Systems – Terms and Symbols. Technical Report – Type 2, International Electrotechnical Commission, TC 82 – Solar photovoltaic energy systems

Ines, A. V., & Hansen, J. W. (2006) Bias correction of daily GCM rainfall for crop simulation studies, Agricultural and forest meteorology, 138(1), 44-53.

Jacob, D., Petersen, J., Eggert, B., Alias, A., Christensen, O. B., Bouwer, L. M., ... & Georgopoulou, E. (2014) EURO-CORDEX: new high-resolution climate change projections for European impact research, Regional Environmental Change, 14(2), 563-578.

Jacovides C.P., Tymvios F.S., Assimakopoulos V.D., Kaltsounides N.A., (2006) Comparative study of various correlations in estimating hourly diffuse fraction of global solar radiation, Renewable Energy 31 (15), 2492-2504.

Janjić ZI (1990) The step-mountain coordinate: physical package, Mon Weather Rev 118:1429–1443

Janjić ZI (1994) The step-mountain eta coordinate model: further developments of the convection, viscous sublayer and turbulence closure schemes, Mon Weather Rev 122:927–945.

Janjić ZI (2000) Comments on ‘‘development and evaluation of a convection scheme for use in climate models’’, J Atmos Sci, 57:3686.

Janjić, Z. I. (2002) Nonsingular implementation of the Mellor–Yamada level 2.5 scheme in the NCEP Meso model, NCEP office note, 437, 61

Jarvis, C. H., & Stuart, N. (2001) A comparison among strategies for interpolating maximum and minimum daily air temperatures, Part II: The interaction between number of guiding variables and the type of interpolation method. Journal of Applied Meteorology, 40(6), 1075-1084.

Jerez, S., Montavez, J. P., Gomez-Navarro, J. J., Lorente-Plazas, R., Garcia-Valero, J. A., & Jimenez-Guerrero, P. (2013a) A multi-physics ensemble of regional climate change projections over the Iberian Peninsula, Climate dynamics, 41(7-8), 1749-1768.

Jerez, S., Trigo, R. M., Sarsa, A., Lorente-Plazas, R., Pozo-Vázquez, D., & Montávez, J. P. (2013b) Spatio-temporal complementarity between solar and wind power in the Iberian Peninsula, Energy Procedia, 40, 48-57

Jerez, S., Tobin, I., Vautard, R., Montávez, J. P., López-Romero, J. M., Thais, F., ... & Nikulin, G. (2015) The impact of climate change on photovoltaic power generation in Europ, Nature communications, 6.

Jimenez, P. A., Hacker, J. P., Dudhia, J., Ellen Haupt, S., Ruiz-Arias, J. A., Gueymard, C. A., ... & Deng, A. (2015) WRF-Solar: An augmented NWP model for solar power prediction - Model description and clear sky assessment, Bulletin of the American Meteorological Society, (2015).

Journée, M., & Bertrand, C. (2010) Improving the spatio-temporal distribution of surface solar radiation data by merging ground and satellite measurements, Remote Sensing of Environment, 114(11), 2692-2704.

Kalma J. D. and Fleming P. M., (1972) A note on estimating the direct and diffuse components of global radiation, Archiv für Meteorologie, Geophysik und Bioklimatologie, Serie B 20, 191-205.

Karatasou S., Santamouris M., Geros V., (2003) Analysis of experimental data on diffuse solar radiation in Athens, Greece, for building applications, International Journal of Sustainable Energy , 23, 1-11

Katragkou, E., García-Díez, M., Vautard, R., Sobolowski, S., Zanis, P., Alexandri, G., ... & Goergen, K. (2015), Regional climate hindcast simulations within EURO-CORDEX:

evaluation of a WRF multi-physics ensemble, Geoscientific model development, 8(3), 603-618.

Kenny, R. P., Huld, T. A., & Iglesias, S. (2006) Energy rating of PV modules based on PVGIS irradiance and temperature database, In Proceedings from 21st European Photovoltaic Solar Energy Conference and Exhibition (pp. 4-8).

Kipp & Zonen (2000) Instruction Manual Pyranometer CM11/14, Kipp & Zonen, Delft

Kipp & Zonen (2015) Instruction Manual: CMP series Pyranometer and CMA series Albedometer, Kipp & Zonen, Delft

Kleissl, J. (2013) Solar energy forecasting and resource assessment, Academic Press.

Kniffka A., Meirink J., Stengel M., (2013) EUMETSAT Satellite Application Facility on Climate Monitoring Product User Manual – SEVIRI dataset cloud products, SAF/CM/DWD/PUM/SEV/CLD, Issue 1.2, 11-13

Kosmopoulos, P. G., Kazadzis, S., Lagouvardos, K., Kotroni, V., & Bais, A. (2015) Solar energy prediction and verification using operational model forecasts and ground-based solar measurements, Energy, 93, 1918-1930.

Kotlarski, S., Keuler, K., Christensen, O. B., Colette, A., Déqué, M., Gobiet, A., ... & Nikulin, G. (2014) Regional climate modeling on European scales: a joint standard evaluation of the EURO-CORDEX RCM ensemble. Geoscientific Model Development, 7(4), 1297-1333.

Lara-Fanego V., Ruiz-Arias J.A., Pozo-Vázquez D., Santos-Alamillos F.J., Tovar-Pescador J. (2012) Evaluation of the WRF model solar irradiance forecasts in Andalusia (southern Spain), Solar Energy, 86-8, 2200-2217

Li, H., Sheffield, J., & Wood, E. F. (2010) Bias correction of monthly precipitation and temperature fields from Intergovernmental Panel on Climate Change AR4 models using equidistant quantile matching, Journal of Geophysical Research: Atmospheres (1984–2012), 115(D10).

Liang, F., and Xia, X. A. (2005) Long-term trends in solar radiation and the associated climatic factors over China for 1961-2000, Annales Geophysicae , 23-7, 2425-2432).

Liepert, B., & Tegen, I. (2002) Multidecadal solar radiation trends in the United States and Germany and direct tropospheric aerosol forcing, Journal of Geophysical Research: Atmospheres (1984–2012), 107(D12), AAC-7.

Liu B.Y.H. and Jordan R.C., (1960) The interrelationship and characteristic distribution of direct, diffuse and total solar radiation, Solar Energy 4, 1-19

Long C.N. and Shi Y., (2006) The QCRad Value Added Product: surface radiation measurements quality control testing, including climatology configurable limits, Technical Report, ARM Climate Research Facility, U.S. Department of Energy.

Lopez, D., Muñoz, R., Valero, S., & Senabre, C. (2011) Analysis of a Ground-Mounted Double Axis Photovoltaic Installation in Spain, In International Conference on Renewable Energies and Power Quality ICREPQ (Vol. 11).

Lorenz, E., Hurka, J., Heinemann, D., & Beyer, H. G. (2009) Irradiance forecasting for the power prediction of grid-connected photovoltaic systems, IEEE Journal of Selected Topics in Applied Earth Observations and Remote Sensing, 2 (1), 2-10.

Maraun, D., Wetterhall, F., Ireson, A. M., Chandler, R. E., Kendon, E. J., Widmann, M., ... & Thiele‐Eich, I. (2010) Precipitation downscaling under climate change: Recent developments to bridge the gap between dynamical models and the end user, Reviews of Geophysics, 48(3).

Maraun, D. (2013) Bias correction, quantile mapping, and downscaling: Revisiting the inflation issue, Journal of Climate, 26(6), 2137-2143.

Maraun, D., Widmann, M., Gutiérrez, J. M., Kotlarski, S., Chandler, R. E., Hertig, E., ... & Wilcke, R. A. (2015) VALUE: A framework to validate downscaling approaches for climate change studies, Earth's Future, 3(1), 1-14.

Martins, J., Cardoso, R. M., Soares, P. M., Trigo, I. F., Belo-Pereira, M., Moreira, N., & Tomé, R. (2015) The summer diurnal cycle of coastal cloudiness over west Iberia using Meteosat/SEVIRI and a WRF regional climate model simulation, International Journal of Climatology.

Martins JPA, Cardoso RM, Soares PMM, Trigo I, Belo-Pereira M, Moreira N, Tomé R (2016) The diurnal cycle of coastal cloudiness over west Iberia using Meteosat/SEVIRI and a WRF regional climate model simulation, International Journal of Climatology.

Mathiesen, P., & Kleissl, J. (2011) Evaluation of numerical weather prediction for intra-day solar forecasting in the continental United States, Solar Energy, 85(5), 967-977.

Mathiesen, P., Collier, C., Parkes, J., Landberg, L., & Kleissl, J. (2014) Improved Solar Power Forecasting Using Cloud Assimilation into WRF, Proceedings of the 52nd Annual Conference, Australian Solar Energy Society (Australian Solar Council) Melbourne

Maxwell E. L., (1987) A quasi-physical model for converting hourly global horizontal to direct normal insolation, Report SERI/TR-215-3087, Solar Energy Research Institute, Colorado.

Medvigy D. and Beaulieu C., (2012) Trends in Daily Solar Radiation and Precipitation Coefficients of Variation since 1984, Journal of Climate, 25, 1330–1339

Meehl G., Stocker T., Collins W., Friedlingstein P. et al. (2007) Global climate projections, In: Solomon S, Qin D, Manning M, Chen Z, Marquis M, Averyt KB, Tignor M, Miller HL (eds) Climate change 2007: the physical science basis. Contribution of working group I to the 4th assessment report of the IPCC, Cambridge University Press, Cambridge, pp 747–846 Lorenz, E., Remund, J., Müller, S., Traunmüller, W., Steinmaurer, G., Pozo, D., Ruiz-Arias, J., Fanego, V., Ramirez, L., Romeo, M., Kurz, C., Pomares, L., Guerrero, C., (2009) Benchmarking of different approaches to forecast solar irradiance. 24th European Photovoltaic Solar Energy Conference, Hamburg, Germany, 21–25

Miguel A., Bilbao J., Aguiar R., Kambezidis H., Negro E., (2001) Diffuse solar irradiation model evaluation in the North Mediterranean Belt area, Solar Energy 70 (2), 143-153

Morcrette, J. J., & Jakob, C. (2000), The response of the ECMWF model to changes in the cloud overlap assumption, Monthly weather review, 128(6), 1707-1732.

Moss, R. H., Edmonds, J. A., Hibbard, K. A., Manning, M. R., Rose, S. K., Van Vuuren, D. P., ... & Meehl, G. A. (2010) The next generation of scenarios for climate change research and assessment, Nature, 463(7282), 747-756.

Ohmura, A. (2009). Observed decadal variations in surface solar radiation and their causes, Journal of Geophysical Research: Atmospheres (1984–2012), 114(D10).

Otkin, J. A., & Greenwald, T. J. (2008) Comparison of WRF model-simulated and MODIS-derived cloud data, Monthly Weather Review, 136(6), 1957-1970.

Ohtake, H., Shimose, K. I., da Silva Fonseca, J. G., Takashima, T., Oozeki, T., & Yamada, Y. (2013) Accuracy of the solar irradiance forecasts of the Japan Meteorological Agency mesoscale model for the Kanto region, Japan, Solar Energy, 98, 138-152.

Oliveira A.P., Escobedo J.F., Machado A.J., Soares J., (2002) Correlation models of diffuse solar-radiation applied to the city of São Paulo, Brazil, Applied Energy 71 (1), 59-73

Orgill J.F., Hollands K.G.T., (1977) Correlation equation for hourly diffuse radiation on a horizontal surface, Solar Energy 19 (4), 357-359

Pagola, I., Gastón, M., Fernández-Peruchena, C., Moreno, S., & Ramírez, L. (2010) New methodology of solar radiation evaluation using free access databases in specific locations, Renewable Energy, 35(12), 2792-2798.

Panagea, I. S., Tsanis, I. K., Koutroulis, A. G., & Grillakis, M. G. (2014) Climate Change Impact on Photovoltaic Energy Output: The Case of Greece, Advances in Meteorology, 2014.

Paulescu, M., Paulesu, E., Gravila, P., Badescu, V. (2013) Weather Modeling and Forecasting of PV Systems Operation, Green Energy and Technology, Springer, London.

Peel, M. C., Finlayson, B. L., & McMahon, T. A. (2007) Updated world map of the Köppen-Geiger climate classification, Hydrology and earth system sciences discussions, 4(2), 439-473.

Pelland, S., Galanis, G., & Kallos, G. (2013) Solar and photovoltaic forecasting through post-processing of the Global Environmental Multiscale numerical weather prediction model, Progress in Photovoltaics: Research and Applications, 21(3), 284-296.

Perez, R., Lorenz, E., Pelland, S., Beauharnois, M., Van Knowe, G., Hemker Jr, K., ... & Pomares, L. M. (2013) Comparison of numerical weather prediction solar irradiance forecasts in the US, Canada and Europe. Solar Energy, 94, 305-326.

Perkins, S. E., A. J. Pitman, N. J. Holbrook, McAneney J., (2007) Evaluation of the ar4 climate models' simulated daily maximum temperature, minimum temperature, and precipitation over australia using probability density functions. Journal of Climate, 20, 4356–4376.

Piani, C., Haerter, J. O., & Coppola, E. (2010) Statistical bias correction for daily precipitation in regional climate models over Europe, Theoretical and Applied Climatology, 99(1-2), 187-192.

Power, H. C. (2003) Trends in solar radiation over Germany and an assessment of the role of aerosols and sunshine duration, Theoretical and Applied Climatology, 76(1-2), 47-63.

Reindl D.T., Beckman W.A., Duffie J.A., (1990) Diffuse fraction correlations, Solar Energy 45 (1), 1-7

Rehman, S., & Ghori, S. G. (2000) Spatial estimation of global solar radiation using geostatistics. Renewable Energy, 21(3), 583-605.

Riahi, K., Rao, S., Krey, V., Cho, C., Chirkov, V., Fischer, G., ... & Rafaj, P. (2011) RCP 8.5—A scenario of comparatively high greenhouse gas emissions, Climatic Change, 109(1-2), 33-57.

Ridley B., Boland J., Lauret P., (2010) Modelling of diffuse solar fraction with multiple predictors, Renewable Energy, 35(2), 478-483

Rincón, A., Jorba, O., & Baldasano, J. M. (2010) Development of a short-term irradiance prediction system using post-processing tools on WRF-ARW meteorological forecasts in Spain. In Extended Abstracts, European Conf. on Applied Meteorology, Vol 7

Rios‐Entenza, A., Soares, P. M., Trigo, R. M., Cardoso, R. M., & Miguez‐Macho, G. (2014) Moisture recycling in the Iberian Peninsula from a regional climate simulation: Spatiotemporal analysis and impact on the precipitation regime, Journal of Geophysical Research: Atmospheres, 119(10), 5895-5912.

Romanou, A., Liepert, B., Schmidt, G. A., Rossow, W. B., Ruedy, R. A., and Zhang, Y. (2007) 20th century changes in surface solar irradiance in simulations and observations, Geophysical Research Letters, 34(5).

Rossow W. B. and Dueñas E. N., (2004) The international satellite cloud climatology project (ISCCP) web site: an online resource for research, Bulletin of the American Meteorological Society, 85, 167–172.

Ruiz-Arias, J. A., Alsamamra, H., Tovar-Pescador, J., & Pozo-Vázquez, D. (2010) Proposal of a regressive model for the hourly diffuse solar radiation under all sky conditions, Energy Conversion and Management, 51(5), 881-893.

Ruiz-Arias, J. A., Pozo-Vázquez, D., Santos-Alamillos, F. J., Lara-Fanego, V., & Tovar-Pescador, J. (2011) A topographic geostatistical approach for mapping monthly mean values of daily global solar radiation: A case study in southern Spain, Agricultural and forest meteorology, 151(12), 1812-1822.

Ruiz-Arias, J., Gueymard, C., Dudhia, J., Pozo-Vazquez, D. (2012) Improvement of the Weather Research and Forecasting (WRF) model for solar resource assessments and forecasts under clear skies, Proc. Amer. Sol. Energy Soc., Denver, USA

Rummukainen, M. (2010) State-of-the-art with Regional Climate Models, Wiley Interdisciplinary Reviews: Climate Change, 1(1), 82-96.

Sanchez - Lorenzo, A., Calbo, J., Brunetti, M., & Deser, C. (2009) Dimming/brightening over the Iberian Peninsula: Trends in sunshine duration and cloud cover and their relations with atmospheric circulation, Journal of Geophysical Research: Atmospheres, 114(D10).

Santos-Alamillos, F. J., Pozo-Vázquez, D., Ruiz-Arias, J. A., Lara-Fanego, V., & Tovar-Pescador, J. (2012) Analysis of spatiotemporal balancing between wind and solar energy resources in the southern Iberian Peninsula, Journal of Applied Meteorology and Climatology, 51-11, 2005-2024

Skamarock, W. C., Klemp, J. B., Dudhia, J., Gill, D. O., Barker, D. M., Wang, W., & Powers, J. G. (2008) A description of the advanced research WRF version 3 (No. NCAR/TN-475_STR). National Center for Atmospheric Research, Boulder Co, Mesoscale and Microscale Meteorology Divc

Skartveit A., Olseth J. A., Tuft M.E., 1998. An hourly diffuse fraction model with correction for variability and surface albedo, Solar Energy 63 (3), 173-183

Soares J., Oliveira A.P., Božnar M.Z., Mlakar P., Escobedo J.F., Machado A.J., (2004) Modeling hourly diffuse solar-radiation in the city of São Paulo using a neural-network technique, Applied Energy 79 (2), 201-214

Soares, P. M., Cardoso, R. M., Miranda, P., Viterbo, P., & Belo‐Pereira, M. (2012a) Assessment of the ENSEMBLES regional climate models in the representation of precipitation variability and extremes over Portugal, Journal of Geophysical Research: Atmospheres, 117(D7)

Soares, P. M. M., Cardoso, R. de Medeiros, M. J., Miranda, P. M. A., Belo-Pereira, M., Espirito-Santo F. (2012b) WRF high resolution dynamical downscaling of ERA-Interim for Portugal, Climate Dynamics, 399/10, 2497-2522

Soares, P.M.M., Cardoso, R.M., Semedo, A., Chinita, M.J., Ranjha, R. (2014) Climatology of Iberia Coastal Low-Level Wind Jet: WRF High Resolution Results, Tellus A, 66, 22377

Stanhill, G. (1998) Long-term trends in, and spatial variation of, solar irradiances in Ireland. International Journal of Climatology, 18(9), 1015-1030.

Stanhill, G. and Ianetz, A. (1997) Long-term trends in, and the spatial variation of, global irradiance in Israel, Tellus B, 49

Stengel, M., Kniffka, A., Meirink, J. F., Lockhoff, M., Tan, J., and Hollmann, R. (2014) CLAAS: the CM SAF cloud property data set using SEVIRI, Atmos. Chem. Phys., 14, 4297-4311

Sundqvist, H., Berge, E., & Kristjánsson, J. E. (1989) Condensation and cloud parameterization studies with a mesoscale numerical weather prediction model, Monthly Weather Review, 117(8), 1641-1657.

Šúri, M., & Hofierka, J. (2004) A new GIS‐based solar radiation model and its application to photovoltaic assessments, Transactions in GIS, 8(2), 175-190.

Šúri, M., Huld, T. A., Dunlop, E. D., Ossenbrink, H. A., (2007) Potential of solar electricity generation in the European Union member states and candidate countries, Solar Energy, 81-10, 1295-1305.

Tardío, J., Pardo de Santayana, M., & Morales, R. (2006) Ethnobotanical review of wild edible plants in Spain. Botanical Journal of Linnean Society, 152, 27–71

Teutschbein, C., & Seibert, J. (2012) Bias correction of regional climate model simulations for hydrological climate-change impact studies: Review and evaluation of different methods, Journal of Hydrology, 456, 12-29.

Themeßl, M., Gobiet, A., & Leuprecht, A. (2011) Empirical-statistical downscaling and error correction of daily precipitation from regional climate models, International Journal of Climatology, 31(10), 1530-1544.

Tomé, R., (2013) *Mudanças climáticas nas regiões insulares*, (Unpublished doctoral thesis), University of Azores, Portugal. Retrieved from http://hdl.handle.net/10400.3/2895.

Torres J.L., De Blas M., García A., de Francisco A., (2010) Comparative study of various models in estimating hourly diffuse solar irradiance, Renewable Energy 35 (6), 1325-1332

Troccoli, A., Dubus, L., & Haupt, S. E. (Eds.) (2014) Weather Matters for Energy, Springer, 2014.

van derLinden, P., and J. Mitchell (2009) ENSEMBLES: Climate change and its impacts: Summary of research and results from the ENSEMBLES project, technical report, Met Off. Hadley Cent., Exeter, U K.

Casanueva, A. V. (2016) Comparison of statistical and dynamical climate downscaling techniques: screening of methods for their use in impact studies, (Unpublished doctoral thesis), University of Cantabria, Spain. Retrieved from ttp://hdl.handle.net/10902/8321

von Storch, H. (1999) On the use of “inflation” in statistical downscaling, Journal of Climate, 12(12), 3505-3506.

von Storch, H., & Zwiers, F. W. (2001) Statistical analysis in climate research, Cambridge University Press.

Wilby, R. L., Dawson, C. W., & Barrow, E. M. (2002) SDSM—a decision support tool for the assessment of regional climate change impacts, Environmental Modelling & Software, 17(2), 145-157.

Wilby, R.L., Charles, S., Mearns, L.O., Whetton, P., Zorito, E. and Timbal, B. (2004) Guidelines for Use of Climate Scenarios Developed from Statistical Downscaling Methods, IPCC Task Group on Scenarios for Climate Impact Assessment (TGCIA)

Wilcke, R. A. I., Mendlik, T., and Gobiet, A. (2013) Multi-Variable Downscaling and Error-Correction of Regional Climate Models. Clim. Change, 120(4), 871–887

Wild, M., Gilgen, H., Roesch, A., Ohmura, A., Long, C. N., Dutton, E. G., ... and Tsvetkov, A. (2005) From dimming to brightening: Decadal changes in solar radiation at Earth's surface. Science, 308(5723), 847-850.

Wild, M., Folini, D., Henschel, F., Fischer, N., and Müller, B. (2015) Projections of long-term changes in solar radiation based on CMIP5 climate models and their influence on energy yields of photovoltaic systems, Solar Energy, 116, 12-24.

Wilks, D. S. (2006) Statistical methods in the atmospheric sciences, Academic press.

Wood AW, Leung LR, Sridhar V, Lettenmaier DP (2004) Hydrologic implications of dynamical and statistical approaches to downscaling climate model outputs, Climatic Change, 62 (1-3), 189-216.

Wong L.T. and Chow W.K., 2001. Solar radiation model, Applied Energy, Volume 69, Issue 3, July 2001, 191-224.

Zhang, M. H., Lin, W. Y., Klein, S. A., Bacmeister, J. T., Bony, S., Cederwall, R. T., ... & Minnis, P. (2005) Comparing clouds and their seasonal variations in 10 atmospheric general circulation models with satellite measurements, Journal of Geophysical Research: Atmospheres, 110(D15).

Zhang, Y., Dulière, V., Mote, P. W., & Salathé Jr, E. P. (2009) Evaluation of WRF and HadRM mesoscale climate simulations over the US Pacific Northwest, Journal of Climate, 22(20), 5511-5526.